

On the design and analysis of near-term quantum network protocols using Markov decision processes

Sumeet Khatri

Dahlem Center for Complex Quantum Systems, Freie Universität Berlin, 14195 Berlin, Germany

(*Electronic mail: sumeet.khatri@fu-berlin.de)

(Dated: 8 July 2022)

The quantum internet is one of the frontiers of quantum information science research. It will revolutionize the way we communicate and do other tasks, and it will allow for tasks that are not possible using the current, classical internet. The backbone of a quantum internet is entanglement distributed globally in order to allow for such novel applications to be performed over long distances. Experimental progress is currently being made to realize quantum networks on a small scale, but much theoretical work is still needed in order to understand how best to distribute entanglement, especially with the limitations of near-term quantum technologies taken into account. This work provides an initial step towards this goal. In this work, we lay out a theory of near-term quantum networks based on Markov decision processes (MDPs), and we show that MDPs provide a precise and systematic mathematical framework to model protocols for near-term quantum networks that is agnostic to the specific implementation platform. We start by simplifying the MDP for elementary links introduced in prior work, and by providing new results on policies for elementary links in the steady-state (infinite-time) limit. In particular, we show that the well-known memory-cutoff policy is optimal in the steady-state limit. Then we show how the elementary link MDP can be used to analyze a quantum network protocol in which we wait for all elementary links to be active before creating end-to-end links. We then provide an extension of the MDP formalism to two elementary links, which is useful for analyzing more sophisticated quantum network protocols. Here, as new results, we derive linear programming relaxations that allow us to obtain optimal steady-state policies with respect to the expected fidelity and waiting time of the end-to-end link.

CONTENTS

I. Introduction	1
II. Markov decision process for elementary links	3
A. Elementary link generation	3
B. Definition of the MDP	4
C. Optimal policies	5
D. The memory-cutoff policy and its optimality	7
III. Entanglement distillation and joining protocols	7
A. Entanglement distillation	7
B. Joining protocols	8
1. Entanglement swapping protocol	9
2. GHZ entanglement swapping protocol	10
3. Graph state distribution protocol	10
IV. Analysis of a quantum network protocol	12
A. Fidelity	13
B. Waiting time	13
C. Key rates for quantum key distribution	14
V. A Markov decision process beyond the elementary link level	15
A. An MDP for two elementary links	15
B. Optimal policies via linear programming	17
VI. Summary and outlook	18
Acknowledgments	19

I. INTRODUCTION

The quantum internet^{1–5} is envisioned to be a global-scale interconnected network of devices that exploits the uniquely quantum-mechanical phenomenon of entanglement. By operating in tandem with today’s internet, it will allow people all over the world to perform quantum communication tasks such as quantum key distribution (QKD)^{6–11}, quantum teleportation^{12–14}, quantum clock synchronization^{15–18}, distributed quantum computation¹⁹, and distributed quantum metrology and sensing^{20–22}. A quantum internet will also allow for exploring fundamental physics²³, and for forming an international time standard²⁴. Quantum teleportation and QKD are perhaps the primary use cases of the quantum internet in the near term. In fact, there are several metropolitan-scale QKD systems already in place^{25–32}.

Scaling up beyond the metropolitan level towards a global-scale quantum internet is a major challenge. All of the aforementioned tasks require the use of shared entanglement between distant locations on the earth, which typically has to be distributed using single-photonic qubits sent through either the atmosphere or optical fibers. It is well known that optical signals transmitted through either the atmosphere or optical fibers undergo an exponential decrease in the transmission success probability with distance^{33–35}, limiting direct transmission distances to roughly hundreds of kilometers. Therefore, one of the central research questions in the theory of quantum networks is how to overcome this exponential loss and thus to distribute entanglement over long distances efficiently and at high rates.

A quantum network can be modelled as a graph $G = (V, E)$,

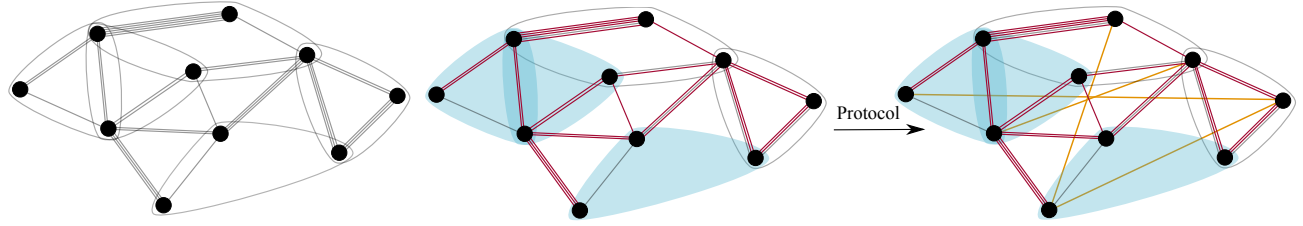


FIG. 1. Graphical depiction of a quantum network and entanglement distribution. (Left) The physical layout of the quantum network is described by a hypergraph G , which should be thought of as fixed, in which the vertices represent the nodes (senders and receivers) in the network and the (hyper)edges represent quantum channels that are used to distribute entangled states (elementary links) shared by the corresponding nodes. (Center) At any point in time only a certain number of elementary links in the network may be active. By “active”, we mean that an entangled state has been distributed successfully to the nodes and the corresponding quantum systems stored in the respective quantum memories. Active bipartite links are indicated by a red line, and active k -partite elementary links, $k \geq 3$, corresponding to the hyperedges are indicated by a blue bubble. (Right) An entanglement distribution protocol transforms elementary links to virtual links, which are indicated in orange, thus leading to a new graph for the network. The protocol is described mathematically by an LOCC channel.

where the vertices V represent the nodes in the network and the edges in E represent quantum channels connecting the nodes; see Fig. 1. Then, the task of entanglement distribution is to transform *elementary links*, i.e., entanglement shared by neighbouring nodes, to *virtual links*, i.e., entanglement between distant nodes; see the right-most panel of Fig. 1. In this context, nodes that are not part of the virtual links to be created can act as *quantum repeaters*, i.e., helper nodes whose purpose is to mitigate the effects of loss and noise along a path connecting the end nodes, thereby making the quantum information transmission more reliable. Specifically, quantum repeaters perform entanglement distillation^{36–38} (or some other form of quantum error correction), entanglement swapping^{12,39}, and possibly some form of routing, in order to create the desired virtual links. Protocols for entanglement distribution in quantum networks have been described from an information-theoretic perspective in Refs. [40–47], and limits on communication in quantum networks have been explored in Refs. [40–54]. Linear programs, and other techniques for obtaining optimal entanglement distribution rates in a quantum network, have been explored in Refs. [53, 55–57]. However, information-theoretic analyses are agnostic to physical implementations, and generally speaking the protocols and the rates derived apply in an idealized scenario, in which quantum memories have high coherence times and quantum gate operations have no error.

What are the fundamental limitations on *near-term quantum networks*? Such quantum networks are characterized by the following elements:

- Small number of nodes;
- Imperfect sources of entanglement;
- Non-deterministic elementary link generation and entanglement swapping;
- Imperfect measurements and gate operations;
- Quantum memories with short coherence times;
- No (or limited) entanglement distillation/error correction.

A theoretical framework taking these practical limitations into account would act as a bridge between statements about what

can be achieved in principle (which can be answered using information-theoretic methods) and statements that are directly useful for the purpose of implementation. The purpose of this work is to present the initial elements of such a theory of near-term quantum networks.

The main contribution of this work is to frame quantum network protocols in terms of Markov decision processes (MDPs), and to place the Markov decision process for elementary links introduced in Ref. [58] within an overall quantum network protocol. More specifically, the contributions of this work are as follows:

1. In Sec. II, we start by recapping the model for elementary link generation presented in Ref. [58]. Then, as a new contribution, we show that the quantum decision process for elementary links introduced in Ref. [58] can be written in a simpler manner as an MDP in terms of different variables. Furthermore, we emphasize that the figure of merit associated with the MDP, as introduced in Ref. [58], takes into account both the fidelity of the elementary link as well as the probability that it is active. To the best of our knowledge, such a figure of merit has not been considered in prior work. The simplified form of the MDP allows us to derive two new results. The first new result is Theorem II.2, which gives us an analytic expression for the steady-state value of an elementary link undergoing an arbitrary time-homogenous policy. The second new result is Theorem II.4, in which we show that the so-called “memory-cutoff policy”—in which the elementary link is kept for some fixed amount of time and then discarded and regenerated—is an optimal policy in the steady-state limit. We demonstrate the usefulness of the MDP approach to modeling elementary links in Appendix C and D.
2. In Sec. III, we describe entanglement distillation protocols and protocols for joining elementary links (in order to create virtual links) in general terms as LOCC quantum instrument channels. We then present three joining protocols and write them down explicitly as LOCC channels. Doing so allows us to determine the output state of the protocol for *any* set of input states,

including input states that are noisy as a result of device imperfections, etc. This in turn allows us to compute the fidelity of the output state with respect to the ideal target state that would be obtained if the input states were ideal. Formulas for the fidelity at the output of the protocols are presented as Proposition III.1, Proposition III.2, and Proposition III.3. In particular, Proposition III.1 provides a formula for the fidelity at the output of the usual entanglement swapping protocol, which to the best of our knowledge is not explicitly found in prior works. Prior works typically use (as an approximation) the product of the individual elementary link fidelities in order to obtain the fidelity after entanglement swapping.

3. In Sec. IV, we present a quantum network protocol that combines the Markov decision process for elementary links with known routing and path-finding algorithms. In essence, the protocol is a simple one in which we first wait for all of the relevant elementary links to become active, and then we perform the required joining operations to establish the virtual links; see Fig. 8 for a summary. For this protocol, we provide a general method for determining waiting times and key rates for quantum key distribution.
4. In Sec. V, we provide a first step towards extending the elementary link MDP by defining an MDP for two elementary links with entanglement swapping. We then show how to approximate waiting times using a linear program, and we find that this linear programming approximation reproduces exactly the known analytic results on the waiting time for such a scenario⁵⁹. However, our result is more general, allowing us to compute waiting times for arbitrary parameter regimes, while the analytic results are true only for restricted parameter regimes. Broadly speaking, having linear-programming approximations to the waiting time and other important quantities of interest (such as fidelity) will be important when considering MDPs for larger networks.

This work is one in a long line of work on quantum repeaters, taking device imperfections and noise into account, beginning with the initial theoretical proposal^{60,61}, and then resulting in a vast body of work^{56,57,59,62–91}. (See also Refs. [92–96] and the references therein.) All of these proposals deal almost exclusively with a single transmission line connecting a sender and a receiver. However, for a quantum internet, we need to go beyond a single transmission line, and we need to consider multiple transmission lines operating in parallel. A unified and self-consistent theoretical framework will help to guide real-world implementations. It is our hope that this work provides a good starting point along this line of thought, and leads to a better understanding of how realistic, near-term quantum devices could be used to realize large-scale quantum networks, and eventually a global-scale quantum internet.

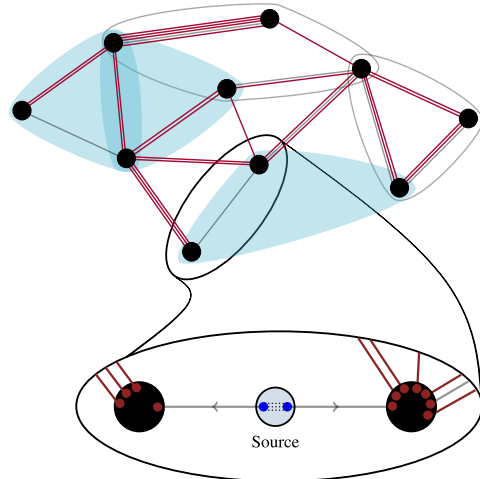


FIG. 2. Our model for elementary link generation in a quantum network consists of source stations associated to every elementary link that distributes entangled states to the corresponding nodes^{76,97–99}. (Adapted from Ref. [58].)

II. MARKOV DECISION PROCESS FOR ELEMENTARY LINKS

We start by presenting a Markov decision process (MDP) for elementary links, based on Ref. [58]. To be specific, this is an MDP for an arbitrary edge of the graph corresponding to a quantum network. We start by describing the physical model of elementary link generation. Then, we define the MDP corresponding to this model of elementary link generation.

A. Elementary link generation

Our model for elementary link generation is the one considered in Ref. [58] and illustrated in Fig. 2, based on the same model considered in prior work^{76,97–99}. Consider an arbitrary physical link in the network. For every such physical link, there is a source station that prepares and distributes an entangled state to the corresponding nodes. In general, all of these source stations operate independently of each other, distributing entangled states as they are requested. Specifically, we have the following.

- The source produces a k -partite quantum state ρ^S , $k \geq 2$, and sends it to the nodes via a quantum channel \mathcal{S} , leading to the state $\mathcal{S}(\rho^S)$. Here, k is the number of nodes belonging to an edge, with $k = 2$ corresponding to ordinary, bipartite edges (such as the red edges in Fig. 2) and $k \geq 3$ corresponding to hyperedges (such as the blue bubbles in Fig. 2).
- The nodes perform a heralding procedure, which is a protocol involving local operations and classical communication. It can be described by a quantum instrument $\{\mathcal{M}^0, \mathcal{M}^1\}$, where \mathcal{M}^0 and \mathcal{M}^1 are completely positive trace non-increasing maps such that $\mathcal{M}^0 + \mathcal{M}^1$ is trace preserving. These maps capture not only the probabilistic nature of the heralding procedure but also the

various imperfections of the devices that are used to perform the procedure. The map \mathcal{M}^0 corresponds to failure of heralding and \mathcal{M}^1 corresponds to success. The probability of successful transmission and heralding is

$$p = \text{Tr}[(\mathcal{M}^1 \circ \mathcal{S})(\rho^S)], \quad (1)$$

and the states conditioned on success and failure are, respectively,

$$\sigma^0 := \frac{1}{p}(\mathcal{M}^1 \circ \mathcal{S})(\rho^S), \quad (2)$$

$$\tau^0 := \frac{1}{1-p}(\mathcal{M}^0 \circ \mathcal{S})(\rho^S). \quad (3)$$

The superscript “0” in σ^0 indicates that, upon success of the heralding procedure, the quantum systems have been immediately stored in local quantum memories at the nodes and have not yet suffered from any decoherence.

- The state of the quantum systems after $m \in \{0, 1, 2, \dots\}$ time steps in the quantum memories is given by

$$\sigma(m) := \mathcal{N}^{\circ m}(\sigma^0), \quad (4)$$

where \mathcal{N} is a quantum channel that describes the decoherence of the individual quantum memories at the nodes.

For specific, realistic noise models for the heralding and for the quantum memories, as well as for other realistic parameters for elementary link generation, we refer to Refs. [57, 100–105]. Also, in Appendix C, we present two specific models of elementary link generation, as special cases of the abstract developments presented here.

B. Definition of the MDP

Having described the physical model of elementary link generation in the previous section, let us now proceed to the definition of the Markov decision process (MDP) for an elementary link. Note that while the formalism of the previous section gives us a mathematical description of the quantum state of an elementary link immediately after it is successfully generated, the MDP formalism provides us with a systematic framework to define actions on an elementary link and their effects on the quantum state over time.

Before starting, let us briefly summarize the definition of a Markov decision process (MDP); we refer to Appendix A for more details and a detailed explanation of the notation being used. An MDP is a mathematical model of an agent performing actions on a system (usually called the environment). The system is described by a set S of (*classical*) states, and the agent picks actions from a set A . Corresponding to every action $a \in A$ is a $|S| \times |S|$ transition matrix T^a , such that the matrix element $T^a(s', s)$ is equal to the probability of transitioning to the state $s' \in S$ given that the current state is $s \in S$ and the action $a \in A$ is taken.

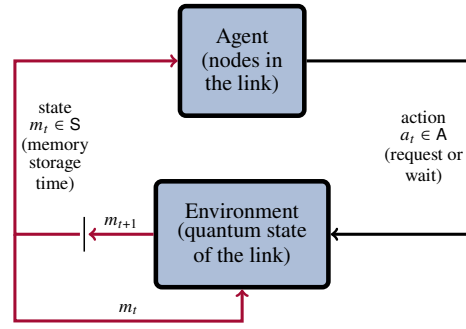


FIG. 3. Schematic depiction of the Markov decision process (MDP) for elementary links presented in Sec. II B. The MDP provides us with a systematic way of keeping track of the quantum state of an elementary link in a quantum network based on the actions at the nodes of the elementary link. Specifically, the states m_t of the MDP encode information about the quantum state via (4).

The results of Ref. [58] show us that, for the purposes of tracking the quantum state of an elementary link over time, as well as its fidelity to a target pure state, it is enough to keep track of the time that the quantum systems of the elementary link reside in their respective quantum memories. With this observation, we can define a simpler MDP for elementary links; see Fig. 3.

- *States:* The states in our elementary link MDP are defined by the set $S = \{-1, 0, 1, \dots, m^*\}$, which correspond to the number of time steps that the quantum systems of the elementary link have been sitting in their respective quantum memories. The state -1 corresponds to the elementary link being inactive, and $m^* \in \mathbb{N}_0 := \{0, 1, 2, \dots\}$ corresponds to the coherence time of the quantum memory. Specifically, if t_{coh} is the coherence time of the quantum memory (say, in seconds), and the duration of every time step (in seconds) is Δt (based on the classical communication time between the nodes in the elementary link), then $m^* = \frac{t_{\text{coh}}}{\Delta t}$. From now on, we refer to m^* as the *maximum storage time* of the elementary link.

We use $M(t)$, $t \in \mathbb{N}$, to refer to the random variables (taking values in S) corresponding to the state of the MDP at time t . We also associate to the elements in S orthonormal vectors $\{|m\rangle\}_{m \in S}$, and we emphasize that these vectors should not be thought of as representing quantum states but as representing the extreme points of a probability simplex associated with the set S ; see Appendix A for details.

- *Actions:* The set of actions is $A = \{0, 1\}$, where 0 corresponds to the action of “wait” and 1 corresponds to “request”. In other words, at every time step, the agent can decide to keep their quantum systems currently in memory (“wait”) or to discard the quantum systems and perform the elementary link generation procedure again (“request”).

The transition matrices T^0 and T^1 corresponding to the

two actions are defined as follows:

$$T^0 = \mathbb{1}^{(-)} + B^{(+)} \quad (5)$$

$$T^1 = |g_p\rangle\langle\gamma|, \quad (6)$$

where

$$\mathbb{1}^{(-)} := |-1\rangle\langle-1|, \quad (7)$$

$$B^{(+)} := \sum_{m=0}^{m^*-1} |m+1\rangle\langle m| + |-1\rangle\langle m^*|, \quad (8)$$

$$|g_p\rangle := (1-p)|-1\rangle + p|0\rangle, \quad (9)$$

$$|\gamma\rangle = \sum_{m=-1}^{m^*} |m\rangle. \quad (10)$$

(Note that we define our transition matrices such that probability vectors are applied to them from the right; see Appendix A for details.) The transition matrix T^0 describes what happens to the elementary link when the action $a = 0$ (“wait”) is taken by the agent: if the elementary link is currently inactive, then it stays inactive; if the elementary link is active, and it is in memory for less than m^* time steps, then the memory time is incremented by one; if the elementary link is active and it has been in memory for m^* time steps, then because the coherence time of the memory has been reached (as per the definition of m^*), the elementary link becomes inactive. If the action $a = 1$ (“request”) is taken, then regardless of the current state of the elementary link, the state changes to -1 (inactive) with probability $1 - p$, meaning that the elementary link generation failed, or it changes to 0 with probability p , meaning that the elementary link generation succeeded. These two possibilities are captured by the probability vector $|g_p\rangle$. We use $A(t)$, $t \in \mathbb{N}$, to refer to the random variable (taking values in the set \mathcal{A}) corresponding to the action taken at time t .

We let $H(t) = (M(1), A(1), M(2), A(2), \dots, A(t-1), M(t))$ be the *history*, consisting of a sequence of states and actions, up to time t , with $H(1) = M(1)$.

- *Figure of merit*: Our figure of merit for an elementary link is the following function:

$$f(m) := \begin{cases} \langle\psi|\sigma(m)|\psi\rangle & \text{if } m \in \{0, 1, 2, \dots, m^*\}, \\ 0 & \text{if } m = -1. \end{cases} \quad (11)$$

$$= (1 - \delta_{m,-1})\langle\psi|\sigma(m)|\psi\rangle, \quad (12)$$

where $\sigma(m)$ is defined in (4) and $|\psi\rangle$ is a target state vector for the elementary link. (For example, if the elementary link contains two nodes, then $|\psi\rangle$ could be the state vector for the two-qubit maximally entangled state.) We emphasize that the function f is not just the fidelity of the elementary link—it also depends implicitly on the probability that the elementary link is active, because if f was simply the fidelity of the elementary link then instead of the definition $f(-1) = 0$ we would have $f(-1) =$

$\langle\psi|\tau^\varnothing|\psi\rangle$, where $\tau^\varnothing = (1/(1-p))(\mathcal{M}^0 \circ \mathcal{S})(\rho^S)$ is the quantum state corresponding to failure of the heralding procedure; see (3). We illustrate the importance of this distinction, and therefore the usefulness of this figure of merit for designing and evaluating protocols, in Sec. D 2, specifically Fig. 16. To the best of our knowledge, this figure of merit has not been considered in prior work.

A *policy* is a sequence $\pi = (d_1, d_2, \dots)$ of *decision functions* $d_t : \mathcal{S} \times \mathcal{A} \rightarrow [0, 1]$, which indicate the probability of performing a particular action conditioned on the state of the system:

$$d_t(s)(a) = \Pr[A(t) = a | S(t) = s]. \quad (13)$$

For a particular policy $\pi = (d_1, d_2, \dots, d_{t-1})$, the probability of a particular history $h^t = (m_1, a_1, m_2, a_2, \dots, a_{t-1}, m_t)$ of states and actions is (see Appendix A 2)

$$\begin{aligned} \Pr[H(t) = h^t]_\pi &= \Pr[M(1) = m_1] \prod_{j=1}^{t-1} T^{a_j}(m_{j+1}; m_j) d_j(m_j)(a_j). \end{aligned} \quad (14)$$

Then, the quantum state of the elementary link is⁵⁸

$$\rho^\pi(t) = \sum_{h^t} \Pr[H(t) = h^t]_\pi |h^t\rangle\langle h^t| \otimes \sigma(t|h^t), \quad (15)$$

$$\sigma(t|h^t) = (1 - \delta_{m_t,-1})\sigma(m_t) + \delta_{m_t,-1}\tau^\varnothing, \quad (16)$$

where we recall that $\sigma(m_t)$ is given by (4).

We are interested primarily in the expected value of the function f defined in (12) at times $t \in \mathbb{N}$:

$$\tilde{F}^\pi(t) := \mathbb{E}[f(M(t))]_\pi = \sum_{m=0}^{m^*} f(m) \Pr[M(t) = m]_\pi, \quad (17)$$

for policies $\pi = (d_1, d_2, \dots, d_{t-1})$. We are also interested in the probability that the elementary link is active at time $t \in \mathbb{N}$, which is given by

$$X^\pi(t) := 1 - \Pr[M(t) = -1]_\pi. \quad (18)$$

From this, the expected fidelity of the elementary link is given by

$$F^\pi(t) := \frac{\tilde{F}^\pi(t)}{X^\pi(t)}. \quad (19)$$

C. Optimal policies

We define an *optimal policy* to be one that achieves the quantity $\sup_\pi \tilde{F}^\pi(t)$, i.e., the maximum value of the function \tilde{F}^π defined in (17) among all policies π . In the steady-state (infinite-time) limit, we are interested in the quantity

$$\sup_d \lim_{t \rightarrow \infty} \tilde{F}^{(d,d,\dots)}(t)$$

$$= \sup_d \sum_{m=0}^{m^*} f(m) \lim_{t \rightarrow \infty} \Pr[M(t) = m]_{(d, d, \dots)} \quad (20)$$

(if the limit exists), which is the maximum value of \tilde{F}^π among all time-homogeneous (stationary) policies $\pi = (d, d, \dots)$, i.e., policies in which a fixed decision function d is used at every time step.

In Ref. [58], it was shown that an optimal policy can be determined using a backward recursion algorithm. We restate this algorithm here for completeness.

Theorem II.1 (Optimal finite-time policy for an elementary link⁵⁸). For all $t \in \mathbb{N}$, the optimal value of an elementary link with success probability $p \in [0, 1]$ and maximum storage time $m^* \in \mathbb{N}_0$ is given by

$$\sup_\pi \tilde{F}^\pi(t) = \sum_{m_1 \in \mathcal{S}} \max_{a_1 \in \mathcal{A}} w_2(m_1, a_1), \quad (21)$$

where

$$w_j(h^{j-1}, a_{j-1}) = \sum_{m_j \in \mathcal{S}} \max_{a_j \in \mathcal{A}} w_{j+1}(h^{j-1}, a_{j-1}, m_j, a_j) \quad (22)$$

for all $j \in \{2, 3, \dots, t-1\}$, and

$$\begin{aligned} w_t(h^{t-1}, a_{t-1}) &= \sum_{m_t \in \mathcal{S}} \langle m_t | g_p \rangle \left(\prod_{j=1}^{t-1} T^{a_j}(m_{j+1}; m_j) \right) f(m_t). \end{aligned} \quad (23)$$

Furthermore, the optimal policy is deterministic and given by $\pi = (d_1^*, d_2^*, \dots, d_{t-1}^*)$, where

$$d_j^*(h^j) = \max_{a \in \mathcal{A}} w_{j+1}(h^j, a) \quad \forall j \in \{1, 2, \dots, t-1\}. \quad (24)$$

Intuitively, the result of Theorem II.1 tells us that, for finite times, an optimal policy can be found by optimizing the individual actions going “backwards in time”, by first optimizing the final action at time $t-1$ and then optimizing the action at time $t-2$, etc., and then finally optimizing the action at time $t=1$. This is indeed the case, because from (24) we see that the optimal action at the first time step is obtained using the function w_2 , but from (22) we see that to calculate w_2 we need w_3 , and to calculate w_3 we need w_4 , etc., until we get to the function w_t for the final time step, which we can calculate using (23).

While the optimal policy for finite times was determined in Ref. [58], the steady-state value of the function \tilde{F} with respect to arbitrary stationary policies (i.e., the value in (20)) was not determined. We now show that the limit in (20) exists, and we determine its value for arbitrary decision functions.

Theorem II.2 (Steady-state expected value of an elementary link). Let $p \in [0, 1]$ be the success probability of generating an elementary link in a quantum network, let $m^* \in \mathbb{N}_0$ be the maximum storage time of the elementary link, and let d be a decision function such that $d(m)(0) = \alpha(m)$, $m \in \{-1, 0, 1, \dots, m^*\}$, is the probability of executing the action

“wait” and $d(m)(1) = 1 - d(m)(0) = \bar{\alpha}(m)$ is the probability of executing the action “request”. If the elementary link undergoes the stationary policy (d, d, \dots) , then

$$\lim_{t \rightarrow \infty} \tilde{F}^{(d, d, \dots)}(t) = \sum_{m=0}^{m^*} f(m) s_d(m), \quad (25)$$

where

$$s_d(-1) = \frac{1}{N_d} \left(1 - p \left(1 - \prod_{m'=0}^{m^*} \alpha(m') \right) \right), \quad (26)$$

$$s_d(0) = \frac{1}{N_d} p \bar{\alpha}(-1), \quad (27)$$

$$s_d(m) = \frac{1}{N_d} p \bar{\alpha}(-1) \prod_{m'=0}^{m-1} \alpha(m'), \quad m \in \{1, \dots, m^*\}, \quad (28)$$

with

$$\begin{aligned} N_d &= 1 - p \left(1 - \prod_{m'=0}^{m^*} \alpha(m') \right) \\ &\quad + p \bar{\alpha}(-1) \left(1 + \sum_{m=1}^{m^*} \prod_{m'=0}^{m-1} \alpha(m') \right). \end{aligned} \quad (29)$$

Proof. See Appendix F. \square

Using Theorem II.2, we can determine the optimal steady-state value of the function $\tilde{F}^{(d, d, \dots)}$, and thus the optimal decision function d , by optimizing the quantity in (25) with respect to m^* independent variables $\alpha(-1), \alpha(0), \dots, \alpha(m^*)$ subject to the constraints $\alpha(m) \in [0, 1]$ for all $m \in \{-1, 0, 1, \dots, m^*\}$. (Recall from the statement of Theorem II.2 that the variables $\alpha(m)$ are directly related to the decision function d .) Alternatively, we can use the following linear program in order to obtain an optimal policy.

Proposition II.3 (Linear program for the optimal steady-state value of an elementary link). Consider an elementary link in a quantum network with generation success probability $p \in [0, 1]$ and maximum storage time $m^* \in \mathbb{N}_0$. Let $|f\rangle := \sum_{m=-1}^{m^*} f(m)|m\rangle$. The optimal steady-state value of the elementary link, namely, the quantity in (20), is equal to the solution to the following linear program:

$$\begin{aligned} &\text{maximize } \langle f | v \rangle \\ \text{subject to } &0 \leq |w_a\rangle \leq |v\rangle \leq 1 \quad \forall a \in \{0, 1\}, \\ &\langle \gamma | v \rangle = 1, \\ &|w_0\rangle + |w_1\rangle = |v\rangle = T^0|w_0\rangle + T^1|w_1\rangle, \end{aligned} \quad (30)$$

where the optimization is with respect to the $(m^* + 1)$ -dimensional vectors $|v\rangle, |w_0\rangle, |w_1\rangle$, and the inequality constraints on the vectors are componentwise. For every feasible point of this linear program, we obtain a decision function d as follows: $d(m)(a) = \frac{\langle m | w_a \rangle}{\langle m | v \rangle}$ for all $m \in \{-1, 0, 1, \dots, m^*\}$ and $a \in \{0, 1\}$. If $\langle m | v \rangle = 0$, then we set $d(m)(0) = \alpha(m)$ and $d(m)(1) = 1 - \alpha(m)$ for an arbitrary $\alpha(m) \in [0, 1]$.

Proof. The linear program in (30) is a special case of the linear program presented in Proposition A.2 in Appendix A. The main assumption of that result is that the MDP be ergodic, which is true in this case by Theorem II.2. \square

D. The memory-cutoff policy and its optimality

An example of a stationary policy is the *memory-cutoff policy*, which has been considered extensively in prior work^{58,59,63–65,98,99,101,106–109}. This is a deterministic policy that is defined by a cutoff time $t^* \in \mathbb{N}_0 \cup \{\infty\}$, where $\mathbb{N}_0 := \{0, 1, 2, \dots\}$, such that $t^* \leq m^*$. Then, the decision function for this policy is defined by the values $d^{t^*}(m)(0)$ and $d^{t^*}(m)(1) = 1 - d^{t^*}(m)(0)$ for all $m \in \{-1, 0, 1, \dots, t^*\}$ as follows:

$$d^{t^*}(m)(0) = \begin{cases} 0 & \text{if } m = -1, t^*, \\ 1 & \text{if } m \in \{0, 1, \dots, t^* - 1\}, \end{cases} \quad (31)$$

for all $t^* \in \mathbb{N}_0$. In other words, the elementary link is kept in memory for t^* time steps, and then it is discarded and regenerated. If $t^* = \infty$,

$$d^\infty(m)(0) = \begin{cases} 0 & \text{if } m = -1, \\ 1 & \text{otherwise,} \end{cases} \quad (32)$$

which means that the elementary link, once generated, is never discarded.

For the memory-cutoff policy, we use the abbreviations $\tilde{F}^{t^*} \equiv \tilde{F}^{(d^{t^*}, d^{t^*}, \dots)}$, $X^{t^*} \equiv X^{(d^{t^*}, d^{t^*}, \dots)}$, and $F^{t^*} \equiv F^{(d^{t^*}, d^{t^*}, \dots)}$. Using Theorem II.2, we have $N_d = 1 + t^*p$ and $s_{d^{t^*}}(m) \equiv s_{t^*}(m) = \frac{p}{1+t^*p}$ for all $m \in \{0, 1, \dots, t^*\}$, so that

$$\lim_{t \rightarrow \infty} \tilde{F}^{t^*}(t) = \frac{p}{1+t^*p} \sum_{m=0}^{t^*} f(m), \quad (33)$$

for all $t^* \in \mathbb{N}_0$, which agrees with Ref. [58, Eq. (4.15)], which was obtained using different methods. We also obtain

$$\lim_{t \rightarrow \infty} X^{t^*}(t) = \frac{(t^* + 1)p}{1 + t^*p}, \quad (34)$$

$$\lim_{t \rightarrow \infty} F^{t^*}(t) = \frac{1}{t^* + 1} \sum_{m=0}^{t^*} f(m), \quad (35)$$

for all $t^* \in \mathbb{N}_0$.

For $t^* = \infty$, we have, for all $t \geq 1$ ⁵⁸,

$$\tilde{F}^\infty(t) = \sum_{m=0}^{t-1} f(m)p(1-p)^{t-(m+1)}, \quad (36)$$

$$X^\infty(t) = 1 - (1-p)^t, \quad (37)$$

$$F^\infty(t) = \sum_{m=0}^{t-1} f(m) \frac{p(1-p)^{t-(m+1)}}{1 - (1-p)^t}. \quad (38)$$

It turns out that, in the steady-state limit, there always exists a cutoff such that the memory-cutoff policy achieves the optimal value of the elementary link.

Theorem II.4 (Optimality of the memory-cutoff policy in the steady-state limit). Consider an elementary link in a quantum network with generation success probability $p \in [0, 1]$ and maximum storage time $m^* \in \mathbb{N}_0$. The optimal steady-state value of the elementary link, namely, the quantity in (20), is achieved by a memory-cutoff policy, i.e.,

$$\sup_d \lim_{t \rightarrow \infty} \tilde{F}^{(d, d, \dots)}(t) = \max_{t^* \in \{0, 1, \dots, m^*\}} \frac{p}{1 + t^*p} \sum_{m=0}^{t^*} f(m). \quad (39)$$

Proof. See Appendix G. \square

III. ENTANGLEMENT DISTILLATION AND JOINING PROTOCOLS

In the previous section, we discussed elementary links in a quantum network, how to model the generation of elementary links and how to model them in time in terms of a Markov decision process. The description of an elementary link in terms of a Markov decision process allows us to determine, as a function of time, the quantum state of an elementary link. Keeping in mind the overall goal of entanglement distribution, i.e., the creation of long-distance virtual links, the next step in an entanglement distribution protocol is to take elementary links and to improve their fidelity using entanglement distillation and then to join them in order to create the virtual links (using, e.g., entanglement swapping). In this section, we explain how to model entanglement distillation protocols and joining protocols using LOCC channels. We refer to Appendix B 2 for a detailed explanation of LOCC channels. The explicit description of these protocols as LOCC channels is important because, as we saw in the previous section, the quantum state of an elementary link will not always be the ideal entangled state with respect to which joining protocols are typically defined. It is therefore important to understand how the protocols will act when the input states are not ideal.

A. Entanglement distillation

The term “entanglement distillation” refers to the task of taking many copies of a given quantum state ρ_{AB} and transforming them, via an LOCC protocol, to several (fewer) copies of the maximally entangled state $\Phi_{AB} := \frac{1}{d} \sum_{i,j=0}^{d-1} |i, i\rangle \langle j, j|$. Typically, with only a finite number of copies of the initial state ρ_{AB} , it is not possible to perfectly obtain copies of the maximally entangled state, so we aim instead for a state σ_{AB} whose fidelity $F(\Phi_{AB}, \sigma_{AB})$ to the maximally entangled state is higher than the fidelity $F(\Phi_{AB}, \rho_{AB})$ of the initial state. Mathematically, the task of entanglement distillation corresponds to the transformation

$$\rho_{AB}^{\otimes n} \mapsto \mathcal{L}_{A^n B^n \rightarrow A^m B^m}(\rho_{AB}^{\otimes n}) = \sigma_{AB}^{\otimes m}, \quad (40)$$

where $n, m \in \mathbb{N}$, $m < n$, and $\mathcal{L}_{A^n B^n \rightarrow A^m B^m}$ is an LOCC channel.

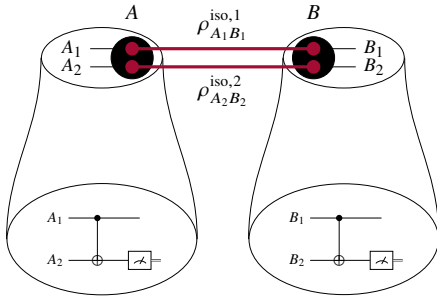


FIG. 4. Depiction of the simple entanglement distillation protocol from Ref. [36]. The protocol takes two isotropic states $\rho_{A_j B_j}^{\text{iso},j}$, $j \in \{1, 2\}$ (see (45)), and transforms them probabilistically to a state with higher fidelity.

Typically, in practice, we have $n = 2$ and $m = 1$, with the task being to transform two two-qubit states $\rho_{A_1 B_1}^1$ and $\rho_{A_2 B_2}^2$ to a two-qubit state $\sigma_{A_1 B_1}$ having a higher fidelity to the maximally entangled state than the initial states. Protocols achieving this aim are typically probabilistic in practice, meaning that the state $\sigma_{A_1 B_1}$ with higher fidelity is obtained only with some non-unit probability.

We are not concerned with any particular entanglement distillation protocol in this work. All we are concerned with is their mathematical structure. In particular, entanglement distillation protocols that are probabilistic can be described mathematically as an LOCC instrument, which we now demonstrate with a simple example, depicted in Fig. 4, which comes from Ref. [36]. In this protocol, Alice and Bob first apply the CNOT gate to their qubits and follow it with a measurement of their second qubit in the standard basis. They then communicate the results of their measurement to each other. The protocol is considered successful if they both obtain the same outcome, and a failure otherwise. This protocol has the following corresponding LOCC instrument channel:

$$\begin{aligned} & \mathcal{L}_{A_1 A_2 B_1 B_2 \rightarrow A_1 B_1} \left(\rho_{A_1 B_1}^1 \otimes \rho_{A_2 B_2}^2 \right) \\ &= |0\rangle\langle 0| \otimes \left((K_A^0 \otimes K_B^1) (\rho_{A_1 B_1}^{\text{iso},1} \otimes \rho_{A_2 B_2}^{\text{iso},2}) (K_A^0 \otimes K_B^1)^\dagger \right. \\ & \quad \left. + (K_A^1 \otimes K_B^0) (\rho_{A_1 B_1}^{\text{iso},1} \otimes \rho_{A_2 B_2}^{\text{iso},2}) (K_A^1 \otimes K_B^0)^\dagger \right) \\ & \quad + |1\rangle\langle 1| \otimes \left((K_A^0 \otimes K_B^0) (\rho_{A_1 B_1}^{\text{iso},1} \otimes \rho_{A_2 B_2}^{\text{iso},2}) (K_A^0 \otimes K_B^0)^\dagger \right. \\ & \quad \left. + (K_A^1 \otimes K_B^1) (\rho_{A_1 B_1}^{\text{iso},1} \otimes \rho_{A_2 B_2}^{\text{iso},2}) (K_A^1 \otimes K_B^1)^\dagger \right), \quad (41) \end{aligned}$$

where

$$K_A^x \equiv K_{A_1 A_2 \rightarrow A_1}^x := \langle x |_{A_2} \text{CNOT}_{A_1 A_2} \quad \forall x \in \{0, 1\}, \quad (42)$$

$$K_B^x \equiv K_{B_1 B_2 \rightarrow B_1}^x := \langle x |_{B_2} \text{CNOT}_{B_1 B_2} \quad \forall x \in \{0, 1\}. \quad (43)$$

Furthermore, the states $\rho_{A_j B_j}^{\text{iso},j}$, $j \in \{1, 2\}$, are defined as

$$\rho_{A_j B_j}^{\text{iso},j} := \mathcal{T}_{A_j B_j}^U (\rho_{A_j B_j}^j) \quad (44)$$

$$:= \int_U \left(U_{A_j} \otimes \overline{U}_{B_j} \right) (\rho_{A_j B_j}^j) \left(U_{A_j} \otimes \overline{U}_{B_j} \right)^\dagger, \quad (45)$$

where \mathcal{T}^U is the *isotropic twirling channel*; see, e.g., Ref. [110, Example 7.25].

It is a straightforward calculation to show that if $f_1 = \langle \Phi | \rho_{A_1 B_1}^1 | \Phi \rangle$ and $f_2 = \langle \Phi | \rho_{A_2 B_2}^2 | \Phi \rangle$ are the fidelities of the initial states with the maximally entangled state, then the protocol depicted in Fig. 4, with corresponding LOCC channel given by (41), succeeds with probability

$$p_{\text{succ}} = \frac{8}{9} f_1 f_2 - \frac{2}{9} (f_1 + f_2) + \frac{5}{9}, \quad (46)$$

and the fidelity of the output state $\sigma_{A_1 B_1}$ with the maximally entangled state (conditioned on success) is

$$\langle \Phi | \sigma_{A_1 B_1} | \Phi \rangle = \frac{1}{p_{\text{succ}}} \left(\frac{10}{9} f_1 f_2 - \frac{1}{9} (f_1 + f_2) + \frac{1}{9} \right). \quad (47)$$

The above example illustrates a general principle, which is that entanglement distillation protocols that are probabilistic (and heralded) can be described using LOCC instrument channels. Specifically, let $G = (V, E)$ be the graph corresponding to the physical links in a quantum network. Given an element $e \in E$ with n parallel edges e^1, e^2, \dots, e^n , every probabilistic entanglement distillation protocol has the form of an LOCC instrument channel of the following form:

$$\begin{aligned} \mathcal{D}_{e^1 \dots e^n \rightarrow e^1 \dots e^n}^e (\cdot) &= |0\rangle\langle 0| \otimes \mathcal{D}_{e^1 \dots e^n \rightarrow e^1 \dots e^n}^{e;0} (\cdot) \\ &+ |1\rangle\langle 1| \otimes \mathcal{D}_{e^1 \dots e^n \rightarrow e^1 \dots e^n}^{e;1} (\cdot), \quad (48) \end{aligned}$$

where $\mathcal{D}_{e^1 \dots e^n \rightarrow e^1 \dots e^n}^{e;0}$ and $\mathcal{D}_{e^1 \dots e^n \rightarrow e^1 \dots e^n}^{e;1}$ are completely positive trace non-increasing LOCC maps such that $\mathcal{D}_{e^1 \dots e^n \rightarrow e^1 \dots e^n}^{e;0} + \mathcal{D}_{e^1 \dots e^n \rightarrow e^1 \dots e^n}^{e;1}$ is a trace-preserving map, and thus an LOCC quantum channel. Specifically, $\mathcal{D}_{e^1 \dots e^n \rightarrow e^1 \dots e^n}^{e;0}$ corresponds to failure of the protocol and $\mathcal{D}_{e^1 \dots e^n \rightarrow e^1 \dots e^n}^{e;1}$ corresponds to success of the protocol.

B. Joining protocols

Let us now discuss joining protocols, such as entanglement swapping. We can describe such protocols using LOCC instrument channels, just as with entanglement distillation protocols. As above, let $G = (V, E)$ be the graph corresponding to the physical links in a quantum network. A path in a graph is a sequence $w = (v_1, e_1, v_2, e_2, \dots, e_{n-1}, v_n)$ of vertices and edges that specifies how to get from the vertex v_1 to the vertex v_n . Given a path w of active elementary links in the network, the joining channel $\mathcal{L}_{w \rightarrow e'}$ that forms the new virtual link e' is given in the probabilistic setting by

$$\mathcal{L}_{w \rightarrow e'} (\cdot) = |0\rangle\langle 0| \otimes \mathcal{L}_{w \rightarrow e'}^0 (\cdot) + |1\rangle\langle 1| \otimes \mathcal{L}_{w \rightarrow e'}^1 (\cdot), \quad (49)$$

where $\mathcal{L}_{w \rightarrow e'}^0$ and $\mathcal{L}_{w \rightarrow e'}^1$ are completely positive trace non-increasing LOCC maps such that $\mathcal{L}_{w \rightarrow e'}^0 + \mathcal{L}_{w \rightarrow e'}^1$ is a trace-preserving map, and thus an LOCC quantum channel. Specifically, $\mathcal{L}_{w \rightarrow e'}^0$ corresponds to failure of the joining protocol and $\mathcal{L}_{w \rightarrow e'}^1$ corresponds to success of the joining protocol. Given

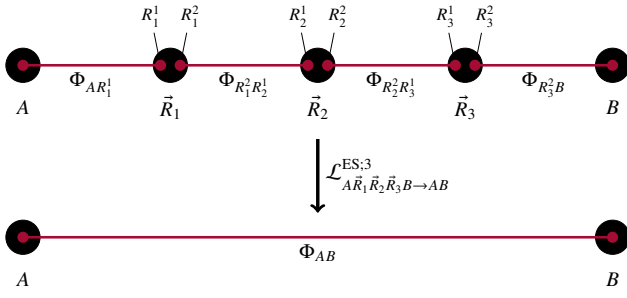


FIG. 5. A chain of five nodes corresponding to the entanglement swapping protocol with $n = 3$ intermediate nodes. The red lines represent maximally entangled states. The goal of the entanglement swapping protocol is to establish entanglement between A and B . The protocol proceeds by first performing a Bell-basis measurement on the systems at the nodes \vec{R}_j , $1 \leq j \leq n$, and communicating the results of the measurement to B , who applies a correction operation based on the outcomes.

an input state ρ_w corresponding to the given path w , the success probability of the joining protocol is $p_{\text{succ}} = \text{Tr}[\mathcal{L}_{w \rightarrow e'}^1(\rho_w)]$, and the state conditioned on success is

$$\frac{1}{p_{\text{succ}}} \mathcal{L}_{w \rightarrow e'}^1(\rho_w). \quad (50)$$

Note that as input states to the maps $\mathcal{L}_{w \rightarrow e'}^0$ and $\mathcal{L}_{w \rightarrow e'}^1$ we could have arbitrary states of the elementary links along the path w . In particular, depending on the elementary link policy, they could be states of the form (15), which take into account the noise in the quantum memories and other device imperfections arising during the process of generating the elementary links.

The precise joining protocol, and thus the explicit form for the maps $\mathcal{L}_{w \rightarrow e'}^0$ and $\mathcal{L}_{w \rightarrow e'}^1$, depends on the type of entanglement that is to be created. For bipartite entanglement, we consider entanglement swapping in Sec. III B 1. For tripartite GHZ entanglement, we describe a protocol in Sec. III B 2, and for multipartite graph states we describe a protocol in Sec. III B 3.

1. Entanglement swapping protocol

Let $\rho_{A\vec{R}_1\vec{R}_2\cdots\vec{R}_nB}$ be a multipartite quantum state, where $n \geq 1$ and $\vec{R}_j \equiv R_j^1 R_j^2$ is an abbreviation for two the quantum systems R_j^1 and R_j^2 . The entanglement swapping protocol with n intermediate nodes is defined by a Bell-basis measurement of the systems \vec{R}_j , i.e., a measurement described by the POVM $\{\Phi^{z,x} : z, x \in [d]\}$, where $[d] = \{0, 1, \dots, d-1\}$, $\Phi^{z,x} = |\Phi^{z,x}\rangle\langle\Phi^{z,x}|$, and

$$|\Phi^{z,x}\rangle := (Z^z X^x \otimes \mathbb{1})|\Phi\rangle \quad (51)$$

are the qudit Bell state vectors, with

$$|\Phi\rangle := \frac{1}{\sqrt{d}} \sum_{k=0}^{d-1} |k, k\rangle. \quad (52)$$

The operators Z and X are the discrete Weyl operators¹¹⁰, which are defined as

$$Z := \sum_{k=0}^{d-1} e^{\frac{2\pi i k}{d}} |k\rangle\langle k|, \quad X := \sum_{k=0}^{d-1} |k+1\rangle\langle k|. \quad (53)$$

Conditioned on the outcomes (z_j, x_j) of the Bell measurement on \vec{R}_j , the unitary $Z_B^{z_1+\dots+z_n} X_B^{x_1+\dots+x_n}$ is applied to the system B , where the addition is performed modulo d . Let $\vec{z}, \vec{x} \in [d]^{n \times n}$, and define

$$M_{\vec{R}_1\vec{R}_2\cdots\vec{R}_n}^{\vec{z},\vec{x}} := \Phi_{\vec{R}_1}^{z_1,x_1} \otimes \Phi_{\vec{R}_2}^{z_2,x_2} \otimes \cdots \otimes \Phi_{\vec{R}_n}^{z_n,x_n}, \quad (54)$$

$$W_B^{\vec{z},\vec{x}} := Z_B^{z_1+\dots+z_n} X_B^{x_1+\dots+x_n}, \quad (55)$$

where the addition in the second line is performed modulo d . Then, the LOCC quantum channel corresponding to the entanglement swapping protocol with $n \geq 1$ intermediate nodes is

$$\begin{aligned} \mathcal{L}_{A\vec{R}_1\cdots\vec{R}_nB\rightarrow AB}^{\text{ES};n} & \left(\rho_{A\vec{R}_1\cdots\vec{R}_nB} \right) \\ & := \sum_{\vec{z}, \vec{x} \in [d]^{n \times n}} \text{Tr}_{\vec{R}_1\cdots\vec{R}_n} \left[M_{\vec{R}_1\cdots\vec{R}_n}^{\vec{z},\vec{x}} W_B^{\vec{z},\vec{x}} \right. \\ & \quad \left. \left(\rho_{A\vec{R}_1\cdots\vec{R}_nB} \right) \left(W_B^{\vec{z},\vec{x}} \right)^\dagger \right]. \end{aligned} \quad (56)$$

The standard entanglement swapping protocol³⁹ corresponds to the input state

$$\rho_{A\vec{R}_1\vec{R}_2\cdots\vec{R}_nB} = \Phi_{AR_1^1} \otimes \Phi_{R_1^2 R_2^1} \otimes \cdots \otimes \Phi_{R_{n-1}^2 R_n^1} \otimes \Phi_{R_n^2 B}. \quad (57)$$

This scenario is shown in Fig. 5. Indeed, it can be shown that

$$\begin{aligned} \mathcal{L}_{A\vec{R}_1\cdots\vec{R}_nB\rightarrow AB}^{\text{ES};n} & \left(\Phi_{AR_1^1} \otimes \Phi_{R_1^2 R_2^1} \otimes \cdots \right. \\ & \quad \left. \otimes \Phi_{R_{n-1}^2 R_n^1} \otimes \Phi_{R_n^2 B} \right) = \Phi_{AB}. \end{aligned} \quad (58)$$

Furthermore, the standard teleportation protocol¹² corresponds to $n = 1$ and the input state

$$\rho_{A\vec{R}_1B} = \sigma_{R_1^1} \otimes \Phi_{R_1^2 B}, \quad (59)$$

where $A = \emptyset$ is a trivial (one-dimensional) system and $\sigma_{R_1^1}$ is an arbitrary d -dimensional quantum state, so that

$$\mathcal{L}_{\vec{R}_1\rightarrow B}^{\text{ES};1} (\sigma_{R_1^1} \otimes \Phi_{R_1^2 B}) = \sigma_B, \quad (60)$$

as expected.

Proposition III.1 (Fidelity after entanglement swapping). For all $n \geq 1$ and all states $\rho_{AR_1^1}^1, \rho_{R_1^2 R_2^1}^2, \dots, \rho_{R_n^2 B}^{n+1}$, the fidelity of the maximally entangled state with the state after entanglement swapping of $\rho_{AR_1^1}^1, \rho_{R_1^2 R_2^1}^2, \dots, \rho_{R_n^2 B}^{n+1}$ is given by

$$\langle \Phi |_{AB} \mathcal{L}_{A\vec{R}_1\cdots\vec{R}_nB\rightarrow AB}^{\text{ES};n} \left(\rho_{AR_1^1}^1 \otimes \rho_{R_1^2 R_2^1}^2 \otimes \cdots \otimes \rho_{R_n^2 B}^{n+1} \right) | \Phi \rangle_{AB}$$

$$= \sum_{\vec{z}, \vec{x} \in [d]^{\times n}}^{d-1} \langle \Phi^{z', x'} | \rho_{AR_1^1}^1 | \Phi^{z', x'} \rangle \langle \Phi^{z_1, x_1} | \rho_{R_1^2 R_2^1}^2 | \Phi^{z_1, x_1} \rangle \cdots \langle \Phi^{z_n, x_n} | \rho_{R_n^2 B}^{n+1} | \Phi^{z_n, x_n} \rangle, \quad (61)$$

where $z' = -z_1 - z_2 - \cdots - z_n$ and $x' = -x_1 - x_2 - \cdots - x_n$.

Proof. See Appendix H 1. \square

2. GHZ entanglement swapping protocol

The previous example takes a chain of Bell states and transforms them into a Bell state shared by the end nodes of the chain. In this example, we look at a protocol that takes the same chain of Bell states and transforms them instead to a multi-qubit GHZ state, which is defined as¹¹

$$|\text{GHZ}_n\rangle := \frac{1}{\sqrt{2}}(|0\rangle^{\otimes n} + |1\rangle^{\otimes n}). \quad (62)$$

We call this protocol the *GHZ entanglement swapping protocol*.

The protocol for transforming a chain of two Bell states to a three-party GHZ state is shown in Fig. 6. First, the two qubits R_1^1 and R_1^2 in the central node are entangled with a CNOT gate, followed by a measurement of R_1^2 in the standard basis (with corresponding POVM $\{|0\rangle\langle 0|, |1\rangle\langle 1|\}$). The result $x \in \{0, 1\}$ is communicated to B , where the correction operation X_B^x is applied. The LOCC channel corresponding to this protocol is

$$\begin{aligned} \mathcal{L}_{A\vec{R}_1 B}^{\text{GHZ};1}(\rho_{A\vec{R}_1 B}) &= \sum_{x=0}^1 \left(K_{\vec{R}_1}^x \otimes X_B^x \right) \rho_{A\vec{R}_1 B} \left(K_{\vec{R}_1}^x \otimes X_B^x \right)^\dagger, \quad (63) \end{aligned}$$

where

$$K_{\vec{R}_1}^x := \langle x |_{R_1^2} \text{CNOT}_{\vec{R}_1}, \quad (64)$$

$$\text{CNOT}_{\vec{R}_1} := |0\rangle\langle 0|_{R_1^1} \otimes \mathbb{I}_{R_1^2} + |1\rangle\langle 1|_{R_1^1} \otimes X_{R_1^2}. \quad (65)$$

The protocol shown in Fig. 6, with corresponding LOCC quantum channel in (63), can be easily extended to a scenario with $n > 1$ intermediate nodes. In this case, the node \vec{R}_1 starts by applying the gate $\text{CNOT}_{\vec{R}_1}$ to its qubits and then measuring the qubit R_1^2 in the standard basis. The outcome of this measurement is sent to the node \vec{R}_2 , and the corresponding correction operation is applied to the qubit R_2^1 . Then, the gate $\text{CNOT}_{\vec{R}_2}$ is applied to the qubits at \vec{R}_2 , followed by a standard-basis measurement of R_2^2 and communication of the outcome to \vec{R}_3 and a correction operation on R_3^1 . This proceeds in sequence until the n^{th} intermediate node \vec{R}_n , which sends its measurement outcome to B , which applies the appropriate correction operation. The LOCC channel for this protocol is

$$\mathcal{L}_{A\vec{R}_1 \cdots \vec{R}_n B \rightarrow A\vec{R}_1^1 \cdots \vec{R}_n^1 B}^{\text{GHZ};n}(\rho_{A\vec{R}_1 \cdots \vec{R}_n B})$$

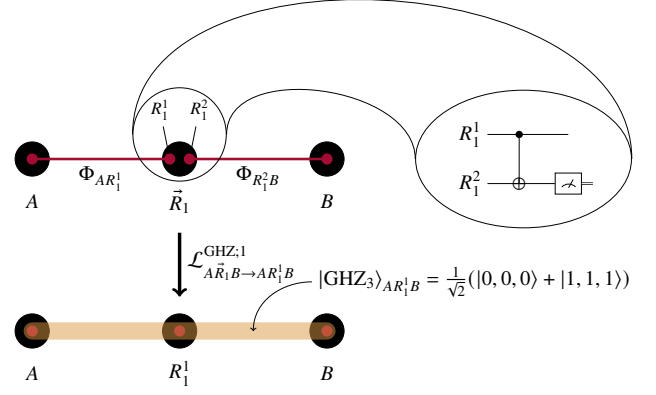


FIG. 6. The GHZ entanglement swapping protocol with one intermediate node. The two qubits in the central node are entangled using the CNOT gate, after which the qubit R_1^2 is measured in the standard basis. The result $x \in \{0, 1\}$ of the measurement is communicated to B , where the gate X_B^x is applied.

$$:= \sum_{\vec{x} \in \{0, 1\}^n} P_{\vec{R}_1 \cdots \vec{R}_n B}^{\vec{x}} \left(\rho_{A\vec{R}_1 \cdots \vec{R}_n B} \right) P_{\vec{R}_1 \cdots \vec{R}_n B}^{\vec{x} \dagger}, \quad (66)$$

where

$$P_{\vec{R}_1 \cdots \vec{R}_n B}^{\vec{x}} := K_{\vec{R}_1}^{x_1} \otimes K_{\vec{R}_2}^{x_2} X_{R_2^1}^{x_1} \otimes \cdots \otimes K_{\vec{R}_n}^{x_n} X_{R_n^1}^{x_{n-1}} \otimes X_B^{x_n} \quad (67)$$

for all $\vec{x} \in \{0, 1\}^n$. If the input state to this channel is

$$\rho_{A\vec{R}_1 \cdots \vec{R}_n B} = \Phi_{AR_1^1} \otimes \Phi_{R_2^1 R_2^1} \otimes \cdots \otimes \Phi_{R_{n-1}^1 R_n^1} \otimes \Phi_{R_n^2 B}, \quad (68)$$

then the output is a $(n+2)$ -party GHZ state given by the state vector $|\text{GHZ}_{n+2}\rangle_{AR_1^1 \cdots R_n^1 B}$ as defined in (62), i.e.,

$$\begin{aligned} \mathcal{L}_{A\vec{R}_1 \cdots \vec{R}_n B \rightarrow A\vec{R}_1^1 \cdots \vec{R}_n^1 B}^{\text{GHZ};n} \left(\Phi_{AR_1^1} \otimes \Phi_{R_2^1 R_2^1} \otimes \cdots \otimes \Phi_{R_{n-1}^1 R_n^1} \otimes \Phi_{R_n^2 B} \right) &= |\text{GHZ}_{n+2}\rangle \langle \text{GHZ}_{n+2}|. \quad (69) \end{aligned}$$

Proposition III.2 (Fidelity after GHZ entanglement swapping). For all $n \geq 1$, and for all states $\rho_{AR_1^1}^1, \rho_{R_2^1 R_2^1}^2, \dots, \rho_{R_n^2 B}^{n+1}$, the fidelity of the $(n+2)$ -party GHZ state with the state after the GHZ entanglement swapping of $\rho_{AR_1^1}^1, \rho_{R_2^1 R_2^1}^2, \dots, \rho_{R_n^2 B}^{n+1}$ is

$$\begin{aligned} &\langle \text{GHZ}_{n+2} | \mathcal{L}_{A\vec{R}_1 \cdots \vec{R}_n B \rightarrow A\vec{R}_1^1 \cdots \vec{R}_n^1 B}^{\text{GHZ};n} \left(\rho_{AR_1^1}^1 \otimes \right. \\ &\quad \left. \rho_{R_2^1 R_2^1}^2 \otimes \cdots \otimes \rho_{R_n^2 B}^{n+1} \right) | \text{GHZ}_{n+2} \rangle \\ &= \sum_{z_1, \dots, z_n=0}^1 \langle \Phi^{z_1+ \cdots + z_n, 0} | \rho_{AR_1^1} | \Phi^{z_1+ \cdots + z_n, 0} \rangle \\ &\quad \langle \Phi^{z_1, 0} | \rho_{R_2^1 R_2^1}^2 | \Phi^{z_1, 0} \rangle \cdots \langle \Phi^{z_n, 0} | \rho_{R_n^2 B}^{n+1} | \Phi^{z_n, 0} \rangle. \quad (70) \end{aligned}$$

Proof. See Appendix H 2. \square

3. Graph state distribution protocol

We now consider an example of distributing an arbitrary graph state, which can be viewed as a special case of the

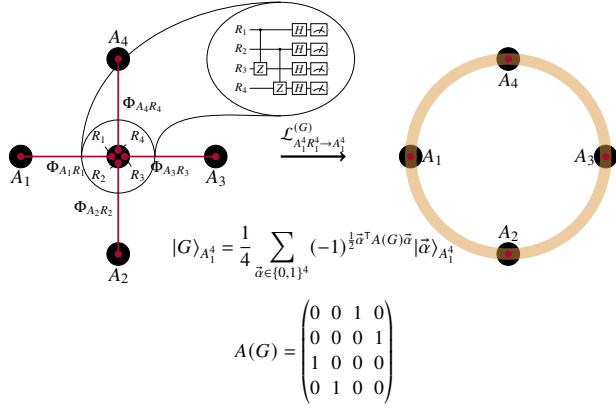


FIG. 7. Depiction of a protocol for distributing a graph state among four nodes A_1, A_2, A_3, A_4 , all of which initially share Bell states with the central node.

procedure considered in Ref. [73]. A graph state^{112–114} is a multi-qubit quantum state defined using graphs.

Consider a graph $G = (V, E)$, which consists of a set V of vertices and a set E of edges. For the purposes of this example, G is an undirected graph, and E is a set of two-element subsets of V . The graph state $|G\rangle$ is an n -qubit quantum state $|G\rangle_{A_1 \dots A_n}$, with $n = |V|$, that is defined as

$$|G\rangle_{A_1 \dots A_n} := \frac{1}{\sqrt{2^n}} \sum_{\vec{\alpha} \in \{0,1\}^n} (-1)^{\frac{1}{2} \vec{\alpha}^T A(G) \vec{\alpha}} |\vec{\alpha}\rangle, \quad (71)$$

where $A(G)$ is the adjacency matrix of G , which is defined as

$$A(G)_{i,j} = \begin{cases} 1 & \text{if } \{v_i, v_j\} \in E, \\ 0 & \text{otherwise,} \end{cases} \quad (72)$$

and $\vec{\alpha}$ is the column vector $(\alpha_1, \dots, \alpha_n)^\top$. It is easy to show that

$$|G\rangle_{A_1 \dots A_n} = \text{CZ}(G)(|+\rangle_{A_1} \otimes \dots \otimes |+\rangle_{A_n}), \quad (73)$$

where $|+\rangle := \frac{1}{\sqrt{2}}(|0\rangle + |1\rangle)$ and

$$\text{CZ}(G) := \bigotimes_{\{v_i, v_j\} \in E} \text{CZ}_{A_i A_j}, \quad (74)$$

with $\text{CZ}_{A_i A_j} := |0\rangle\langle 0|_{A_i} \otimes \mathbb{1}_{A_j} + |1\rangle\langle 1|_{A_i} \otimes Z_{A_j}$ being the controlled-Z gate.

Now, consider the scenario depicted in Fig. 7, in which $n = 4$ nodes share Bell states with a central node. The task is for the central node to distribute the graph state $|G\rangle$ to the outer nodes. One possible procedure is for the central node to locally prepare the graph state and then to teleport the individual qubits using the Bell states. However, it is possible to perform a slightly simpler procedure that does not require the additional qubits needed to prepare the graph state locally. In fact, the following deterministic procedure produces the required graph state $|G\rangle$ shared by the nodes A_1, \dots, A_n .

1. The central node applies $\text{CZ}(G)$ to the qubits R_1, \dots, R_n .

2. On each of the qubits R_1, \dots, R_n , the central node performs the measurement defined by the POVM $\{|+\rangle\langle +|, |-\rangle\langle -|\}$, where $|\pm\rangle = \frac{1}{\sqrt{2}}(|0\rangle \pm |1\rangle)$. The outcome is an n -bit string $\vec{x} = (x_1, \dots, x_n)$, where $x_i = 0$ corresponds to the “+” outcome and $x_i = 1$ corresponds to the “-” outcome. The central node communicates outcome x_i to the node A_i .
3. The nodes A_i apply Z^{x_i} to their qubit. In other words, if $x_i = 0$, then A_i does nothing, and if $x_i = 1$, then A_i applies Z to their qubit.

Let us prove that this protocol achieves the desired outcome. First, observe that

$$\begin{aligned} |\Phi\rangle_{A_1 R_1} \otimes \dots \otimes |\Phi\rangle_{A_n R_n} \\ = \frac{1}{\sqrt{2^n}} \sum_{\vec{\alpha} \in \{0,1\}^n} |\vec{\alpha}\rangle_{A_1 \dots A_n} |\vec{\alpha}\rangle_{R_1 \dots R_n}. \end{aligned} \quad (75)$$

Then, after the first step, the state is

$$\begin{aligned} \frac{1}{\sqrt{2^n}} \sum_{\vec{\alpha} \in \{0,1\}^n} |\vec{\alpha}\rangle_{A_1 \dots A_n} \text{CZ}(G) |\vec{\alpha}\rangle_{R_1 \dots R_n} \\ = \frac{1}{\sqrt{2^n}} \sum_{\vec{\alpha} \in \{0,1\}^n} (-1)^{\frac{1}{2} \vec{\alpha}^T A(G) \vec{\alpha}} |\vec{\alpha}\rangle_{A_1 \dots A_n} |\vec{\alpha}\rangle_{R_1 \dots R_n}, \end{aligned} \quad (76)$$

where we have used the fact that

$$\text{CZ}(G) |\vec{\alpha}\rangle = (-1)^{\sum_{i,j: \{v_i, v_j\} \in E} \alpha_i \alpha_j} |\vec{\alpha}\rangle \quad (77)$$

$$= (-1)^{\frac{1}{2} \vec{\alpha}^T A(G) \vec{\alpha}} |\vec{\alpha}\rangle. \quad (78)$$

Then, we find that for every outcome string (x_1, \dots, x_n) of the measurement on the qubits R_1, \dots, R_n the corresponding (unnormalized) post-measurement state is

$$\frac{1}{2^n} \sum_{\vec{\alpha} \in \{0,1\}^n} (-1)^{\frac{1}{2} \vec{\alpha}^T A(G) \vec{\alpha}} (-1)^{\alpha_1 x_1 + \dots + \alpha_n x_n} |\vec{\alpha}\rangle_{A_1 \dots A_n}. \quad (79)$$

Then, using the fact that $Z^x |\alpha\rangle = (-1)^{\alpha x} |\alpha\rangle$ for all $x, \alpha \in \{0, 1\}$, we find that at the end of the second step the (unnormalized) state is

$$\begin{aligned} \frac{1}{2^n} (Z_{A_1}^{x_1} \otimes \dots \otimes Z_{A_n}^{x_n}) \sum_{\vec{\alpha} \in \{0,1\}^n} (-1)^{\frac{1}{2} \vec{\alpha}^T A(G) \vec{\alpha}} |\vec{\alpha}\rangle_{A_1 \dots A_n} \\ = \frac{1}{\sqrt{2^n}} (Z_{A_1}^{x_1} \otimes \dots \otimes Z_{A_n}^{x_n}) |G\rangle_{A_1 \dots A_n} \end{aligned} \quad (80)$$

for all $(x_1, \dots, x_n) \in \{0, 1\}^n$. From this, we see that, up to local Pauli- z corrections, the post-measurement state is equal to the desired graph state $|G\rangle$ with probability $\frac{1}{2^n}$ for every measurement outcome string (x_1, \dots, x_n) . Once all of the nodes A_i receive their corresponding outcome x_i and apply the correction $Z_{A_i}^{x_i}$, the nodes A_1, \dots, A_n share the graph state $|G\rangle$. As a result of the classical communication of the measurement outcomes and the subsequent correction operations, the protocol is deterministic.

The protocol described above has the following representation as an LOCC channel:

$$\begin{aligned} \mathcal{L}_{A_1^n R_1^n \rightarrow A_1^n}^{(G)} & \left(\rho_{A_1^n R_1^n} \right) \\ & := \sum_{\vec{x} \in \{0,1\}^n} \left(Z_{A_1^n}^{\vec{x}} \otimes \langle \vec{x} |_{R_1^n} H^{\otimes n} \text{CZ}(G)_{R_1^n} \right) \left(\rho_{A_1^n R_1^n} \right) \\ & \quad \left(Z_{A_1^n}^{\vec{x}} \otimes \text{CZ}(G)_{R_1^n}^\dagger H^{\otimes n} | \vec{x} \rangle_{R_1^n} \right), \quad (81) \end{aligned}$$

for every state $\rho_{A_1^n R_1^n}$, where $H = |+\rangle\langle 0| + |-\rangle\langle 1|$ is the Hadamard operator, and we have let

$$Z_{A_1 \dots A_n}^{\vec{x}} := Z_{A_1}^{x_1} \otimes \dots \otimes Z_{A_n}^{x_n}. \quad (82)$$

We have also used the abbreviation $A_1^n \equiv A_1 A_2 \dots A_n$, and similarly for R_1^n . Using the fact that

$$\text{CZ}(G) H^{\otimes n} | \vec{x} \rangle = Z^{\vec{x}} | G \rangle \quad (83)$$

for all $\vec{x} \in \{0,1\}^n$, and letting

$$|G^{\vec{x}}\rangle := Z^{\vec{x}} |G\rangle, \quad (84)$$

we can write the channel in the following simpler form:

$$\begin{aligned} \mathcal{L}_{A_1^n R_1^n \rightarrow A_1^n}^{(G)} & \left(\rho_{A_1^n R_1^n} \right) \\ & = \sum_{\vec{x} \in \{0,1\}^n} \left(Z_{A_1^n}^{\vec{x}} \otimes \langle G^{\vec{x}} |_{R_1^n} \right) \left(\rho_{A_1^n R_1^n} \right) \left(Z_{A_1^n}^{\vec{x}} \otimes |G^{\vec{x}}\rangle_{R_1^n} \right). \quad (85) \end{aligned}$$

From this, we see that the protocol can be thought of as measuring the systems R_1, \dots, R_n according to the POVM $\{|G^{\vec{x}}\rangle\langle G^{\vec{x}}|\}_{\vec{x} \in \{0,1\}^n}$ and, conditioned on the outcome \vec{x} , applying the correction operation $Z^{\vec{x}}$ to the systems A_1, \dots, A_n . Note that $\{|G^{\vec{x}}\rangle\langle G^{\vec{x}}|\}_{\vec{x} \in \{0,1\}^n}$ is indeed a POVM due to the fact that

$$|G^{\vec{x}}\rangle = \text{CZ}(G) H^{\otimes n} | \vec{x} \rangle \quad (86)$$

for all $\vec{x} \in \{0,1\}^n$, which follows from (83) and (84), so that

$$\begin{aligned} & \sum_{\vec{x} \in \{0,1\}^n} |G^{\vec{x}}\rangle\langle G^{\vec{x}}| \\ & = \text{CZ}(G) H^{\otimes n} \underbrace{\sum_{\vec{x} \in \{0,1\}^n} | \vec{x} \rangle\langle \vec{x} |}_{\mathbb{1}} H^{\otimes n} \text{CZ}(G)^\dagger = \mathbb{1}. \quad (87) \end{aligned}$$

Proposition III.3 (Fidelity after graph state distribution). For all $n \geq 2$, every graph G with n vertices, and all two-qubit states $\rho_{A_1 R_1}^1, \rho_{A_2 R_2}^2, \dots, \rho_{A_n R_n}^n$, the fidelity of the graph state $|G\rangle$ with the state after the graph state distribution protocol applied to $\rho_{A_1 R_1}^1, \rho_{A_2 R_2}^2, \dots, \rho_{A_n R_n}^n$ is

$$\langle G | \mathcal{L}_{A_1^n R_1^n \rightarrow A_1^n}^{(G)} \left(\rho_{A_1 R_1}^1 \otimes \dots \otimes \rho_{A_n R_n}^n \right) | G \rangle$$

$$= \sum_{\vec{x} \in \{0,1\}^n} \langle \Phi^{z_1, x_1} | \rho_{A_1 R_1}^1 | \Phi^{z_1, x_1} \rangle \langle \Phi^{z_2, x_2} | \rho_{A_2 R_2}^2 | \Phi^{z_2, x_2} \rangle \dots \langle \Phi^{z_n, x_n} | \rho_{A_n R_n}^n | \Phi^{z_n, x_n} \rangle, \quad (88)$$

where the column vector $\vec{z} = (z_1, \dots, z_n)^\top$ is given by $\vec{z} = A(G)\vec{x}$, with $A(G)$ the adjacency matrix of G .

Proof. See Appendix H 3. \square

IV. ANALYSIS OF A QUANTUM NETWORK PROTOCOL

In the previous two sections, we described in detail how to model elementary links in a quantum network using Markov decision processes. Then, we showed how to model entanglement distillation protocols and joining protocols (such as entanglement swapping) as LOCC channels. The upshot of these developments is that they give us a method for determining the quantum states of elementary and virtual links in a quantum network that depend explicitly on the underlying device parameters and noise processes that characterize the device, thereby allowing us to perform a more realistic analysis of entanglement distribution protocols, as we now show in this section.

In this section, we analyze a simple entanglement distribution protocol. Recall from Sec. I that entanglement distribution refers to the task of creating virtual links—entanglement between non-adjacent nodes—from elementary links, which are entangled states shared by adjacent (physically connected) nodes. An entanglement distribution protocol can be thought of as a graph transformation, as done in Refs. [115 and 116] and depicted in Fig. 1. Starting with the graph $G = (V, E)$ of physical links in the network, the goal is to realize a new graph $G_{\text{target}} = (V, E_{\text{target}})$ consisting of virtual links in addition to elementary links, such as the graph in the right-most panel of Fig. 1.

The protocol that we consider consists of two steps: generate elementary links, and then perform joining protocols based on the given target graph. The protocol is described more formally in Fig. 8. Starting with the graph $G = (V, E)$ of elementary links, all of the elementary links independently undergo policies π_e , with $e \in E$. After $t \geq 1$ time steps, an algorithm finds paths for creating the virtual links specified by the target graph G_{target} and the corresponding joining protocols are performed. If entire target network cannot be achieved in t time steps, then a decision is made to either conclude the protocol with the current configuration or to continue for another t time steps under the same policies.

Remark IV.1. Note that in the protocol described in Fig. 8, the virtual links are created only when all of the required elementary links are active. This is of course not the most general procedure, because it is in general possible to join some of the elementary links along a path while waiting for the others to become active. To handle such general procedures requires developing MDPs for systems of multiple elementary links. While this is the subject of ongoing future work, we provide an example of how to extend the elementary-link MDP framework

Quantum network protocol via Markov decision processes	
Given	
	<ul style="list-style-type: none"> • Graph $G = (V, E)$ of elementary links. • Source states ρ_e^S, transmission channels S_e, and heralding instruments $\{\mathcal{M}_e^0, \mathcal{M}_e^1\}$ for every edge $e \in E$. • Time $t \geq 1$. • A policy π_e for every edge $e \in E$.
Required	
	<p>A target graph $G_{\text{target}} = (V, E_{\text{target}})$, with corresponding target states ρ_e^{target} and fidelity thresholds for every edge $e \in E_{\text{target}}$.</p>
Protocol	
	<ol style="list-style-type: none"> 1. Every elementary link corresponding to $e \in E$ follows the policy π_e for t time steps. 2. Given the configuration of active elementary links at the end of t time steps, an algorithm determines paths for forming the virtual links specified by E_{target}, and the corresponding joining protocols are performed. 3. If the required target graph and fidelity thresholds are reached, then STOP; otherwise, decide: <ol style="list-style-type: none"> (a) STOP; or (b) CONTINUE: repeat Steps 1–3.

FIG. 8. Outline of a quantum network protocol based on Markov decision processes. Every elementary link in the network follows a policy for $t \geq 1$ time steps. At the end of the t time steps, the appropriate paths in the network are found and the corresponding joining protocols are performed in order to achieve the network corresponding to the target graph G_{target} .

of Sec. II to a system of two elementary links, in which entanglement swapping is included, in Sec. V. We also note that the protocol in Fig. 8 uses fixed routing and path-finding algorithms from Refs. [115–117]. It is possible, in principle, to develop an MDP that takes into account routing. Doing so would allow us to obtain protocols that simultaneously optimize the actions of the elementary links, the joining operations, and the actions corresponding to routing, either directly using dynamic programming algorithms such as the one in Theorem II.1, or through reinforcement learning. These possibilities, and other possibilities for developing more sophisticated protocols using MDPs, are interesting directions for future work.

A. Fidelity

In order to quantify the performance of the protocol described in Fig. 8, it is natural to ask what the fidelity of the resulting states of the elementary and virtual links are to prescribed target states. Thus, let us begin by showing, in general terms, how we could calculate the fidelity after t time steps of our protocol.

First, we note that all of the elementary links are independent of each other. This is due to the fact that we assume that every node has a separate quantum system for every one of the elementary links associated to that node. Furthermore, we assume that every elementary link undergoes its own policy independent of the other elementary links. Therefore, after t

time steps the quantum state of the network is

$$\rho_G^{\vec{\pi}}(t) = \bigotimes_{e \in E} \rho_e^{\pi_e}(t), \quad (89)$$

where $\vec{\pi} = \{\pi_e : e \in E\}$ is a collection of policies for the individual elementary links, and every state $\rho_e^{\pi_e}(t)$ is given by (15), namely,

$$\rho_e^{\pi_e}(t) = \sum_{h^t} \Pr[H_e(t) = h^t]_{\pi_e} |h^t\rangle\langle h^t| \otimes \sigma_e(t|h^t). \quad (90)$$

Recall from (14) that $\Pr[H_e(t) = h^t]_{\pi_e}$ is the probability of the history h^t with respect to the policy π_e , and $\sigma_e(t|h^t)$ is the quantum state of the elementary link conditioned on the history h^t , given by (16).

The state in (90) is a classical-quantum state that contains both classical information about the history of elementary link as well as the quantum state of the elementary link conditioned on every history. If we condition on an elementary link corresponding to $e \in E$ being active at time t , then the expected quantum state of the elementary link at time t is⁵⁸

$$\bar{\rho}_e^{\pi_e}(t) := \frac{1}{X_e^{\pi_e}(t)} \sum_{h^t: m_t \neq -1} \Pr[H_e(t) = h^t]_{\pi_e} \sigma_e(t|h^t). \quad (91)$$

From these states, we can calculate the quantum states of the virtual links in the target graph that are created via joining protocols. In general, the states are of the form (50). As a concrete example, let us consider the usual entanglement swapping protocol from Sec. III B 1. Let $w = (v_1, e_1, v_2, e_2, \dots, e_n, v_{n+1})$ be a path between two non-neighbouring nodes v_1 and v_{n+1} , such that the entanglement swapping protocol along this path creates the virtual link given by the edge $\{v_1, v_{n+1}\}$. The quantum state at the input of the entanglement swapping protocol is $\bigotimes_{j=1}^n \bar{\rho}_{e_j}^{\pi_{e_j}}(t)$, and the output state, conditioned on success of the protocol is $\mathcal{L}^{\text{ES};n}(\bigotimes_{j=1}^n \bar{\rho}_{e_j}^{\pi_{e_j}}(t))$, where we recall the definition of $\mathcal{L}^{\text{ES};n}$ in (56).

After the appropriate joining protocols are performed, and conditioned on their success, we obtain the target graph $G_{\text{target}} = (V, E_{\text{target}})$, and the corresponding quantum state has the form $\bigotimes_{e \in E_{\text{target}}} \omega_e$, where if e is a virtual link, obtained via a joining protocol, then ω_e is given by (50). Now, the target quantum state is simply a tensor product of the target states corresponding to the edges of the target graph, i.e., $\bigotimes_{e \in E_{\text{target}}} \omega_e^{\text{target}}$. Therefore, by multiplicativity of fidelity with respect to the tensor product, the fidelity of the quantum state after the protocol is equal to $\prod_{e \in E_{\text{target}}} F(\omega_e, \omega_e^{\text{target}})$. For the virtual links, individual fidelities in this product can be calculated using the formulas presented in Sec. III B.

B. Waiting time

In addition to the fidelity, another relevant figure of merit is the *expected waiting time*, which is a figure of merit that indicates how long it takes (on average) to establish an elementary or virtual link. This figure of merit has been considered

in prior work in the context of both a linear chain of quantum repeaters and general quantum networks^{59,65,99,107,118–120}.

When defining the waiting times, we imagine a scenario in which elementary link generation is continuously occurring in the network¹¹⁶ and that an end-user request for entanglement occurs at a time $t_{\text{req}} \geq 0$. The waiting time is then the number of time steps from time t_{req} onward that it takes to establish the entanglement.

Definition IV.2 (Elementary link waiting time). Let $G = (V, E)$ be the graph corresponding to the elementary links of a quantum network and let $e \in E$. For all $t_{\text{req}} \geq 0$, the waiting time for the elementary link corresponding to the edge e is defined to be

$$W_e(t_{\text{req}}) := \sum_{t=t_{\text{req}}+1}^{\infty} t X_e(t) \prod_{i=t_{\text{req}}+1}^{t-1} (1 - X_e(i)). \quad (92)$$

Then, the expected waiting time is

$$\begin{aligned} \mathbb{E}[W_e(t_{\text{req}})]_{\pi} &= \sum_{t=t_{\text{req}}+1}^{\infty} t \Pr[X_e(t_{\text{req}}+1) = 1] = 0, \\ &\dots, X_e(t_{\text{req}}+t) = 1]_{\pi}, \end{aligned} \quad (93)$$

where π is an arbitrary policy for the elementary link corresponding to the edge e .

We make the following definition for the waiting time for a collection of elementary links.

Definition IV.3 (Collective elementary link waiting time). Let $G = (V, E)$ be the graph corresponding to the elementary links of a quantum network, and let $t_{\text{req}} \geq 0$. For every subset $E' \subseteq E$, the waiting time for the elementary links corresponding to the elements of E' is defined to be

$$W_{E'}(t_{\text{req}}) := \sum_{t=t_{\text{req}}+1}^{\infty} t X_{E'}(t) \prod_{i=t_{\text{req}}+1}^{t-1} (1 - X_{E'}(i)) \quad (94)$$

where $X_{E'}(t) := \prod_{e \in E'} X_e(t)$.

In other words, the collective elementary link waiting time is the time it takes for all of the elementary links given by E' to be simultaneously active, and its expected value is

$$\begin{aligned} \mathbb{E}[W_{E'}(t_{\text{req}})]_{\pi} &= \sum_{t=t_{\text{req}}+1}^{\infty} t \Pr[X_{E'}(t_{\text{req}}+1) = 1] = 0, \\ &\dots, X_{E'}(t_{\text{req}}+t) = 1]_{\vec{\pi}}, \end{aligned} \quad (95)$$

where $\vec{\pi} = (\pi_e : e \in E')$ is an arbitrary collection of policies for the elementary links corresponding to E' . If we consider a collection of elementary links, all undergoing the $t^* = \infty$ memory-cutoff policy, then

$$\mathbb{E}[W_{E'}(t_{\text{req}})]_{\infty} = \sum_{k=1}^M \binom{M}{k} (-1)^{k+1} \left(1 + \frac{(1 - p_k)^{t_{\text{req}}+1}}{p_k} \right),$$

$$p_k := 1 - (1 - p)^k. \quad (96)$$

Proofs of this result using various different techniques can be found in Refs. [65, 99, and 121]. In Appendix I, we prove this result within the framework introduced here by explicitly evaluating the formula in (95).

Definition IV.4 (Virtual link waiting time). Let $G = (V, E)$ be the graph corresponding to the elementary links of a quantum network, and let $t_{\text{req}} \geq 0$. Given a pair $v_1, v_n \in V$ of distinct non-adjacent vertices and a path $w = (v_1, e_1, v_2, e_2, \dots, e_{n-1}, v_n)$ between them for some $n \geq 2$, the *virtual link waiting time* along this path is defined to be the amount of time it takes to establish the virtual link given by the edge $\{v_1, v_n\}$:

$$W_{\{v_1, v_n\}; w}(t_{\text{req}}) := W_{E_w}(t_{\text{req}}) \sum_{t=t_{\text{req}}+1}^{\infty} t Y_w (1 - Y_w)^{t-1}, \quad (97)$$

where $E_w = \{e_1, e_2, \dots, e_{n-1}\}$ is the set of edges corresponding to the path w , $W_{E_w}(t_{\text{req}})$ is the collective elementary link waiting time from Definition IV.3, and Y_w is a binary random variable for the success of the joining protocol along the path w , so that $Y_w = 1$ corresponds to success of the joining protocol and $Y_w = 0$ to failure. We define Y_w and W_{E_w} to be independent random variables.

The formula for the virtual link waiting time in Definition IV.4 is based on the formula in Ref. [59]. It corresponds to the simple strategy of waiting for all of the elementary links along the path w to be established and then performing the measurements for the joining protocol. Note that this strategy is consistent with our overall quantum network protocol in Fig. 8.

C. Key rates for quantum key distribution

In order to determine secret key rates between arbitrary pairs of nodes in a quantum network, we need to keep track of the quantum state of the relevant elementary links as a function of time. The following discussion and formulas for secret key rates are based on Ref. [122].

Suppose that K is a function that gives the number of secret key bits per entangled state shared by the nodes of either an elementary link or virtual link. (K is, for example, the formula for the asymptotic secret key rate of the BB84, six-state, or device-independent protocol.) Then, suppose that $G = (V, E)$ is the graph corresponding to the elementary links of a quantum network. Consider a collection $e' := \{v_1, \dots, v_k\} \notin E$ of distinct nodes corresponding to a virtual link for some $k \geq 2$, and let w be a path in the physical graph leading to the virtual link given by e' . An entanglement swapping protocol is performed along the path w in order to establish the bipartite virtual link. Conditioned on success of the joining protocol, the quantum state of the virtual link is given by (50), namely,

$$\frac{1}{p_{\text{succ}}} \mathcal{L}_{w \rightarrow e'}^1(\rho_w), \quad (98)$$

where

$$p_{\text{succ}} = \text{Tr}[\mathcal{L}_{w \rightarrow e'}^1(\rho_w)] \quad (99)$$

is the success probability of the joining protocol. Then, the secret key rate (in units of secret key bits per second) for the virtual link along the path w is

$$\tilde{K}_{e';w} = p_{\text{succ}} v_{e'}^{\text{rep}} K. \quad (100)$$

Here, K is calculated using the state in (98). The repetition rate $v_{e'}^{\text{rep}}$ in this case is a function of the end-to-end classical communication time required for executing the joining protocol.

V. A MARKOV DECISION PROCESS BEYOND THE ELEMENTARY LINK LEVEL

The developments so far in this work constitute an analysis of quantum networks using a Markov decision process (MDP) for elementary links. As we have seen, the framework of MDPs is useful because it allows us to model noise processes and imperfections that are present in near-term quantum technologies, and thus allows us to understand the limits on the performance of near-term quantum networks. An important question is how useful the MDP formalism will be in practice when scaling up to model systems of more than one elementary link. In this section, we provide an MDP for a system of two elementary links, taking entanglement swapping into account. We note that in recent work¹²³ an MDPs for repeater chains with two, three and four elementary links have been considered, but the definition of the MDP here differs from the one in Ref. [123], because here we take decoherence of the quantum memories into account.

We start this section by defining the basic elements of the MDP, and then we show how to obtain optimal policies using linear programming. In particular, we formulate the optimal expected waiting time to obtain the end-to-end virtual link and the optimal expected fidelity of the end-to-end virtual link as linear programs. Then, we show that prior analytical results on the expected waiting time for two elementary links under the memory-cutoff policy⁵⁹, known only in the “symmetric” scenario when the two elementary links have the same transmission-heralding success probability and the same memory cutoff, can be reproduced. However, we note that our linear programming procedure can be applied even in non-symmetric scenarios.

A. An MDP for two elementary links

Let p_1 and p_2 be the success probabilities for generating the two elementary links, and let q be the probability of successful entanglement swapping. Note that p_1 and p_2 are defined exactly as in Sec. II A. In particular,

$$p_1 = \text{Tr}[(\mathcal{M}_1^1 \circ \mathcal{S}_1)(\rho_1^S)], \quad (101)$$

$$p_2 = \text{Tr}[(\mathcal{M}_2^1 \circ \mathcal{S}_2)(\rho_2^S)], \quad (102)$$

where \mathcal{M}_j^1 , $j \in \{1, 2\}$, are the completely positive maps corresponding to success of the heralding procedure for the j^{th} elementary link, \mathcal{S}_j is the transmission channel from the



FIG. 9. Two elementary links with entanglement swapping at the central node.

source to the nodes for the j^{th} elementary link, and ρ_j^S is the state produced by the source associated with the j^{th} elementary link; see Fig. 9. We also define the states

$$\sigma_j^0 = \frac{1}{p_j} (\mathcal{M}_j^1 \circ \mathcal{S}_j)(\rho_j^S), \quad (103)$$

$$\sigma_j(m) = \mathcal{N}_j^{\text{om}}(\sigma_j^0), \quad j \in \{1, 2\}, \quad (104)$$

where \mathcal{N}_j is the quantum channel describing the decoherence of the quantum memories associated with the j^{th} elementary link.

Now, recall that in the case of one elementary link considered in Sec. II B, the state variable was just the memory time $M(t)$, referring to the time for which the quantum state of the elementary link was held in the memories of the nodes, and the actions consisted of either keeping the elementary link or discarding it and generating a new one. Now, in the case of two elementary links, we must keep track of the memory time of both elementary links, and we also store information about whether or not the virtual (end-to-end) link is active. The actions are similar to before, consisting of the same elementary link actions as before, but now we define an additional action for performing the entanglement swapping operation. Formally, we have the following.

- **States:** The states of the MDP are elements of the set $S = X \times M_1 \times M_2$, where $X = \{0, 1\}$ indicates whether or not the end-to-end link is active, $M_1 = \{-1, 0, 1, \dots, m_1^*\}$ is the set of possible states of the first elementary link (with the elements of the set having the same interpretation as in the elementary link MDP), and $M_2 = \{-1, 0, 1, \dots, m_2^*\}$ is the set of possible states of the second elementary link. In particular, m_1^* and m_2^* are the maximum storage times of the two elementary links, corresponding to their coherence times; see Sec. II B. To these states, we associate the (standard) probability simplex spanned by the orthonormal vectors $|x\rangle \otimes |m_1\rangle \otimes |m_2\rangle$, with $x \in X$, $m_1 \in M_1$, and $m_2 \in M_2$, and we often use the abbreviation $|s\rangle \equiv |x, m_1, m_2\rangle \equiv |x\rangle \otimes |m_1\rangle \otimes |m_2\rangle$ for every $s = (x, m_1, m_2) \in S$.

We use $S(t) = (X(t), M_1(t), M_2(t))$, $t \in \mathbb{N}$, to refer to the random variables (taking values in S) corresponding to the state of the MDP.

- **Actions:** The set of actions is $A = \{00, 01, 10, 11, \bowtie\}$, where the different actions have the following meanings:

- 00: Keep both elementary links.
- 01: Keep the first elementary link, discard and regenerate the second.

- 10: Discard and regenerate the first elementary link, keep the second.
- 11: Discard and regenerate both elementary links.
- \bowtie : Perform entanglement swapping.

We use $A(t)$, $t \in \mathbb{N}$, to refer to the random variables (taking values in the set \mathcal{A}) corresponding to the actions taken.

$$f(x, m_1, m_2) = \begin{cases} \langle \psi | \mathcal{L}^{\text{ES};1}(\sigma_1(m_1) \otimes \sigma_2(m_2)) | \psi \rangle & \text{if } x = 1, m_1, m_2 \geq 0, \\ 0 & \text{otherwise,} \end{cases} \quad (105)$$

where we recall that $\mathcal{L}^{\text{ES};1}$ is the entanglement swapping channel for one intermediate node, as defined in Sec. III B 1, and $|\psi\rangle$ is a target pure state vector, which in this context is typically the maximally entangled state vector $|\Phi\rangle$, as defined in (52).

Let us now proceed to the definition of the transition matrices for our MDP. Unlike the elementary link scenario, in this scenario of two elementary links we want not only for the fidelity and success probability of the end-to-end link to be high, but we also want the average amount of time it takes to generate the end-to-end link to be low—in other words, we want the expected waiting time to be low as well. Therefore, in order to address the expected waiting time in our MDP, we define the transition matrices in such a way that states corresponding to an active end-to-end link (i.e., states $s = (x, m_1, m_2) \in \mathcal{S}$ such that $x = 1$) are *absorbing states*. By doing this, the expected waiting time is nothing but the expected time to absorption, which is a standard result in the theory of Markov chains; see, e.g., Ref. [124]. We note that this idea of relating the expected waiting time of a quantum repeater chain to the absorption time of a Markov chain has already been used in Ref. [107]; however, here, we apply this idea in the more general context of an MDP, while also taking memory decoherence and other device imperfections explicitly into account.

Let T_j^a denote the transition matrix for the j^{th} elementary link, as defined in (5) and (6), for $a \in \{0, 1\}$. Then, using those elementary link transition matrices, we define the transition matrices for our MDP for two elementary links as follows:

$$T^{00} := |0\rangle\langle 0| \otimes T_1^0 \otimes T_2^0 + |1\rangle\langle 1| \otimes \mathbb{1}_1 \otimes \mathbb{1}_2, \quad (106)$$

$$T^{01} := |0\rangle\langle 0| \otimes T_1^0 \otimes T_2^1 + |1\rangle\langle 1| \otimes \mathbb{1}_1 \otimes \mathbb{1}_2, \quad (107)$$

$$T^{10} := |0\rangle\langle 0| \otimes T_1^1 \otimes T_2^0 + |1\rangle\langle 1| \otimes \mathbb{1}_1 \otimes \mathbb{1}_2, \quad (108)$$

$$T^{11} := |0\rangle\langle 0| \otimes T_1^1 \otimes T_2^1 + |1\rangle\langle 1| \otimes \mathbb{1}_1 \otimes \mathbb{1}_2, \quad (109)$$

$$\begin{aligned} T^{\bowtie} := & |0\rangle\langle 0| \otimes ((1-q)|g_{p_1}, g_{p_2}\rangle\langle \gamma_1^+, \gamma_2^+| \\ & + S_1 \otimes |-1\rangle\langle -1| + |-1\rangle\langle -1| \otimes S_2 \\ & + |-1, -1\rangle\langle -1, -1| + |-1, -1\rangle\langle -1, m_2^{\star}| \\ & + |-1, -1\rangle\langle m_1^{\star}, -1|) \\ & + |1\rangle\langle 0| \otimes q\mathbb{1}_1^+ \otimes \mathbb{1}_2^+ + |1\rangle\langle 1| \otimes \mathbb{1}_1 \otimes \mathbb{1}_2, \end{aligned} \quad (110)$$

We let $H(t) = (S(1), A(1), S(2), A(2), \dots, A(t-1), S(t))$ be the history, consisting of a sequence of states and actions, up to time $t \in \mathbb{N}$, with $H(1) = S(1)$.

- *Figure of merit*: For the elementary link MDP defined in Sec. II B, recall that the figure of merit was essentially the fidelity of the elementary link, but scaled by a factor corresponding to the probability that the elementary link is active. We define the figure of merit here in an analogous fashion as follows:

where

$$|\gamma_j^+\rangle = \sum_{m=0}^{m_j^{\star}} |m\rangle, \quad (111)$$

$$\mathbb{1}_j = \sum_{m=-1}^{m_j^{\star}} |m\rangle\langle m|, \quad (112)$$

$$\mathbb{1}_j^+ = \sum_{m=0}^{m_j^{\star}} |m\rangle\langle m|, \quad (113)$$

$$S_j = \sum_{m=0}^{m_j^{\star}-1} |m+1\rangle\langle m|, \quad (114)$$

and $|g_{p_j}\rangle$, $j \in \{1, 2\}$, is defined exactly as in (9).

First, let us observe that every transition matrix has a block structure, with the blocks defined by the transitions of the status of the end-to-end link. Specifically, we can write every transition matrix T^a as

$$T^a = \begin{pmatrix} T_{0 \rightarrow 0}^a & T_{1 \rightarrow 0}^a \\ T_{0 \rightarrow 1}^a & T_{1 \rightarrow 1}^a \end{pmatrix}, \quad a \in \mathcal{A}, \quad (115)$$

where the sub-blocks $T_{x \rightarrow x'}^a$ is the block corresponding to the transition of the status of the virtual link from $x \in \{0, 1\}$ to $x' \in \{0, 1\}$. (We note, as before, that probability vectors are applied to transition matrices from the right; see Appendix A.) From this, we see that for the actions 00, 01, 10, 11, the transition matrices are of the following block-diagonal form:

$$T^{jk} = \begin{pmatrix} T_1^j \otimes T_2^k & 0 \\ 0 & \mathbb{1}_1 \otimes \mathbb{1}_2 \end{pmatrix}, \quad j, k \in \{0, 1\}. \quad (116)$$

Therefore, for these transition matrices, because the entanglement swapping action is not performed, the transition from $x = 0$ to $x = 1$ is not possible. Consequently, if the end-to-end is initially inactive ($x = 0$), then it stays inactive and each elementary link transitions independently according to the elementary link transition matrices from Sec. II B. If the end-to-end link is initially active ($x = 1$), then nothing happens to the states of

the elementary links, in accordance with the definition of an absorbing state. For the action \bowtie of entanglement swapping, we have three non-zero blocks. The block $T_{0 \rightarrow 0}^{\bowtie}$ means that the end-to-end link is initially inactive and stays inactive, which can happen in one of several ways:

- Both elementary links are initially active but the entanglement swapping fails, after which both elementary links are regenerated. This possibility is given by the term $(1 - q)|g_{p_1}, g_{p_2}\rangle\langle\gamma_1^+, \gamma_2^+|$.
- Both elementary links are initially inactive. In this case, they both remain inactive after the entanglement swapping action, and this is given by the term $| - 1, - 1\rangle\langle - 1, - 1|$.
- One of the elementary links is active but the other is not. In this case, the memory time of the active elementary link is incremented by one, corresponding to the “shift” operator S_j on the active elementary link, while the inactive elementary link remains inactive. These possibilities are given by the terms $S_1 \otimes | - 1\rangle\langle - 1|$ and $| - 1\rangle\langle - 1| \otimes S_2$.
- One of the elementary links is inactive and the other has reached its maximum storage time. In this case, the inactive elementary link remains inactive, and the other elementary link transitions to the -1 state, because the maximum time m_j^* was reached. These possibilities are given by the terms $| - 1, - 1\rangle\langle m_1^*, - 1|$ and $| - 1, - 1\rangle\langle - 1, m_2^*|$.

The block $T_{0 \rightarrow 1}^{\bowtie}$ corresponds to a transition from the end-to-end link initially being inactive to being active, which happens when the entanglement swapping succeeds. Since the entanglement swapping is possible only when both elementary links are active, and because we want to keep track of the memory times of the elementary links at the moment the entanglement swapping is performed, this block is given by $q\mathbb{1}_1^+ \otimes \mathbb{1}_2^+$. Finally, the block $T_{1 \rightarrow 1}^{\bowtie}$ corresponds to the end-to-end link being active already; thus, in accordance with the definition of an absorbing state, this block is given simply by $\mathbb{1}_1 \otimes \mathbb{1}_2$, as with the other actions.

Now, just as we defined a memory-cutoff policy for elementary links in Sec. II D, we can define a memory-cutoff policy for the system of two elementary links that we are considering here. Suppose that the first elementary link has cutoff time $t_1^* \leq m_1^*$ and the second elementary link has cutoff time $t_2^* \leq m_2^*$. Then, we define the decision function such that, if both elementary links are active, then an entanglement swap is attempted; otherwise, one of the actions 01, 10, or 11 is performed, depending on which elementary links are active. This leads to the following definition of the deterministic decision function.

$$d(0, m_1, m_2) = \begin{cases} 01, & m_1 \in \{0, \dots, t_1^* - 1\}, m_2 = -1, \\ 10, & m_1 = -1, m_2 \in \{0, \dots, t_2^* - 1\}, \\ 11, & (m_1, m_2) = (-1, -1), (-1, t_2^*), (t_1^*, -1), \\ \bowtie, & m_1 \in \{0, \dots, t_1^*\}, m_2 \in \{0, \dots, t_2^*\}, \end{cases} \quad (117)$$

for all $m_1 \in M_1$ and $m_2 \in M_2$. Note that it is only necessary to define the decision function on the transient states $(0, m_1, m_2)$ and not the absorbing states $(1, m_1, m_2)$, because the figures of merit that we are concerned with (such as the expected value of the function f in (105) and the expected waiting time to absorption) do not depend on the values of the decision function on absorbing states.

B. Optimal policies via linear programming

Having defined the basic elements of the MDP for two elementary links with entanglement swapping, let us now look at optimal policies. We are concerned both with the figure of merit defined in (105) and with the expected waiting time to obtain an end-to-end link. In Appendix A 4, we show that both quantities can be bounded using linear programs. In fact, the results in Appendix A 4 go beyond the MDP for two elementary links that we consider here, because the linear programs apply to general MDPs with arbitrary state and action sets and transition matrices.

Theorem V.1 (Linear program for the optimal expected value for two elementary links). Given a system of two elementary links, along with the associated MDP defined in Sec. V A, the optimal expected value of the function f defined in (105) is bounded from above by the following linear program:

$$\begin{aligned} & \text{maximize } \langle f | 1, x \rangle \\ & \text{subject to } 0 \leq |w_a\rangle \leq |x\rangle \quad \forall a \in A, \\ & \quad 0 \leq |v_a\rangle \leq |y\rangle \quad \forall a \in A, \\ & \quad \sum_{a \in A} \sum_{i=0}^1 T_{0 \rightarrow i}^a |w_a\rangle = |0\rangle |x\rangle, \\ & \quad \sum_{a \in A} |w_a\rangle = |x\rangle, \\ & \quad |y\rangle - \sum_{a \in A} T_{0 \rightarrow 0}^a |v_a\rangle = |g_{p_1}\rangle |g_{p_2}\rangle, \\ & \quad \sum_{a \in A} |v_a\rangle = |y\rangle, \\ & \quad T_{0 \rightarrow 1}^{\bowtie} |v_{\bowtie}\rangle = |x\rangle, \end{aligned} \quad (118)$$

where the optimization is with respect to the $(m_1^* + 2) \cdot (m_2^* + 2)$ -dimensional vectors $|x\rangle$, $|y\rangle$, $|w_a\rangle$, $|v_a\rangle$, $a \in A$, and the inequality constraints are component-wise. Every set of feasible points $|x\rangle$, $|y\rangle$, $|w_a\rangle$, $|v_a\rangle$, $a \in A$, of this linear program defines a stationary policy with decision function d , whose values for the transient states $(0, m_1, m_2)$ are as follows:

$$d(0, m_1, m_2)(a) = \frac{\langle 0, m_1, m_2 | w_a \rangle}{\langle 0, m_1, m_2 | x \rangle}, \quad (119)$$

for all $m_1 \in M_1$, $m_2 \in M_2$, and $a \in A$. If $\langle 0, m_1, m_2 | x \rangle = 0$, then we can set $d(0, m_1, m_2)$ to be an arbitrary probability distribution over the set A of actions.

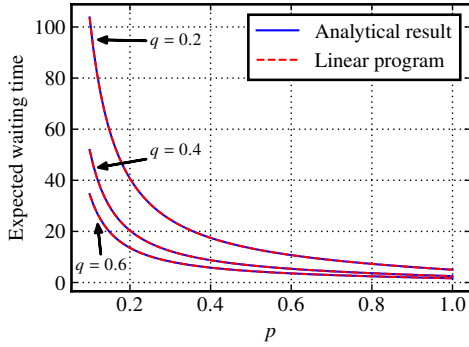


FIG. 10. The expected waiting time for an end-to-end for a system of two elementary links, as depicted in Fig. 9. We let $p_1 = p_2 = p$ be the transmission-heralding success probability for both elementary links, and we denote by q the success probability for entanglement swapping. We compare the known analytical result for this scenario [59, Eq. (5)], with cutoff $t^* = 5$ (see (122)), to the solution obtained by the linear program in (120), with maximum storage time $m^* = 5$.

Remark V.2. Note that in the theorem statement above we defined the action of the decision function only for the transient states. For the absorbing states, we can set the decision function to be arbitrary, because neither the expected value of the MDP nor the expected waiting time to absorption is affected by the value of the decision function on absorbing states; see Appendix A 3.

Theorem V.3 (Linear program for the optimal expected waiting time for two elementary links). Given a system of two elementary links, along with the associated MDP defined in Sec. V A, the optimal expected waiting time is bounded from below by the following linear program:

$$\begin{aligned} & \text{minimize } \langle \gamma | x \rangle \\ & \text{subject to } 0 \leq |w_a\rangle \leq |x\rangle \quad \forall a \in A, \\ & |x\rangle - \sum_{a \in A} T_{0 \rightarrow 0}^a |w_a\rangle = |g_{p_1}\rangle |g_{p_2}\rangle, \quad (120) \\ & \sum_{a \in A} |w_a\rangle = |x\rangle, \end{aligned}$$

where the optimization is with respect to the $(m_1^* + 2) \cdot (m_2^* + 2)$ -dimensional vectors $|x\rangle$ and $|w_a\rangle$, $a \in A$, and the inequality constraints are component-wise. Every set of feasible points $|x\rangle$, $|w_a\rangle$, $a \in A$, of this linear program defines a stationary policy with decision d , whose values for the transient states $(0, m_1, m_2)$ (see Remark V.2 above) are as follows:

$$d(0, m_1, m_2)(a) = \frac{\langle 0, m_1, m_2 | w_a \rangle}{\langle 0, m_1, m_2 | x \rangle}, \quad (121)$$

for all $m_1 \in M_1$, $m_2 \in M_2$, and $a \in A$. If $\langle 0, m_1, m_2 | x \rangle = 0$, then we can set $d(0, m_1, m_2)$ to be an arbitrary probability distribution over the set A of actions.

We now show that the linear program in (120) reproduces the known analytical result in Ref. [59, Eq. (5)] for the expected

waiting time for two elementary links with the same success probability p and cutoff time t^* :

$$\frac{3 - 2p(1 - (1 - p)^{t^*}) - 2(1 - p)^{t^*}}{qp(2 - p(1 - 2(1 - p)^{t^*}) - 2(1 - p)^{t^*})}. \quad (122)$$

In Fig. 10, we plot this function along with the optimal value obtained for the linear program in (120). We find that the two curves coincide for all values of the transmission-heralding probability p and the entanglement swapping success probability q considered. This provides us not only with a sanity check on the linear program, but it also provides evidence that the memory-cutoff policy in (117) is optimal, at least in the symmetric scenario. We also note that the result in (122) holds only in the “symmetric” scenario in which both elementary links have the same transmission-heralding success probability, while the linear program in (120) can be used to determine the optimal expected waiting time in arbitrary parameter regimes.

VI. SUMMARY AND OUTLOOK

The central topic of this work is the theory of near-term quantum networks—specifically, how to describe them and how to develop protocols for entanglement distribution in practical scenarios with near-term quantum technologies. The goal in this area of research is to develop protocols that can handle multiple-user requests, work for any given network topology, and can adapt to changes in topology and attacks to the network infrastructure, with the ultimate goal being the realization of the quantum internet. In this work, we have laid some of the foundations for this research program. The core idea is that Markov decision processes (MDPs) provide a natural setting in which to analyze near-term quantum network protocols. We illustrated this idea in this work by first analyzing the MDP for elementary links first introduced in Ref. [58], simplifying its formulation and presenting some new results about it. Notably, in Theorem II.4, we show that the memory-cutoff policy is optimal in the steady-state limit. We then showed how the elementary link MDP can be used as part of an overall quantum network protocol. Finally, we provided a first step towards using the MDP formalism for more realistic, larger networks, by providing an MDP for two elementary links. We showed that important figures of merit such as the fidelity of the end-to-end link as well as the expected waiting time for the end-to-end link, can be obtained using linear programs.

Moving forward, there are many interesting directions to pursue. The MDPs introduced in this work are not entirely general, because they do not model protocols for arbitrary repeater chains nor arbitrary networks. Thus, to start with, extending the MDP for two elementary links to repeater chains of arbitrary length is an interesting direction for future work. In this direction, we expect that linear, and possibly even semi-definite relaxations of the expected value of the end-to-end link and of the expected waiting time, such as those in Theorem V.1 and Theorem V.3, are going to be crucial in the analysis of longer repeater chains, because the size of the MDP (the number of states and actions) will grow exponentially with the number of elementary links.

Going beyond repeater chains to general quantum networks, it is of interest to examine protocols involving multiple co-operating agents. When we say that agents “cooperate”, we mean that they are allowed to communicate with each other. In the context of quantum networks, agents who cooperate have knowledge beyond that of their own nodes. If every agent cooperates with an agent corresponding to a neighbouring elementary link, then the agents would have knowledge of the network in their local vicinity, and this would in principle improve waiting times and rates for entanglement distribution. Furthermore, the quantum state of the network would not be a simple tensor product of the quantum states corresponding to the individual edges, as we have in (89) when all the agents are independent. See Refs. [116 and 117] for a discussion of nodes with local and global knowledge of a quantum network in the context of routing.

Finally, another interesting direction for future work is to develop quantum network protocols based on decision processes that incorporate queuing models for requests for links of a

specific type between specific nodes; see, e.g., Refs. [90 and 125]. Then, one can calculate quantities such as the time needed to fulfill all requests. We can also calculate the “capacity” of the network, defined in the context of queuing systems as the maximum number of requests that can be fulfilled per unit time.

ACKNOWLEDGMENTS

Much of this work is based on the author’s PhD thesis research¹²⁶, which was conducted at the Hearne Institute for Theoretical Physics, Department of Physics and Astronomy, Louisiana State University. During this time, financial support was provided by the National Science Foundation and the National Science and Engineering Research Council of Canada Postgraduate Scholarship. The author also acknowledges support from the BMBF (QR.X). The plots in this work were made using the Python package matplotlib¹²⁷.

Appendix A: Overview of Markov decision processes

In this section, we provide a brief overview of the concepts from the theory of Markov decision processes (MDPs) that are relevant for this work. We mostly follow the definitions and results as presented in Ref. [128] while using the notation defined in Sec. A 1.

1. Notation

Throughout this work, we deal with probability distributions defined on a discrete, finite set of points. It is very helpful to write these probability distributions as vectors in a (standard) probability simplex. We do this as follows. Consider a finite set X . To this set, we associate the orthonormal vectors $\{|x\rangle\}_{x \in X}$ in $\mathbb{R}^{|X|}$, which means that $\langle x|x' \rangle = \delta_{x,x'}$ for all $x, x' \in X$. The probability simplex corresponding to X is then formally defined as all convex combinations of the vectors in $\{|x\rangle\}_{x \in X}$:

$$\Delta_X := \left\{ \sum_{x \in X} p_x |x\rangle : 0 \leq p_x \leq 1, \sum_{x \in X} p_x = 1 \right\}. \quad (\text{A1})$$

This set is in one-to-one correspondence with the set of all probability distributions defined on X . Specifically, let $P : X \rightarrow [0, 1]$ be a probability distribution (probability mass function) on X , i.e., $P(x) \in [0, 1]$ for all $x \in X$ and $\sum_{x \in X} P(x) = 1$. The unique probability vector $|P\rangle_X \in \Delta_X$ corresponding to P is

$$|P\rangle_X := \sum_{x \in X} P(x) |x\rangle. \quad (\text{A2})$$

We drop the subscript X from $|P\rangle_X$ whenever the underlying set X is clear from context. It is important to note and to emphasize that the vector $|P\rangle$ does not represent a quantum state—the bra-ket notation is used merely for convenience. Normalization of the probability vector is then captured by defining the following vector:

$$|\gamma_X\rangle := \sum_{x \in X} |x\rangle. \quad (\text{A3})$$

We often omit the subscript X in $|\gamma_X\rangle$ when the underlying set X is clear from context. Then

$$\langle \gamma | P \rangle = \sum_{x \in X} P(x) = 1. \quad (\text{A4})$$

It is often the case that a probability distribution is associated with a random variable X taking values in X , so that $P(x) \equiv P_X(x) = \Pr[X = x]$ for all $x \in X$. In this case, for brevity, we sometimes write the probability vector as

$$|X\rangle \equiv |P_X\rangle = \sum_{x \in X} \Pr[X = x] |x\rangle. \quad (\text{A5})$$

Now, consider another random variable Y taking values in the finite set Y . We regard stochastic matrices mapping X to Y (i.e., matrices of conditional probabilities $\Pr[Y = y | X = x]$) as linear operators with domain Δ_X and codomain Δ_Y :

$$T_{Y|X} := \sum_{\substack{x \in X \\ y \in Y}} \Pr[Y = y | X = x] |y\rangle \langle x|, \quad (\text{A6})$$

and we denote the matrix elements by

$$T_{Y|X}(y; x) := \langle y | T_{Y|X} | x \rangle = \Pr[Y = y | X = x] \quad \forall x \in X, y \in Y. \quad (\text{A7})$$

We then have, by definition of a stochastic matrix,

$$\langle \gamma_Y | T_{Y|X} = \langle \gamma_X |, \quad (\text{A8})$$

which captures the fact that the columns of a stochastic matrix sum to one. Then, if $|P_X\rangle \in \Delta_X$ is a probability distribution corresponding to X , then the action of the matrix $T_{Y|X}$ on $|P_X\rangle$, which results in the probability distribution $|P_Y\rangle \in \Delta_Y$ corresponding to Y , can be written as

$$|P_Y\rangle := T_{Y|X} |P_X\rangle. \quad (\text{A9})$$

In particular, for all $y \in Y$,

$$P_Y(y) := \langle y | P_Y \rangle \quad (\text{A10})$$

$$= \langle y | T_{Y|X} | P_X \rangle \quad (\text{A11})$$

$$= \sum_{x \in X} \Pr[Y = y | X = x] P_X(x). \quad (\text{A12})$$

Finally, we discuss joint probability distributions. Consider two finite sets X and Y and the set $\Delta_{X \times Y} \subset \mathbb{R}^{|X \times Y|}$ of all (joint) probability distributions on $X \times Y$. Now, because $\mathbb{R}^{|X \times Y|} \cong \mathbb{R}^{|X|} \otimes \mathbb{R}^{|Y|}$, we can regard $\Delta_{X \times Y}$ as the convex span (convex hull) of tensor product orthonormal vectors $|x\rangle \otimes |y\rangle$, $x \in X$, $y \in Y$. Thus, every $|Q\rangle_{XY} \in \Delta_{X \times Y}$ can be written as

$$|Q\rangle_{XY} = \sum_{(x,y) \in X \times Y} Q_{x,y} |x\rangle \otimes |y\rangle. \quad (\text{A13})$$

We frequently use the abbreviation $|x, y\rangle \equiv |x\rangle \otimes |y\rangle$ in this paper. Then, marginal distributions can be obtained as follows:

$$|Q\rangle_X := (\mathbb{1}_X \otimes \langle \gamma_Y |) |Q\rangle_{XY} = \sum_{x \in X} \left(\sum_{y \in Y} Q_{x,y} \right) |x\rangle, \quad (\text{A14})$$

$$|Q\rangle_Y := (\langle \gamma_X | \otimes \mathbb{1}_Y) |Q\rangle_{XY} = \sum_{y \in Y} \left(\sum_{x \in X} Q_{x,y} \right) |y\rangle, \quad (\text{A15})$$

where

$$\mathbb{1}_X := \sum_{x \in X} |x\rangle \langle x|, \quad \mathbb{1}_Y := \sum_{y \in Y} |y\rangle \langle y|. \quad (\text{A16})$$

These concepts for probability distributions defined on two sets can be readily extended to probability distributions defined on sets of the form $X_1 \times X_2 \times \dots \times X_n$ for all $n \geq 2$.

2. Definitions

A *Markov decision process (MDP)* is a stochastic process that models the evolution of a system with which an agent is allowed to interact. Formally, an MDP is defined as a collection

$$\langle S, A, \{T^a\}_{a \in A}, r \rangle \quad (\text{A17})$$

consisting of the following elements:

- A set S of the allowed *states* of the system. We consider finite state sets throughout this work. The sequence $(S(t) : t \in \mathbb{N})$ of random variables taking values in S describes the state of the system at all times $t \in \mathbb{N}$.
- A set A of *actions* that the agent is allowed to perform on the system. We consider finite action sets throughout this work. The sequence $(A(t) : t \in \mathbb{N})$ of random variables taking values in S describes the action taken by the agent at all times $t \in \mathbb{N}$.
- A set $\{T^a\}_{a \in A}$ of *transition matrices*, which are stochastic matrices with domain Δ_S and codomain Δ_S . Specifically,

$$T^a = \sum_{s, s' \in S} \Pr[S(t+1) = s' | S(t) = s, A(t) = a] |s'\rangle \langle s| \quad (\text{A18})$$

for all $t \in \mathbb{N}$. These matrices determine how the system evolves from one time to the next conditioned on the actions of the agent.

- A function $r : S \times A \rightarrow \mathbb{R}$ that quantifies the *reward* that the agent receives at every time step based on the current state of the system and the action that it takes.

The *history* up to time $t \in \mathbb{N}$ of an MDP is the random sequence $H(t) := (S(1), A(1), \dots, A(t-1), S(t))$, with $H(1) = S(1)$. By the Markovian nature of an MDP, the probability distribution of every history $h^t = (s_1, a_1, \dots, a_{t-1}, s_t)$ is equal to

$$\Pr[H(t) = h^t] = \Pr[S(1) = s_1] \prod_{j=1}^{t-1} T^{a_j}(s_{j+1}; s_j) d_j(s_j)(a_j), \quad (\text{A19})$$

where

$$d_j(s_j)(a_j) := \Pr[A(j) = a_j | S(j) = s_j] \quad (\text{A20})$$

is the probability distribution of actions at time j conditioned on the current state of the system. We refer to $d_j : \mathbb{S} \times \mathbb{A} \rightarrow [0, 1]$ as a *decision function*. Note that $\sum_{a \in \mathbb{A}} d_j(s)(a) = 1$ for all $s \in \mathbb{S}$. The sequence

$$\pi = (d_1, d_2, \dots) \quad (\text{A21})$$

of decision functions at all times $t \in \mathbb{N}$ is known as a *policy* of the agent. In the context of this work, policies should be thought of as synonymous with *protocols* for quantum networks.

Given a decision function d , we define the following linear operators acting on $\Delta_{\mathbb{S}}$:

$$D_a^d := \sum_{s \in \mathbb{S}} d(s)(a) |s\rangle\langle s|, \quad \forall a \in \mathbb{A}. \quad (\text{A22})$$

Then, it is straightforward to show that the linear operator

$$P^d := \sum_{a \in \mathbb{A}} T^a D_a^d \quad (\text{A23})$$

from $\Delta_{\mathbb{S}}$ to $\Delta_{\mathbb{S}}$ is a stochastic matrix with elements

$$\langle s' | P^d | s \rangle = \Pr[S(t+1) = s' | S(t) = s] \quad (\text{A24})$$

for all $t \in \mathbb{N}$ and all $s, s' \in \mathbb{S}$.

Remark A.1. Observe that for a fixed decision function d , the set $\{D_a^d\}_{a \in \mathbb{A}}$ of linear operators defined in (A22) forms a positive operator-valued measure (POVM). Indeed, by definition, all of the operators are positive semidefinite; furthermore, by definition of the decision function in (A20),

$$\sum_{a \in \mathbb{A}} D_a^d = \sum_{a \in \mathbb{A}} \sum_{s \in \mathbb{S}} d(s)(a) |s\rangle\langle s| \quad (\text{A25})$$

$$= \sum_{s \in \mathbb{S}} \underbrace{\left(\sum_{a \in \mathbb{A}} d(s)(a) \right)}_{=1 \ \forall s \in \mathbb{S}} |s\rangle\langle s| \quad (\text{A26})$$

$$= \sum_{s \in \mathbb{S}} |s\rangle\langle s| \quad (\text{A27})$$

$$= \mathbb{1}_{\mathbb{S}}. \quad (\text{A28})$$

The transition matrices P^d as defined in (A23) allow us to determine the probability distribution of the state of the system at every time $t \in \mathbb{N}$ for a given policy. Specifically, for a policy $\pi = (d_1, d_2, \dots)$,

$$|S(t)\rangle_{\pi} := \sum_{s \in \mathbb{S}} \Pr[S(t) = s]_{\pi} |s\rangle \quad (\text{A29})$$

$$= P^{d_{t-1}} \dots P^{d_2} P^{d_1} |S(1)\rangle, \quad (\text{A30})$$

where

$$|S(1)\rangle := \sum_{s \in \mathbb{S}} \Pr[S(1) = s] |s\rangle \quad (\text{A31})$$

is the probability distribution for the system at the initial time $t = 1$.

a. MDPs with absorbing states

We call a state $s \in \mathbb{S}$ *absorbing* if $T^a |s\rangle = |s\rangle$ for all $a \in \mathbb{A}$. In other words, once the system reaches the state s it always stays there, meaning that $P^d |s\rangle = |s\rangle$ for all decision functions d . Every state that is not absorbing is called *transient* if there is non-zero

probability that, starting from such a state, the system will eventually reach an absorbing state. We can partition the set \mathbb{S} of all states into disjoint sets: $\mathbb{S} = \mathbb{S}_{\text{tra}} \cup \mathbb{S}_{\text{abs}}$, where \mathbb{S}_{abs} is the set of absorbing states and \mathbb{S}_{tra} is the set of transient states. We can then rewrite the set $\{|s\rangle\}_{s \in \mathbb{S}}$ as $\{|0, s\rangle\}_{s \in \mathbb{S}_{\text{tra}}} \cup \{|1, s\rangle\}_{s \in \mathbb{S}_{\text{abs}}}$, leading to the following block structure for the transition matrices T^a :

$$T^a = |0\rangle\langle 0| \otimes T_{0 \rightarrow 0}^a + |0\rangle\langle 1| \otimes T_{1 \rightarrow 0}^a + |1\rangle\langle 0| \otimes T_{0 \rightarrow 1}^a + |1\rangle\langle 1| \otimes T_{1 \rightarrow 1}^a, \quad (\text{A32})$$

where $T_{0 \rightarrow 0}^a$ is the block describing transitions between transient states, $T_{1 \rightarrow 0}^a$ is the block describing transition between an absorbing state and a transient state, $T_{0 \rightarrow 1}^a$ is the block describing transitions between a transient state and an absorbing state, and $T_{1 \rightarrow 1}^a$ is the block describing transitions between absorbing states. Note that by our definition of an absorbing state, $T_{1 \rightarrow 0}^a = 0$ and $T_{1 \rightarrow 1}^a = \mathbb{1}_{\mathbb{S}_{\text{abs}}}$ for all $a \in \mathbb{A}$. Similarly, for a decision function d , we can write the matrices D_a^d , $a \in \mathbb{A}$, in block form as

$$D_a^d = |0\rangle\langle 0| \otimes D_a^d(0) + |1\rangle\langle 1| \otimes D_a^d(1), \quad (\text{A33})$$

$$D_a^d(0) = \sum_{s \in \mathbb{S}_{\text{trans}}} d(s)(a)|s\rangle\langle s|, \quad (\text{A34})$$

$$D_a^d(1) = \sum_{s \in \mathbb{S}_{\text{abs}}} d(s)(a)|s\rangle\langle s|. \quad (\text{A35})$$

Consequently, the transition matrix P^d in (A23) has the form

$$P^d = |0\rangle\langle 0| \otimes Q^d + |1\rangle\langle 0| \otimes R^d + |1\rangle\langle 1| \otimes \mathbb{1}_{\mathbb{S}_{\text{abs}}} \quad (\text{A36})$$

$$\equiv \begin{pmatrix} Q^d & 0 \\ R^d & \mathbb{1}_{\mathbb{S}_{\text{abs}}} \end{pmatrix}, \quad (\text{A37})$$

where

$$Q^d = \sum_{a \in \mathbb{A}} T_{0 \rightarrow 0}^a D_a^d(0), \quad (\text{A38})$$

$$R^d = \sum_{a \in \mathbb{A}} T_{0 \rightarrow 1}^a D_a^d(0). \quad (\text{A39})$$

3. Figures of merit

While the primary figure of merit in a Markov decision process is the expected reward, in this work we are mostly interested in what we call *functions of state* (such as the fidelity) and the absorption time (corresponding to the waiting time for a virtual link).

Functions of state. In this work, we are also interested in functions $f : \mathbb{S} \rightarrow \mathbb{R}$ of the state of the system. We can associate to such functions the vector

$$|f\rangle := \sum_{s \in \mathbb{S}} f(s)|s\rangle. \quad (\text{A40})$$

Then, for a policy $\pi = (d_1, d_2, \dots)$, we are interested in the expected value of the random variable $f(S(t))$ for all $t \in \mathbb{N}$, i.e., the quantity

$$\mathbb{E}[f(S(t))]_{\pi} = \sum_{s \in \mathbb{S}} f(s) \Pr[S(t) = s]_{\pi}. \quad (\text{A41})$$

Using (A29) and (A30), we immediately obtain

$$\mathbb{E}[f(S(t))]_{\pi} = \langle f | S(t) \rangle_{\pi} \quad (\text{A42})$$

$$= \langle f | P^{d_{t-1}} \dots P^{d_2} P^{d_1} | S(1) \rangle. \quad (\text{A43})$$

With respect to stationary policies $\pi = (d, d, \dots)$, we are also interested in the asymptotic quantity

$$\lim_{t \rightarrow \infty} \mathbb{E}[f(S(t))]_{(d, d, \dots)} = \lim_{t \rightarrow \infty} \langle f | (P^d)^{t-1} | S(1) \rangle, \quad (\text{A44})$$

if the limit exists, along with the optimal value

$$\sup_d \lim_{t \rightarrow \infty} \langle f | (P^d)^{t-1} | S(1) \rangle. \quad (\text{A45})$$

Expected waiting time to absorption. Finally, for MDPs with absorbing states, we are interested in the expected waiting time to absorption with respect to stationary policies, i.e., the expected number of time steps needed to reach an absorbing state when starting from a transient state and following a stationary policy. It is a standard result of the theory of Markov chains (see, e.g., Ref. [124, Theorem 9.6.1]) that in this setting, with a transition matrix as in (A37), if the initial distribution of states is given by the probability vector $|0, S_{\text{tr}}(1)\rangle$ (entirely in the transient block), then the expected waiting time to absorption with respect to the policy (d, d, \dots) is $\langle \gamma |_{S_{\text{tra}}} (\mathbb{1}_{S_{\text{tra}}} - Q^d)^{-1} |S_{\text{tra}}(1)\rangle$. We are then interested in the following optimal value:

$$\inf_d \langle \gamma |_{S_{\text{tra}}} (\mathbb{1}_{S_{\text{tra}}} - Q^d)^{-1} |S_{\text{tra}}(1)\rangle. \quad (\text{A46})$$

4. Linear programs

We now present linear programs for estimating the values of the figures of merit presented in the previous section in the steady-state limit with a time-homogeneous (stationary) policy. Linear programs have been used for MDPs in various different ways^{128–132}. The linear programs we consider here are similar to those in the aforementioned references, but we present them here in the notation introduced at the beginning of this section. We start by considering a general MDP, not necessarily with absorbing states.

Proposition A.2 (Linear program for the steady-state expected function value). Consider an MDP as defined in Sec. A 2 along with a function $f : S \rightarrow \mathbb{R}$ of the state of the MDP. Among decision functions d for which the limit $\lim_{t \rightarrow \infty} (P^d)^{t-1}$ exists, the optimal steady-state expected value of f , namely the quantity in (A45), is equal to the solution of the following linear program:

$$\begin{aligned} & \text{maximize } \langle f | v \rangle \\ & \text{subject to } 0 \leq |w_a\rangle \leq |v\rangle \leq 1 \quad \forall a \in A, \\ & \quad \sum_{s \in S} \langle s | v \rangle = 1, \\ & \quad \sum_{a \in A} |w_a\rangle = |v\rangle = \sum_{a \in A} T^a |w_a\rangle, \end{aligned} \quad (\text{A47})$$

where the optimization is with respect to $|S|$ -dimensional vectors $|v\rangle$ and $|w_a\rangle$, $a \in A$, and the inequality constraints are component-wise. Every set of feasible points $|v\rangle$, $|w_a\rangle$, $a \in A$, of this linear program defines a stationary policy with decision function d as follows:

$$d(s)(a) = \frac{\langle s | w_a \rangle}{\langle s | v \rangle}, \quad \forall s \in S, a \in A. \quad (\text{A48})$$

Proof. By the assumption that $\lim_{t \rightarrow \infty} (P^d)^{t-1}$ exists and is unique, we have that $\lim_{t \rightarrow \infty} (P^d)^{t-1} = |v\rangle \langle \gamma|$ for some probability vector $|v\rangle$ such that $\langle s | v \rangle \in (0, 1]$ for all $s \in S$ and $P^d |v\rangle = |v\rangle$. (Note that all elements $\langle s | v \rangle$ are strictly greater than zero; see, e.g., Ref. [128, Theorem A.2].) Therefore, $\lim_{t \rightarrow \infty} \mathbb{E}[f(S(t))]_{(d, d, \dots)} = \langle f | v \rangle$. Furthermore, using the fact that $P^d = \sum_{a \in A} T^a D_a^d$, we have $\sum_{a \in A} T_a D_a^d |v\rangle = |v\rangle$. Now, let $|w_a\rangle := D_a^d |v\rangle$. By recalling that $D_a^d = \sum_{s \in S, a \in A} d(s)(a) |s\rangle \langle s|$, we see that $\langle s | w_a \rangle = d(s)(a) \langle s | v \rangle$, so that the elements $\langle s | w_a \rangle$ can be thought of as the joint probabilities $\Pr[S(t) = s, A(t) = a]$ (in the steady state). This means that $\langle s | w_a \rangle \in [0, 1]$, and also that $\langle s | w_a \rangle \leq \langle s | v \rangle$, for all $s \in S$ and $a \in A$. Then, using the fact that $\sum_{a \in A} D_a^d = \mathbb{1}_S$, we obtain $\sum_{a \in A} |w_a\rangle = |v\rangle$. By uniqueness of the stationary probability vector $|v\rangle$, the result follows.

The construction of the decision function d in (A48) follows from Ref. [128, Theorem 8.8.2]. Both $\langle s | w_a \rangle$ and $\langle s | v \rangle$ are obtained from the linear program, and because $\langle s | v \rangle$ is strictly positive, we can divide in order to get $d(s)(a)$, and the condition $\sum_{a \in A} |w_a\rangle$ guarantees that $\sum_{a \in A} d(s)(a) = 1$ for all $s \in S$, as required for a conditional probability. This completes the proof. \square

We now consider the optimal expected value of a function $f : S \rightarrow \mathbb{R}$ in the steady-state limit when there are absorbing states in the MDP. We now show how to obtain an upper bound using a linear program.

Proposition A.3 (Linear programming relaxation for the steady-state expected function value for an MDP with absorbing states). Consider an MDP with absorbing states, as defined in Sec. A 2 a, along with a function $f : S \rightarrow \mathbb{R}$ of the state of the MDP. Then, the optimal steady-state expected value of f , namely the quantity in (A45), is bounded from above by the solution to the following

linear program:

$$\begin{aligned}
& \text{maximize } \langle f | 1, x \rangle \\
& \text{subject to } 0 \leq |w_a\rangle \leq |x\rangle \quad \forall a \in \mathcal{A}, \\
& \quad 0 \leq |v_a\rangle \leq |y\rangle \quad \forall a \in \mathcal{A}, \\
& \quad \sum_{a \in \mathcal{A}} \sum_{i=0}^1 T_{0 \rightarrow i}^a |w_a\rangle = |0\rangle |x\rangle, \\
& \quad \sum_{a \in \mathcal{A}} |w_a\rangle = |x\rangle, \\
& \quad |y\rangle - \sum_{a \in \mathcal{A}} T_{0 \rightarrow 0}^a |v_a\rangle = |S_{\text{tra}}(1)\rangle, \\
& \quad \sum_{a \in \mathcal{A}} |v_a\rangle = |y\rangle, \\
& \quad \sum_{a \in \mathcal{A}} T_{0 \rightarrow 1}^a |v_a\rangle = |x\rangle,
\end{aligned} \tag{A49}$$

where $|S_{\text{tra}}(1)\rangle$ is the initial $|\mathcal{S}_{\text{tra}}|$ -dimensional probability vector of the MDP (entirely in the transient block), and the optimization is with respect to $|\mathcal{S}_{\text{tra}}|$ -dimensional vectors $|x\rangle, |y\rangle, |v_a\rangle, |w_a\rangle, a \in \mathcal{A}$, and the inequality constraints are component-wise. Every set of feasible points $|x\rangle, |y\rangle, |v_a\rangle, |w_a\rangle, a \in \mathcal{A}$, of this linear program defines a stationary policy with decision function d for the transient states as follows:

$$\forall s \in \mathcal{S}_{\text{tra}}, a \in \mathcal{A} : d(s)(a) = \frac{\langle s | w_a \rangle}{\langle s | x \rangle}. \tag{A50}$$

If $\langle s | x \rangle = 0$, as well as for $s \in \mathcal{S}_{\text{abs}}$, we can set $d(s)$ to an arbitrary probability distribution.

Proof. For every decision function d , for the transition matrix in (A37) it is known that¹²⁴

$$\lim_{t \rightarrow \infty} (P^d)^{t-1} = \begin{pmatrix} 0 & & 0 \\ R^d (\mathbb{1}_{\mathcal{S}_{\text{tra}}} - Q^d)^{-1} & & 0 \end{pmatrix}. \tag{A51}$$

Therefore,

$$\lim_{t \rightarrow \infty} \mathbb{E}[f(S(t))]_{(d, d, \dots)} = \langle f | \left(|1\rangle \langle 0| \otimes (R^d (\mathbb{1}_{\mathcal{S}_{\text{tra}}} - Q^d)^{-1}) \right) |0\rangle |S_{\text{tra}}(1)\rangle. \tag{A52}$$

Now, let

$$|x\rangle = R^d (\mathbb{1}_{\mathcal{S}_{\text{tra}}} - Q^d)^{-1} |S_{\text{tra}}(1)\rangle, \tag{A53}$$

$$|y\rangle = (\mathbb{1}_{\mathcal{S}_{\text{tra}}} - Q^d)^{-1} |S_{\text{tra}}(1)\rangle. \tag{A54}$$

Then, it is easy to verify that

$$P^d |0\rangle |x\rangle = |0\rangle |x\rangle, \tag{A55}$$

$$(\mathbb{1}_{\mathcal{S}_{\text{tra}}} - Q^d) |y\rangle = |S_{\text{tra}}(1)\rangle, \tag{A56}$$

$$R^d |y\rangle = |x\rangle. \tag{A57}$$

Then, as in the proof of Proposition A.2, we define

$$|w_a\rangle = D_a^d(0) |x\rangle, \tag{A58}$$

$$|v_a\rangle = D_a^d(0) |y\rangle, \tag{A59}$$

for all $a \in \mathcal{A}$. Then, by the same arguments as in the proof of Proposition A.2, we have that $0 \leq |w_a\rangle \leq |x\rangle$ and $0 \leq |v_a\rangle |y\rangle$ for all $a \in \mathcal{A}$, and $\sum_{a \in \mathcal{A}} |w_a\rangle = |x\rangle$, $\sum_{a \in \mathcal{A}} |v_a\rangle = |y\rangle$. Combining the constraints in (A55)–(A57) along with the definitions and constraints for the vectors $|w_a\rangle$ and $|v_a\rangle$ leads to the constraints in (A49). Optimizing with respect to these constraints therefore results in a value that cannot be less than the value in (A45), leading to the desired result. The construction of the decision function in (A50) results from the definition of $|w_a\rangle$ and the reasoning analogous to that given in the proof of Proposition A.2. This completes the proof. \square

Finally, we show how to bound the expected absorption time of an MDP with absorbing states using a linear program.

Proposition A.4 (Linear programming relaxation for the expected waiting time to absorption). Consider an MDP with absorbing states, as defined in Sec. A 2 a. The minimum expected waiting time to reach an absorbing state, namely the quantity in (A46), is bounded from below by the following linear program:

$$\begin{aligned}
& \text{minimize} \quad \langle \gamma | x \rangle \\
& \text{subject to} \quad 0 \leq |w_a\rangle \leq |x\rangle \quad \forall a \in A, \\
& \quad |x\rangle - \sum_{a \in A} T_{0 \rightarrow 0}^a |w_a\rangle = |S_{\text{tra}}(1)\rangle \\
& \quad \sum_{a \in A} |w_a\rangle = |x\rangle,
\end{aligned} \tag{A60}$$

where $|S_{\text{tra}}(1)\rangle$ is the initial $|S_{\text{tra}}|$ -dimensional probability vector of the MDP (entirely in the transient block), and the optimization is with respect to $|S_{\text{tra}}|$ -dimensional vectors $|x\rangle, |w_a\rangle, a \in A$, and the inequality constraints are component-wise. Every set of feasible points $|x\rangle, |w_a\rangle, a \in A$, of this linear program defines a stationary policy with decision function d for the transient states as follows:

$$d(s)(a) = \frac{\langle s | w_a \rangle}{\langle s | x \rangle} \quad \forall s \in S, a \in A. \tag{A61}$$

If $\langle s | x \rangle = 0$, then we can set $d(s)$ to be an arbitrary probability distribution.

Proof. We start with the fact that, for a given decision function d , the expected waiting time to absorption is given by $\langle \gamma | S_{\text{tra}}(\mathbb{1}_{S_{\text{tra}}} - Q^d)^{-1} | S_{\text{tra}}(1) \rangle$. Now, let

$$|x\rangle = (\mathbb{1}_{S_{\text{tra}}} - Q^d)^{-1} |S_{\text{tra}}(1)\rangle. \tag{A62}$$

Then, we have that $(\mathbb{1}_{S_{\text{tra}}} - Q^d)|x\rangle = |S_{\text{tra}}(1)\rangle$. Using the definition of Q^d in (A38), we obtain $|x\rangle - \sum_{a \in A} T_{0 \rightarrow 0}^a |w_a\rangle = |S_{\text{tra}}(1)\rangle$, where $|w_a\rangle = D_a^d(0)|x\rangle, a \in A$. The definition of $|w_a\rangle$ is the same as in the proof of Proposition A.3, thus for the same reasons as in that proof we have that $0 \leq |w_a\rangle \leq |x\rangle$ for all $a \in A$ and $\sum_{a \in A} |w_a\rangle = |x\rangle$. It is then clear that, by optimizing the quantity $\langle \gamma | x \rangle$ with respect to $|x\rangle$ and $|w_a\rangle, a \in A$, the result can be no greater than the optimal expected time to reach an absorbing state, leading to the desired result. Then, given feasible points $|x\rangle$ and $|w_a\rangle, a \in A$, the function d defined by (A61) is a valid decision function whenever $\langle s | x \rangle$ is non-zero. This completes the proof. \square

Appendix B: Quantum states and channels

In this section, we summarize some standard material on quantum states and channels, which can be found in Refs. [110, 133–136]. Given a quantum system A with associated Hilbert space H_A , the *quantum state* of A is given by a density operator acting on H_A : a linear operator $\rho_A : H_A \rightarrow H_A$ that is positive semi-definite and has unit trace, i.e., $\rho_A \geq 0$ and $\text{Tr}[\rho_A] = 1$.

A type of quantum state that we frequently encounter in this work is a *classical-quantum* state, which is a quantum state of the form

$$\rho_{XA} = \sum_{x \in X} p(x) |x\rangle \langle x|_X \otimes \rho_A^x, \tag{B1}$$

where X is a finite set, $p : X \rightarrow [0, 1]$ is a probability mass function, and $\{\rho_A^x\}_{x \in X}$ is a set of quantum states. Classical-quantum states can be used to model scenarios in which classical information accompanies the state of a quantum system. Specifically, if a quantum system A is prepared in a state from the set $\{\rho_A^x\}_{x \in X}$ according to the probability distribution defined by p , then knowledge of the label $x \in X$ is stored in the classical register X .

Given two quantum states ρ and σ , their *fidelity* is defined to be¹³⁷

$$F(\rho, \sigma) := \left(\text{Tr} \left[\sqrt{\sqrt{\rho} \sigma \sqrt{\rho}} \right] \right)^2. \tag{B2}$$

The fidelity quantifies the closeness of two quantum states. In particular, $F(\rho, \sigma) = 1$ if and only if $\rho = \sigma$, and $F(\rho, \sigma) = 0$ if and only if ρ and σ are supported on orthogonal subspaces. If one of the states, say σ , is pure, then it is straightforward to show that

$$F(\rho, |\psi\rangle \langle \psi|) = \langle \psi | \rho | \psi \rangle. \tag{B3}$$

The fidelity is also *multiplicative*, meaning that

$$F(\rho_1 \otimes \rho_2, \sigma_1 \otimes \sigma_2) = F(\rho_1, \sigma_1)F(\rho_2, \sigma_2), \quad (\text{B4})$$

for all states $\rho_1, \rho_2, \sigma_1, \sigma_2$.

A *quantum channel* is a mathematical description of the evolution of a quantum system. Let $L(H_A)$ denote the vector space of linear operators acting on the Hilbert space H_A . A linear map $\mathcal{T} : L(H_A) \rightarrow L(H_B)$ is often called a *superoperator*, and it is such that

$$\mathcal{T}(\alpha X + \beta Y) = \alpha \mathcal{T}(X) + \beta \mathcal{T}(Y) \quad (\text{B5})$$

for all $\alpha, \beta \in \mathbb{C}$ and all $X, Y \in L(H_A)$. It is often helpful to explicitly indicate the input and output Hilbert spaces of a superoperator $\mathcal{T} : L(H_A) \rightarrow L(H_B)$ by writing $\mathcal{T}_{A \rightarrow B}$. The identity superoperator is denoted by id_A , and it satisfies $\text{id}_A(X) = X$ for all $X \in L(H_A)$.

A quantum channel $\mathcal{N}_{A \rightarrow B}$ is a linear, *completely positive*, and *trace-preserving* superoperator acting on the vector space $L(H_A)$ of linear operators of the Hilbert space H_A of the quantum system A . Given an input state ρ_A of the system A , the output is the state of a new quantum system B given by $\mathcal{N}_{A \rightarrow B}(\rho_A)$.

- A superoperator \mathcal{N} is *completely positive* if the map $\text{id}_k \otimes \mathcal{N}$ is positive for all $k \in \mathbb{N}$, where $\text{id}_k : L(\mathbb{C}^k) \rightarrow L(\mathbb{C}^k)$ is the identity superoperator. In other words, $(\text{id}_k \otimes \mathcal{N})(X) \geq 0$ for every linear operator $X \geq 0$.
- A superoperator \mathcal{N} is *trace preserving* if $\text{Tr}[\mathcal{N}(X)] = \text{Tr}[X]$ for every linear operator X .

1. Quantum instruments

Let A be a quantum system with associated Hilbert space H_A . A *measurement* of A is defined by a finite set $\{M_A^x\}_{x \in X}$ of linear operators acting on H_A , called a *positive operator-valued measure (POVM)*, that satisfies the following two properties.

- $M_A^x \geq 0$ for all $x \in X$;

$$\bullet \sum_{x \in X} M_A^x = \mathbb{1}_A.$$

Elements of the set X label the possible outcomes of the measurement. Given a state ρ_A , the probability of obtaining the outcome $x \in X$ is given by the Born rule as $\text{Tr}[M_A^x \rho_A]$.

As a generalization of a measurement, a *quantum instrument* is a finite set $\{\mathcal{M}^x\}_{x \in X}$ of completely positive trace non-increasing maps such that the sum $\sum_{x \in X} \mathcal{M}^x$ is a trace-preserving map, and thus a quantum channel. (A trace non-increasing map $\mathcal{N}_{A \rightarrow B}$ satisfies $\text{Tr}[\mathcal{N}_{A \rightarrow B}(X_A)] \leq \text{Tr}[X_A]$ for every positive semi-definite linear operator X_A .) The *quantum instrument channel* \mathcal{M} associated to the quantum instrument $\{\mathcal{M}^x\}_{x \in X}$ is defined as

$$\mathcal{M}(\cdot) := \sum_{x \in X} |x\rangle\langle x| \otimes \mathcal{M}^x(\cdot). \quad (\text{B6})$$

A quantum instrument $\{\mathcal{M}^x\}_{x \in X}$ can be thought of as a generalized form of a measurement, in which the completely positive maps \mathcal{M}^x represent the evolution of the quantum system conditioned on the outcome x . The trace non-increasing property of the maps \mathcal{M}^x represents the fact that the outcome x occurs probabilistically. Specifically, the probability of obtaining the outcome x is equal to $\text{Tr}[\mathcal{M}^x(\rho)]$, which can be thought of as a generalized form of the Born rule stated above. The quantum instrument channel in (B6) can be thought of as an operation that stores both the outcome x of the instrument in the classical register as well as the corresponding output state.

2. LOCC channels

Consider two parties, Alice and Bob, who are spatially separated. Suppose that they have the ability to perform arbitrary quantum operations (quantum channels, measurements, instruments) in their respective labs and that they are connected by a classical communication channel. It is often the case that Alice and Bob are also connected by a quantum channel and/or share an entangled quantum state, and their task is to make use of these *resources* as sparingly as possible in order to accomplish their desired goal. Their local operations and classical communication (LOCC) can be used freely to help with achieving the goal, which could be feedback-assisted quantum communication³⁸ (see also Ref. [136]), which includes quantum teleportation and entanglement swapping^{12–14,39}, or it could be entanglement distillation³⁸. In the network setting, the task is repeater-assisted

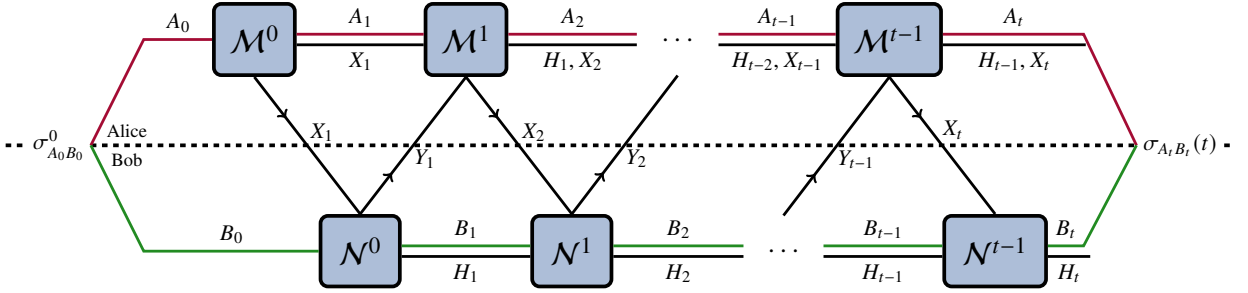


FIG. 11. Depiction of a t -round LOCC protocol between Alice and Bob. The channels $\mathcal{M}^0, \mathcal{M}^1, \dots, \mathcal{M}^{t-1}$ represent Alice's local operations, the channels $\mathcal{N}^0, \mathcal{N}^1, \dots, \mathcal{N}^{t-1}$ represent Bob's local operations, and the registers H_1, H_2, \dots, H_t represent the classical communication to and from Alice and Bob. The final quantum state $\sigma_{A_t B_t}^0(t)$ shared by Alice and Bob has the form shown in (B30).

quantum communication. Here, we focus on the basic mathematical definition of an LOCC channel and provide some examples. For more mathematical details about LOCC channels, we refer to Ref. [138].

Consider the scenario shown in Fig. 11, which is an *LOCC protocol* with t rounds. The LOCC channel corresponding to this protocol, i.e., the channel mapping the input systems $A_0 B_0$ to the output systems $A_t B_t$ at the end of the t^{th} round of the protocol, can be derived as follows.

We start with the initial state $\sigma_{A_0 B_0}^0$ shared by Alice and Bob. In the first round, Alice acts on her system A_0 with a quantum instrument channel $\mathcal{M}_{A_0 \rightarrow X_1 A_1}^0$, which leads to the following output:

$$\sigma_{A_0 B_0}^0 \mapsto \mathcal{M}_{A_0 \rightarrow X_1 A_1}(\sigma_{A_0 B_0}^0) = \sum_{x_1 \in X_1} |x_1><x_1|_{X_1} \otimes \mathcal{M}_{A_0 \rightarrow A_1}^{0;x_1}(\sigma_{A_0 B_0}^0), \quad (\text{B7})$$

where X_1 is a finite set and $\{\mathcal{M}_{A_0 \rightarrow A_1}^{0;x_1}\}_{x_1 \in X_1}$ is a quantum instrument. The classical register X_1 is then communicated to Bob, who applies the conditional quantum instrument channel given by

$$\mathcal{N}_{X_1 B_0 \rightarrow X_1 Y_1 B_1}^0 (|x_1><x_1|_{X_1} \otimes \tau_{B_0}) = |x_1><x_1|_{X_1} \otimes \mathcal{N}_{B_0 \rightarrow Y_1 B_1}^{0;x_1}(\tau_{B_0}), \quad (\text{B8})$$

where $\mathcal{N}_{B_0 \rightarrow Y_1 B_1}^{0;x_1}$ is a quantum instrument channel, i.e.,

$$\mathcal{N}_{B_0 \rightarrow Y_1 B_1}^{0;x_1}(\tau_{B_0}) = \sum_{y_1 \in Y_1} |y_1><y_1|_{Y_1} \otimes \mathcal{N}_{B_0 \rightarrow B_1}^{0;x_1, y_1}(\tau_{B_0}), \quad (\text{B9})$$

with $\{\mathcal{N}_{B_0 \rightarrow B_1}^{0;x_1, y_1}\}_{y_1 \in Y_1}$ being a quantum instrument, i.e., every $\mathcal{N}_{B_0 \rightarrow B_1}^{0;x_1, y_1}$ is a completely positive trace non-increasing map and $\sum_{y_1 \in Y_1} \mathcal{N}_{B_0 \rightarrow B_1}^{0;x_1, y_1}$ is a trace-preserving map. Bob sends the outcome $y_1 \in Y_1$ of the quantum instrument to Alice. This completes the first round, and the quantum state shared by Alice and Bob is

$$\rho_{X_1 Y_1 A_1 B_1}(1) := \left(\mathcal{M}_{A_0 \rightarrow X_1 A_1}^0 \otimes \mathcal{N}_{X_1 B_0 \rightarrow X_1 Y_1 B_1}^0 \right) (\sigma_{A_0 B_0}^0) \quad (\text{B10})$$

$$= \sum_{\substack{x_1 \in X_1 \\ y_1 \in Y_1}} |x_1, y_1><x_1, y_1|_{X_1 Y_1} \otimes \left(\mathcal{M}_{A_0 \rightarrow A_1}^{0;x_1} \otimes \mathcal{N}_{B_0 \rightarrow B_1}^{0;x_1, y_1} \right) (\sigma_{A_0 B_0}^0) \quad (\text{B11})$$

$$= \sum_{\substack{x_1 \in X_1 \\ y_1 \in Y_1}} |x_1, y_1><x_1, y_1|_{X_1 Y_1} \otimes \tilde{\sigma}_{A_1 B_1}(1; x_1, y_1), \quad (\text{B12})$$

where in the last line we let

$$\tilde{\sigma}_{A_1 B_1}(1; x_1, y_1) := \left(\mathcal{M}_{A_0 \rightarrow A_1}^{0;x_1} \otimes \mathcal{N}_{B_0 \rightarrow B_1}^{0;x_1, y_1} \right) (\sigma_{A_0 B_0}^0). \quad (\text{B13})$$

Now, in the second round, Alice applies the conditional quantum instrument channel given by

$$\mathcal{M}_{X_1 Y_1 A_1 \rightarrow X_1 Y_1 X_2 A_2}^1 (|x_1, y_1><x_1, y_1|_{X_1 Y_1} \otimes \rho_{A_1}) := |x_1, y_1><x_1, y_1|_{X_1 Y_1} \otimes \mathcal{M}_{A_1 \rightarrow X_2 A_2}^{1;x_1, y_1}(\rho_{A_1}), \quad (\text{B14})$$

where $\mathcal{M}_{A_1 \rightarrow X_2 A_2}^{1;x_1, y_1}$ is a quantum instrument channel in which the underlying quantum instrument $\{\mathcal{M}_{A_1 \rightarrow A_2}^{1;x_1, y_1, x_2}\}_{x_2 \in X_2}$ is conditioned on the histories $\{(x_1, y_1) : x_1 \in X_1, y_1 \in Y_1\}$ of hers and Bob's prior outcomes. She sends the outcome $x_2 \in X_2$ of the quantum instrument to Bob, who then applies the conditional quantum instrument channel given by

$$\mathcal{N}_{X_1 Y_1 X_2 B_1 \rightarrow X_1 Y_1 X_2 Y_2 B_2}^1(|x_1, y_1, x_2\rangle\langle x_1, y_1, x_2|_{X_1 Y_1 X_2} \otimes \tau_{B_1}) := |x_1, y_1, x_2\rangle\langle x_1, y_1, x_2|_{X_1 Y_1 X_2} \otimes \mathcal{N}_{B_1 \rightarrow Y_2 B_2}^{1;x_1, y_1, x_2}(\tau_{B_1}), \quad (\text{B15})$$

where $\mathcal{N}_{B_1 \rightarrow Y_2 B_2}^{1;x_1, y_1, x_2}$ is a quantum instrument channel in which the underlying quantum instrument $\{\mathcal{N}_{B_1 \rightarrow B_2}^{1;x_1, y_1, x_2, y_2}\}_{y_2 \in Y_2}$ depends on the prior outcomes $x_1 \in X_1, y_1 \in Y_1, x_2 \in X_2$. The outcome of the instrument is $y_2 \in Y_2$, so that, at the end of the second round, the state shared by Alice and Bob is

$$\rho_{X_1 Y_1 X_2 Y_2 A_2 B_2}(2) = \sum_{h^2} |h^2\rangle\langle h^2|_{H_2} \otimes \tilde{\sigma}_{A_2 B_2}(2; h^2), \quad (\text{B16})$$

where we used the abbreviations

$$H_2 \equiv X_1 Y_1 X_2 Y_2, \quad (\text{B17})$$

$$h^2 \equiv (x_1, y_1, x_2, y_2) \in X_1 \times Y_1 \times X_2 \times Y_2, \quad (\text{B18})$$

and

$$\tilde{\sigma}(2; h^2) := \left(\mathcal{M}_{A_1 \rightarrow A_2}^{1;x_1, y_1, x_2} \circ \mathcal{M}_{A_0 \rightarrow A_1}^{0;x_1} \otimes \mathcal{N}_{B_1 \rightarrow B_2}^{1;h^2} \circ \mathcal{N}_{B_0 \rightarrow B_1}^{0;x_1, y_1} \right) (\sigma_{A_0 B_0}^0). \quad (\text{B19})$$

Let $h^j := (x_1, y_1, \dots, x_j, y_j) \in X_1 \times Y_1 \times \dots \times X_j \times Y_j$ be the history up to j steps, $j \in \{1, 2, \dots\}$. Proceeding in the manner presented above, at the j^{th} step of the protocol, Alice and Bob apply conditional quantum instrument channels of the form

$$\mathcal{M}_{H_j A_j \rightarrow H_j X_{j+1} A_{j+1}}^j \left(|h^j\rangle\langle h^j|_{H_j} \otimes \rho_{A_j} \right) = |h^j\rangle\langle h^j|_{H_j} \otimes \mathcal{M}_{A_j \rightarrow X_{j+1} A_{j+1}}^{j;h^j}(\rho_{A_j}) \quad (\text{B20})$$

and

$$\mathcal{N}_{H_j X_{j+1} B_j \rightarrow H_{j+1} B_{j+1}}^j \left(|h^j, x_{j+1}\rangle\langle h^j, x_{j+1}|_{H_j X_{j+1}} \otimes \sigma_{B_j} \right) = |h^j, x_{j+1}\rangle\langle h^j, x_{j+1}|_{H_j X_{j+1}} \otimes \mathcal{N}_{B_j \rightarrow Y_{j+1} B_{j+1}}^{j;h^j, x_{j+1}}(\sigma_{B_j}), \quad (\text{B21})$$

where

$$\mathcal{M}_{A_j \rightarrow X_{j+1} A_{j+1}}^{j;h^j}(\rho_{A_j}) = \sum_{x_{j+1} \in X_{j+1}} |x_{j+1}\rangle\langle x_{j+1}|_{X_{j+1}} \otimes \mathcal{M}_{A_j \rightarrow A_{j+1}}^{j;h^j, x_{j+1}}(\rho_{A_j}) \quad (\text{B22})$$

and

$$\mathcal{N}_{B_j \rightarrow Y_{j+1} B_{j+1}}^{j;h^j, x_{j+1}}(\sigma_{B_j}) = \sum_{y_{j+1} \in Y_{j+1}} |y_{j+1}\rangle\langle y_{j+1}|_{Y_{j+1}} \otimes \mathcal{N}_{B_j \rightarrow B_{j+1}}^{j;h^j, x_{j+1}, y_{j+1}}(\sigma_{B_j}). \quad (\text{B23})$$

Therefore, at the end of the t^{th} round, the classical-quantum state shared by Alice and Bob is

$$\rho_{H_t A_t B_t}(t) = \sum_{h^t} |h^t\rangle\langle h^t|_{H_t} \otimes \tilde{\sigma}_{A_t B_t}(t; h^t), \quad (\text{B24})$$

where $H_t \equiv X_1 Y_1 \dots X_t Y_t$, $h^t = (x_1, y_1, x_2, y_2, \dots, x_t, y_t)$,

$$\tilde{\sigma}(t; h^t) = \left(\mathcal{S}_{A_0 \rightarrow A_t}^{t;h^t} \otimes \mathcal{T}_{B_0 \rightarrow B_t}^{t;h^t} \right) (\sigma_{A_0 B_0}^0), \quad (\text{B25})$$

$$\mathcal{S}_{A_0 \rightarrow A_t}^{t;h^t} := \mathcal{M}_{A_{t-1} \rightarrow A_t}^{t-1;h_{t-1}^t, x_t} \circ \dots \circ \mathcal{M}_{A_1 \rightarrow A_2}^{1;h_1^t, x_2} \circ \mathcal{M}_{A_0 \rightarrow A_1}^{0;x_1}, \quad (\text{B26})$$

$$\mathcal{T}_{B_0 \rightarrow B_t}^{t;h^t} := \mathcal{N}_{B_{t-1} \rightarrow B_t}^{t-1;h^t} \circ \dots \circ \mathcal{N}_{B_1 \rightarrow B_2}^{1;h_2^t} \circ \mathcal{N}_{B_0 \rightarrow B_1}^{0;h_1^t}, \quad (\text{B27})$$

and we have defined $h_j^t := (x_1, y_1, x_2, y_2, \dots, x_j, y_j)$ for all $j \in \{1, 2, \dots, t-1\}$.

Now, if Alice and Bob discard the history of their outcomes, then this corresponds to tracing out the classical history register H_t , and it results in the state

$$\sigma_{A_t B_t}(t) := \text{Tr}_{H_t} [\rho_{H_t A_t B_t}(t)] \quad (\text{B28})$$

$$= \sum_{h^t} \tilde{\sigma}_{A_t B_t}(t; h^t) \quad (\text{B29})$$

$$= \sum_{h^t} (\mathcal{S}_{A_0 \rightarrow A_t}^{t; h^t} \otimes \mathcal{T}_{B_0 \rightarrow B_t}^{t; h^t})(\sigma_{A_0 B_0}^0), \quad (\text{B30})$$

which is of the form

$$\mathcal{L}_{AB \rightarrow \hat{A}\hat{B}}(\cdot) := \sum_{x \in \mathcal{X}} (\mathcal{S}_{A \rightarrow \hat{A}}^x \otimes \mathcal{T}_{B \rightarrow \hat{B}}^x)(\cdot). \quad (\text{B31})$$

Here, $\{\mathcal{S}^x\}_{x \in \mathcal{X}}$ and $\{\mathcal{T}^x\}_{x \in \mathcal{X}}$ are completely positive trace non-increasing maps such that the sum $\sum_{x \in \mathcal{X}} \mathcal{S}^x \otimes \mathcal{T}^x$ is a trace-preserving map.

Note that the sum $\sum_{h^t} \mathcal{S}^{t; h^t} \otimes \mathcal{T}^{t; h^t}$ in (B30) is indeed a trace-preserving map, because for every $j \in \{1, 2, \dots, t-1\}$, history h^{j-1} up to time $j-1$, and linear operator $X_{A_{j-1} B_{j-1}}$,

$$\begin{aligned} & \sum_{x_j, y_j} \text{Tr} \left[\left(\mathcal{M}_{A_{j-1} \rightarrow A_j}^{j-1; h^{j-1}, x_j} \otimes \mathcal{N}_{B_{j-1} \rightarrow B_j}^{j-1; h^{j-1}, x_j, y_j} \right) (X_{A_{j-1} B_{j-1}}) \right] \\ &= \sum_{x_j} \text{Tr} \left[\left(\mathcal{M}_{A_{j-1} \rightarrow A_j}^{j-1; h^{j-1}, x_j} \otimes \sum_{y_j} \mathcal{N}_{B_{j-1} \rightarrow B_j}^{j-1; h^{j-1}, x_j, y_j} \right) (X_{A_{j-1} B_{j-1}}) \right] \quad (\text{B32}) \end{aligned}$$

$$= \sum_{x_j} \text{Tr}_{A_j} \left[\mathcal{M}_{A_{j-1} \rightarrow A_j}^{j-1; h^{j-1}, x_j} (\text{Tr}_{B_{j-1}} [X_{A_{j-1} B_{j-1}}]) \right] \quad (\text{B33})$$

$$= \text{Tr}_{A_j} \left[\sum_{x_j} \mathcal{M}_{A_{j-1} \rightarrow A_j}^{j-1; h^{j-1}, x_j} (\text{Tr}_{B_{j-1}} [X_{A_{j-1} B_{j-1}}]) \right] \quad (\text{B34})$$

$$= \text{Tr}[X_{A_{j-1} B_{j-1}}], \quad (\text{B35})$$

where we have used the fact that $\sum_{y_j} \mathcal{N}_{B_{j-1} \rightarrow B_j}^{j-1; h^{j-1}, x_j, y_j}$ and $\sum_{x_j} \mathcal{M}_{A_{j-1} \rightarrow A_j}^{j-1; h^{j-1}, x_j}$ are trace-preserving maps. By applying this recursively at all time steps, it follows that for every linear operator $X_{A_0 B_0}$,

$$\text{Tr} \left[\sum_{h^t} (\mathcal{S}_{A_0 \rightarrow A_t}^{t; h^t} \otimes \mathcal{T}_{B_0 \rightarrow B_t}^{t; h^t})(X_{A_0 B_0}) \right] = \text{Tr}[X_{A_0 B_0}]. \quad (\text{B36})$$

So we conclude that the sum $\sum_{h^t} \mathcal{S}^{t; h^t} \otimes \mathcal{T}^{t; h^t}$ is a trace-preserving map.

Remark B.1 (LOCC instruments). From (B24) and (B25), the classical-quantum state $\rho_{H_t A_t B_t}(t)$ after t rounds of an LOCC protocol is

$$\rho_{H_t A_t B_t}(t) = \sum_{h^t} |h^t\rangle\langle h^t|_{H_t} \otimes \left(\mathcal{S}_{A_0 \rightarrow A_t}^{t; h^t} \otimes \mathcal{T}_{B_0 \rightarrow B_t}^{t; h^t} \right) (\sigma_{A_0 B_0}^0). \quad (\text{B37})$$

Observe that this state has exactly the form of the output state of a quantum instrument channel. In particular, letting

$$\mathcal{L}_{A_0 B_0 \rightarrow A_t B_t}^{t; h^t} := \mathcal{S}_{A_0 \rightarrow A_t}^{t; h^t} \otimes \mathcal{T}_{B_0 \rightarrow B_t}^{t; h^t}, \quad (\text{B38})$$

we see that the state $\rho_{H_t A_t B_t}(t)$ can be regarded as the output state of an *LOCC instrument*, i.e., a finite set $\{\mathcal{L}_{AB \rightarrow \hat{A}\hat{B}}^x\}_{x \in \mathcal{X}}$ of completely positive trace non-increasing LOCC maps such that sum $\sum_{x \in \mathcal{X}} \mathcal{L}_{AB \rightarrow \hat{A}\hat{B}}^x$ is a trace-preserving map, and thus an LOCC quantum channel.

Appendix C: Examples of elementary link generation

1. Ground-based transmission

The most common medium for quantum information transmission for communication purposes is photons traveling either through either free space or fiber-optic cables. These transmission media are modeled well by a bosonic pure-loss/attenuation

channel \mathcal{L}^η ¹³⁹, where $\eta \in (0, 1]$ is the transmittance of the medium, which for fiber-optic or free-space transmission has the form $\eta = e^{-\frac{L}{L_0}}$ ^{33–35}, where L is the transmission distance and L_0 is the attenuation length of the fiber.

Before the k quantum systems corresponding to the source state ρ^S are transmitted through the pure-loss channel, they are each encoded into d bosonic modes with $d \geq 2$. A simple encoding is the following:

$$|0_d\rangle := |1, 0, 0, \dots, 0\rangle, \quad (\text{C1})$$

$$|1_d\rangle := |0, 1, 0, \dots, 0\rangle, \quad (\text{C2})$$

⋮

$$|(d-1)_d\rangle := |0, 0, 0, \dots, 1\rangle, \quad (\text{C3})$$

sometimes called the *d-rail encoding*. In other words, using d bosonic modes, we form a qudit quantum system by defining the standard basis elements of the associated Hilbert space by the states corresponding to a single photon in each of the d modes. We let

$$|\text{vac}\rangle := |0, 0, \dots, 0\rangle \quad (\text{C4})$$

denote the vacuum state of the d modes, which is the state containing no photons.

In the context of photonic state transmission, the source state ρ^S is typically of the form $|\psi^S\rangle\langle\psi^S|$, where

$$|\psi^S\rangle = \sqrt{p_0^S}|\text{vac}\rangle + \sqrt{p_1^S}|\psi_1^S\rangle + \sqrt{p_2^S}|\psi_2^S\rangle + \dots, \quad (\text{C5})$$

where $|\psi_n^S\rangle$ is a state vector with n photons in total for each of the k parties and the numbers $p_n^S \geq 0$ are probabilities, so that $\sum_{n=0}^{\infty} p_n^S = 1$. For example, in the case $k = 2$ and $d = 2$, the following source state is generated from a parametric down-conversion process (see, e.g., Refs. [140 and 141]):

$$|\psi^S\rangle = \sum_{n=0}^{\infty} \frac{\sqrt{n+1}r^n}{e^q} |\psi_n^S\rangle, \quad (\text{C6})$$

$$|\psi_n^S\rangle = \frac{1}{\sqrt{n+1}} \sum_{m=0}^n (-1)^m |n-m, m; m, n-m\rangle, \quad (\text{C7})$$

where r and q are parameters characterizing the process. One often considers a truncated version of this state as an approximation, so that¹⁴¹

$$|\psi^S\rangle = \sqrt{p_0} |0, 0; 0, 0\rangle + \sqrt{\frac{p_1}{2}} (|1, 0; 0, 1\rangle + |0, 1; 1, 0\rangle) + \sqrt{\frac{p_2}{3}} (|2, 0; 0, 2\rangle + |1, 1; 1, 1\rangle + |0, 2; 2, 0\rangle), \quad (\text{C8})$$

where $p_0 + p_1 + p_2 = 1$.

Typically, the encoding into bosonic modes is not perfect, which means that a source state of the form (C5) is not ideal and that the desired state is given by one of the state vectors $|\psi_j^S\rangle$, and the other terms arise due to the naturally imperfect nature of the source. For example, for the state in (C8), the desired bipartite state is the maximally entangled state

$$|\Psi^+\rangle = \frac{1}{\sqrt{2}} (|1, 0; 0, 1\rangle + |0, 1; 1, 0\rangle). \quad (\text{C9})$$

Once the source state is prepared, each mode is sent through the pure-loss channel. Letting

$$\mathcal{L}^{\eta, (d)} := (\mathcal{L}^\eta)^{\otimes d} \quad (\text{C10})$$

denote the quantum channel that acts on the d modes of each of the k systems, the overall quantum channel through which the source state ρ^S is sent is

$$\mathcal{S}^{\vec{\eta}, (k; d)} := \mathcal{L}^{\eta_1, (d)} \otimes \mathcal{L}^{\eta_2, (d)} \otimes \dots \otimes \mathcal{L}^{\eta_k, (d)}, \quad (\text{C11})$$

where $\vec{\eta} = (\eta_1, \eta_2, \dots, \eta_k)$ and η_j is the transmittance of the medium to the j^{th} node in the edge. The quantum state shared by the k nodes after transmission from the source is then $\rho^{S, \text{out}} = \mathcal{S}^{\vec{\eta}, (k; d)}(\rho^S)$.

Now, it is known (see, e.g., Ref. [142]) that the action of the bosonic pure-loss channel on any linear operator σ_d encoded in d modes according to the encoding in (C3) is equivalent to the output of an erasure channel^{143,144}. In general, a d -dimensional

quantum erasure channel $\mathcal{E}_p^{(d)}$, with $p \in [0, 1]$, is defined as follows. Consider the vector space \mathbb{C}^d with orthonormal basis elements $\{|0\rangle, |1\rangle, \dots, |d-1\rangle\}$, and the vector space \mathbb{C}^{d+1} with orthonormal basis elements $\{|0\rangle, |1\rangle, \dots, |d-1\rangle, |d\rangle\}$. Then, for every linear operator $X \in \mathcal{L}(\mathbb{C}^d)$, $\mathcal{E}_p^{(d)}(X) = pX + (1-p)|d\rangle\langle d|$. Note that the output is an element of $\mathcal{L}(\mathbb{C}^{d+1})$. In particular, note that the vector $|d\rangle$ is orthogonal to the input vector space \mathbb{C}^d .

Lemma C.1 (Pure-loss channel with a d -rail encoding¹⁴²). Let $d \geq 2$. For every linear operator X acting on a d -dimensional Hilbert space defined by the basis elements in (C1)–(C3), we have that

$$\mathcal{L}^{\eta, (d)}(X) = (\mathcal{L}^{\eta})^{\otimes d}(\sigma_d) \quad (\text{C12})$$

$$= \eta X + (1-\eta)\text{Tr}[X]|\text{vac}\rangle\langle\text{vac}|. \quad (\text{C13})$$

Proof. To start, the bosonic pure-loss channel has the following Kraus representation^{145,146}:

$$\mathcal{L}^{\eta}(\rho) = \sum_{\ell=0}^{\infty} \frac{(1-\eta)^{\ell}}{\ell!} \sqrt{\eta}^{a^{\dagger}a} a^k \rho a^{k\dagger} \sqrt{\eta}^{a^{\dagger}a}, \quad (\text{C14})$$

where a and a^{\dagger} are the annihilation and creation operators of the bosonic mode, which are defined as $a|n\rangle = \sqrt{n}|n-1\rangle$ for all $n \geq 1$ (with $a|0\rangle = 0$), and $a^{\dagger}|n\rangle = \sqrt{n+1}|n+1\rangle$ for all $n \geq 0$.

Now, every linear operator X acting on a d -dimensional space that is encoded into d bosonic modes as in (C1)–(C3) can be written as

$$X = \sum_{\ell, \ell'=0}^{d-1} \alpha_{\ell, \ell'} |\ell_d\rangle\langle\ell'_d|, \quad (\text{C15})$$

for $\alpha_{\ell, \ell'} \in \mathbb{C}$. Using (C14), it is straightforward to show that

$$\mathcal{L}^{\eta}(|0\rangle\langle 0|) = |0\rangle\langle 0|, \quad (\text{C16})$$

$$\mathcal{L}^{\eta}(|0\rangle\langle 1|) = \sqrt{\eta}|0\rangle\langle 1|, \quad (\text{C17})$$

$$\mathcal{L}^{\eta}(|1\rangle\langle 0|) = \sqrt{\eta}|1\rangle\langle 0|, \quad (\text{C18})$$

$$\mathcal{L}^{\eta}(|1\rangle\langle 1|) = (1-\eta)|0\rangle\langle 0| + \eta|1\rangle\langle 1|. \quad (\text{C19})$$

Using this, we find that

$$(\mathcal{L}^{\eta})^{\otimes d}(|\ell_d\rangle\langle\ell'_d|) = \begin{cases} \eta|\ell_d\rangle\langle\ell_d| + (1-\eta)|\text{vac}\rangle\langle\text{vac}| & \text{if } \ell = \ell', \\ \eta|\ell_d\rangle\langle\ell'_d| & \text{if } \ell \neq \ell'. \end{cases} \quad (\text{C20})$$

Therefore,

$$(\mathcal{L}^{\eta})^{\otimes d}(X) = \eta \sum_{\ell, \ell'=0}^{d-1} \alpha_{\ell, \ell'} |\ell_d\rangle\langle\ell'_d| + (1-\eta) \left(\sum_{\ell=0}^{d-1} \alpha_{\ell, \ell} \right) |\text{vac}\rangle\langle\text{vac}| \quad (\text{C21})$$

$$= \eta X + (1-\eta)\text{Tr}[X]|\text{vac}\rangle\langle\text{vac}|, \quad (\text{C22})$$

as required. \square

After transmission from the source to the nodes, the heralding procedure typically involves doing measurements at the nodes to check whether all of the photons arrived. In the ideal case the quantum instrument $\{\mathcal{M}^0, \mathcal{M}^1\}$ for the heralding procedure corresponds simply to a measurement in the single-photon subspace defined by (C1)–(C3). To be specific, let

$$\Lambda^1 := \Pi^{(d)} \quad (\text{C23})$$

$$:= |0_d\rangle\langle 0_d| + |1_d\rangle\langle 1_d| + \dots + |(d-1)_d\rangle\langle(d-1)_d|, \quad (\text{C24})$$

$$\Lambda^0 := \mathbb{1}_{\mathcal{H}_d} - \Lambda^1, \quad (\text{C25})$$

where $\Pi^{(d)}$ is the projection onto the d -dimensional single-photon subspace defined by (C1)–(C3), and $\mathbb{1}_{\mathcal{H}_d}$ is the identity operator of the full Hilbert space \mathcal{H}_d of d bosonic modes. Then, letting $\vec{x} \in \{0, 1\}^k$ and defining

$$\Lambda^{\vec{x}} := \Lambda^{x_1} \otimes \Lambda^{x_2} \otimes \dots \otimes \Lambda^{x_k}, \quad (\text{C26})$$

the maps \mathcal{M}^0 and \mathcal{M}^1 have the form

$$\mathcal{M}^1(\cdot) = \Lambda^{\vec{1}}(\cdot)\Lambda^{\vec{1}}, \quad (\text{C27})$$

$$\mathcal{M}^0(\cdot) = \sum_{\substack{\vec{x} \in \{0,1\}^k \\ \vec{x} \neq \vec{1}}} \Lambda^{\vec{x}}(\cdot)\Lambda^{\vec{x}}. \quad (\text{C28})$$

These maps correspond to perfect photon-number-resolving detectors. However, the detectors are typically noisy due to dark counts and other imperfections (see, e.g., Refs. [141]), so that in practice the maps \mathcal{M}^0 and \mathcal{M}^1 will not have the ideal forms presented in (C27) and (C28).

Let

$$\tilde{\sigma}(0) := (\mathcal{M}^0 \circ \mathcal{S})(\rho^S), \quad (\text{C29})$$

$$\tilde{\sigma}(1) := (\mathcal{M}^1 \circ \mathcal{S})(\rho^S). \quad (\text{C30})$$

Then, if the source produces the ideal quantum state, such as the state in (C9), so that $\rho^S = \Psi^+ = |\Psi^+\rangle\langle\Psi^+|$, and if the heralding procedure is also ideal, then using (C12) we obtain

$$\tilde{\sigma}(1) = \eta_1 \eta_2 \Psi^+, \quad (\text{C31})$$

$$\begin{aligned} \tilde{\sigma}(0) = \eta_1 (1 - \eta_2) \frac{\Pi^{(2)}}{2} \otimes |\text{vac}\rangle\langle\text{vac}| \\ + (1 - \eta_1) \eta_2 |\text{vac}\rangle\langle\text{vac}| \otimes \frac{\Pi^{(2)}}{2} \\ + (1 - \eta_1)(1 - \eta_2) |\text{vac}\rangle\langle\text{vac}| \otimes |\text{vac}\rangle\langle\text{vac}|, \end{aligned} \quad (\text{C32})$$

which means that the transmission-heralding success probability as defined in (1) is simply $p = \text{Tr}[\tilde{\sigma}(1)] = \eta_1 \eta_2$.

Remark C.2 (Multiplexing). In practice, in order to increase the transmission-heralding success probability, multiplexing strategies are used. The term ‘‘multiplexing’’ here refers to the use of a single transmission channel to send multiple signals simultaneously, with the signals being encoded into distinct (i.e., orthogonal) frequency modes; see, e.g., Ref. [122]. If $M \geq 1$ distinct frequency modes are used, then the source state being transmitted is $(\rho^S)^{\otimes M}$. If p denotes the probability that any single one of the signals is received and heralded successfully, then the probability that at least one of the M signals is received and heralded successfully is $1 - (1 - p)^M$.

2. Transmission from satellites

Let us now consider the model of elementary link generation proposed in Ref. [147], in which the entanglement sources are placed on satellites orbiting the earth. For further information on satellite-based quantum communication, we refer to Ref. [148] for a review, and we refer to Refs. [149–152] for more detailed modeling of the satellite-to-ground quantum channel than what we consider here.

When modeling photon transmission from satellites to ground stations, we must take into account background photons. Here, we analyze the scenario in which a source on board a satellite generates an entangled photon pair and distributes the individual photons to two parties, Alice (A) and Bob (B), on the ground. We allow the distributed photons to mix with background photons from an uncorrelated thermal source. Also, as before, we use the bosonic encoding defined in (C1)–(C3), but we stick to $d = 2$, i.e., qubit source states and thus bipartite elementary links. In this scenario, it is common for the two modes to represent the polarization degrees of freedom of the photons, so that

$$|H\rangle \equiv |0_2\rangle = |1, 0\rangle, \quad (\text{C33})$$

$$|V\rangle \equiv |1_2\rangle = |0, 1\rangle \quad (\text{C34})$$

represent the state of one horizontally and vertically polarized photon, respectively.

Let \bar{n} be the average number of background photons. Then, as done in Ref. [147], we can define an approximate thermal background state as

$$\tilde{\Theta}^{\bar{n}} := (1 - \bar{n}) |\text{vac}\rangle\langle\text{vac}| + \frac{\bar{n}}{2} (|H\rangle\langle H| + |V\rangle\langle V|). \quad (\text{C35})$$

The transmission channel from the satellite to the ground stations is then

$$\mathcal{L}^{\eta_{\text{sg}}, \bar{n}}(\rho_{A_1 A_2}) := \text{Tr}_{E_1 E_2} \left[\left(U_{A_1 E_1}^{\eta_{\text{sg}}} \otimes U_{A_2 E_2}^{\eta_{\text{sg}}} \right) \left(\rho_{A_1 A_2} \otimes \tilde{\Theta}_{E_1 E_2}^{\bar{n}} \right) \left(U_{A_1 E_1}^{\eta_{\text{sg}}} \otimes U_{A_2 E_2}^{\eta_{\text{sg}}} \right)^{\dagger} \right], \quad (\text{C36})$$

where $U^{\eta_{\text{sg}}}$ is the beamsplitter unitary (see, e.g., Ref. [139]), and A_1 and A_2 refer to the horizontal and vertical polarization modes, respectively, of the dual-rail quantum system being transmitted; similarly for E_1 and E_2 . Note that for $\bar{n} = 0$, the transformation in (C36) reduces to the one in (C12) with $d = 2$.

For a source state ρ_{AB}^S , with $A \equiv A_1 A_2$ and $B \equiv B_1 B_2$, the quantum state shared by Alice and Bob after transmission of the state ρ_{AB}^S from the satellite to the ground stations is

$$\rho_{AB}^{S, \text{out}} = \left(\mathcal{L}_A^{\eta_{\text{sg}}^{(1)}, \bar{n}_1} \otimes \mathcal{L}_B^{\eta_{\text{sg}}^{(2)}, \bar{n}_2} \right) (\rho_{AB}^S), \quad (\text{C37})$$

where $\eta_{\text{sg}}^{(1)}$ and $\eta_{\text{sg}}^{(2)}$ are the transmittances to the ground stations and \bar{n}_1 and \bar{n}_2 are the corresponding thermal background noise parameters. In Sec. D, we look at a specific example of a source state ρ_{AB}^S , and thus provide an explicit form for the state $\rho_{AB}^{S, \text{out}}$. We also consider the heralding procedure defined by (C24)–(C28), and thus provide explicit forms for the states σ^0 and τ^\varnothing in (2) and (3) corresponding to success and failure, respectively, of the heralding procedure.

The transmittance η_{sg} generally depends on atmospheric conditions (such as turbulence and weather conditions) and on orbital parameters (such as altitude and zenith angle)^{150–152}. In general, if the satellite is at altitude h and the path length from the satellite to the ground station is L , then

$$\eta_{\text{sg}}(L, h) = \eta_{\text{fs}}(L) \eta_{\text{atm}}(L, h), \quad (\text{C38})$$

where

$$\eta_{\text{fs}}(L) = 1 - \exp \left(-\frac{2r^2}{w(L)^2} \right), \quad (\text{C39})$$

$$w(L) := w_0 \sqrt{1 + \left(\frac{L}{L_R} \right)^2}, \quad (\text{C40})$$

$$L_R := \pi w_0^2 \lambda^{-1}, \quad (\text{C41})$$

and

$$\eta_{\text{atm}}(L, h) = \begin{cases} (\eta_{\text{atm}}^{\text{zen}})^{\sec \zeta} & \text{if } -\frac{\pi}{2} < \zeta < \frac{\pi}{2}, \\ 0 & \text{if } |\zeta| \geq \frac{\pi}{2}, \end{cases} \quad (\text{C42})$$

with $\eta_{\text{atm}}^{\text{zen}}$ the transmittance at zenith ($\zeta = 0$). In general, the zenith angle ζ is given by

$$\cos \zeta = \frac{h}{L} - \frac{1}{2} \frac{L^2 - h^2}{R_{\oplus} L} \quad (\text{C43})$$

for a circular orbit of altitude h , with $R_{\oplus} \approx 6378$ km being the earth's radius. The following parameters thus characterize the total transmittance from satellite to ground: the initial beam waist w_0 , the receiving aperture radius r , the wavelength λ of the satellite-to-ground signals, and the atmospheric transmittance $\eta_{\text{atm}}^{\text{zen}}$ at zenith. Throughout the rest of this section, we take¹⁴⁷ $r = 0.75$ m, $w_0 = 2.5$ cm, $\lambda = 810$ nm, and $\eta_{\text{atm}}^{\text{zen}} = 0.5$ at 810 nm¹⁴⁹.

After transmission, we assume a heralding procedure defined by post-selecting on coincident events using (perfect) photon-number-resolving detectors. One can justify this assumption because, in the high-loss and low-noise regimes ($\eta_{\text{sg}}^{(1)}, \eta_{\text{sg}}^{(2)}, \bar{n} \ll 1$), the probability of four-photon and three-photon occurrences is negligible compared to two-photon events. Therefore, upon successful heralding, the (unnormalized) quantum state shared by Alice and Bob is

$$\tilde{\sigma}_{AB}(1) := \Pi_{AB} \left(\mathcal{L}_A^{\eta_{\text{sg}}^{(1)}, \bar{n}_1} \otimes \mathcal{L}_B^{\eta_{\text{sg}}^{(2)}, \bar{n}_2} \right) (\rho_{AB}^S) \Pi_{AB}, \quad (\text{C44})$$

where

$$\Pi_{AB} := (|H\rangle\langle H|_A + |V\rangle\langle V|_A) \otimes (|H\rangle\langle H|_B + |V\rangle\langle V|_B) \quad (\text{C45})$$

is the projection onto the two-photon-coincidence subspace. Note that the projection Π_{AB} is exactly the projection $\Lambda^1 \otimes \Lambda^1$, with Λ^1 defined in (C24). Then, the transmission-heralding success probability is, as per the definition in (1),

$$p := \text{Tr}[\tilde{\sigma}_{AB}(1)] \quad (\text{C46})$$

$$= \text{Tr}\left[\Pi_{AB} \left(\mathcal{L}_A^{\eta_{\text{sg}}^{(1)}, \bar{n}_1} \otimes \mathcal{L}_B^{\eta_{\text{sg}}^{(2)}, \bar{n}_2}\right) (\rho_{AB}^S)\right]. \quad (\text{C47})$$

Now, let us take the source state ρ_{AB}^S to be the following:

$$\rho_{AB}^S = f_S \Phi_{AB}^+ + \left(\frac{1-f_S}{3}\right) (\Phi_{AB}^- + \Psi_{AB}^+ + \Psi_{AB}^-), \quad (\text{C48})$$

where $f_S \in [0, 1]$ and

$$\Phi_{AB}^\pm := |\Phi^\pm\rangle\langle\Phi^\pm|_{AB}, \quad (\text{C49})$$

$$\Psi_{AB}^\pm := |\Psi^\pm\rangle\langle\Psi^\pm|_{AB}, \quad (\text{C50})$$

$$|\Phi^\pm\rangle_{AB} := \frac{1}{\sqrt{2}}(|H, H\rangle_{AB} \pm |V, V\rangle_{AB}), \quad (\text{C51})$$

$$|\Psi^\pm\rangle_{AB} := \frac{1}{\sqrt{2}}(|H, V\rangle_{AB} \pm |V, H\rangle_{AB}). \quad (\text{C52})$$

Using (C48), we obtain an explicit form for the (unnormalized) state $\tilde{\sigma}_{AB}(1)$ in (C44).

Proposition C.3 (Quantum state of a satellite-to-ground elementary link¹⁴⁷). Let $\eta_{\text{sg}}^{(1)}, \eta_{\text{sg}}^{(2)}, \bar{n}_1, \bar{n}_2 \in [0, 1]$, and consider the source state ρ_{AB}^S given by (C48). Then, after successful heralding, the (unnormalized) state $\tilde{\sigma}_{AB}(1)$ given by (C44) is equal to

$$\begin{aligned} \tilde{\sigma}_{AB}(1) &= \Pi_{AB} \left(\mathcal{L}_A^{\eta_{\text{sg}}^{(1)}, \bar{n}_1} \otimes \mathcal{L}_B^{\eta_{\text{sg}}^{(2)}, \bar{n}_2}\right) (\rho_{AB}^S) \Pi_{AB} \\ &= \frac{1}{2} \left(f_S(a+b) + \left(\frac{1-f_S}{3}\right)(a+2c-b)\right) \Phi_{AB}^+ \\ &\quad + \frac{1}{2} \left(f_S(a-b) + \left(\frac{1-f_S}{3}\right)(a+2c+b)\right) \Phi_{AB}^- \\ &\quad + \frac{1}{2} \left(f_S c + \left(\frac{1-f_S}{3}\right)(2a+c)\right) \Psi_{AB}^+ \\ &\quad + \frac{1}{2} \left(f_S c + \left(\frac{1-f_S}{3}\right)(2a+c)\right) \Psi_{AB}^-, \end{aligned} \quad (\text{C53})$$

where

$$a := x_1 x_2 + y_1 y_2, \quad b := z_1 z_2, \quad c := x_1 y_2 + y_1 x_2, \quad (\text{C54})$$

and

$$x_i := (1 - \bar{n}_i) \eta_{\text{sg}}^{(i)} + \frac{\bar{n}_i}{2} \left(\left(1 - 2\eta_{\text{sg}}^{(i)}\right)^2 + \left(\eta_{\text{sg}}^{(i)}\right)^2 \right), \quad (\text{C55})$$

$$y_i := \frac{\bar{n}_i}{2} \left(1 - \eta_{\text{sg}}^{(i)}\right)^2, \quad (\text{C56})$$

$$z_i := (1 - \bar{n}_i) \eta_{\text{sg}}^{(i)} - \bar{n}_i \eta_{\text{sg}}^{(i)} \left(1 - 2\eta_{\text{sg}}^{(i)}\right), \quad (\text{C57})$$

for $i \in \{1, 2\}$.

From (C53), we have that the transmission-heralding success probability is given by

$$p = \text{Tr}[\tilde{\sigma}_{AB}(1)] = a + c = (x_1 + y_1)(x_2 + y_2), \quad (\text{C58})$$

so that the quantum state shared by Alice and Bob conditioned on successful heralding is, as per the definition in (2),

$$\sigma_{AB}^0 = \frac{\tilde{\sigma}_{AB}(1)}{p}. \quad (\text{C59})$$

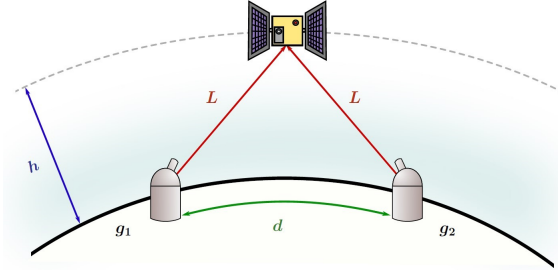


FIG. 12. Optical satellite-to-ground transmission¹⁴⁷. Two ground stations g_1 and g_2 are separated by a distance d with a satellite at altitude h at the midpoint. Both ground stations are the same distance L away from the satellite, so that the total transmittance for two-qubit entanglement transmission (one qubit to each ground station) is η_{sg}^2 , where $\eta_{\text{sg}} = \eta_{\text{fs}}\eta_{\text{atm}}$, with η_{fs} given by (C39) and η_{atm} given by (C42).

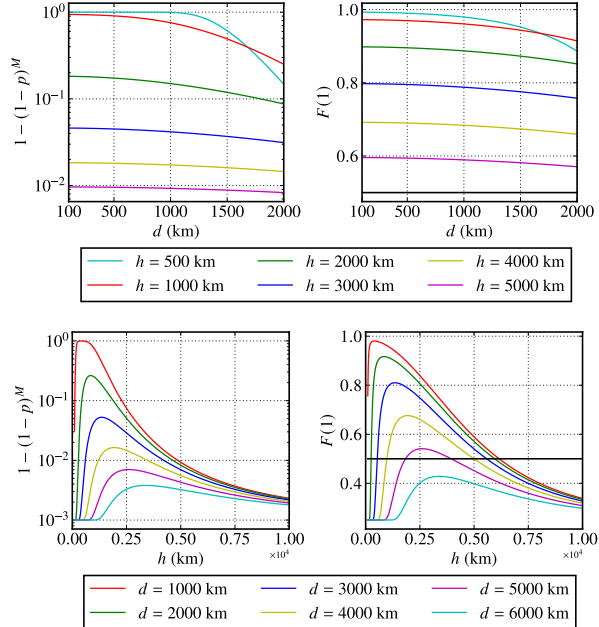


FIG. 13. Plots of the transmission-heralding success probability as well as the initial fidelity of the quantum state σ_{AB}^0 conditioned on successful heralding for the situation depicted in Fig. 12, in which $\eta_{\text{sg}}^{(1)} = \eta_{\text{sg}}^{(2)} = \eta_{\text{sg}}$ and $\bar{n}_1 = \bar{n}_2 = \bar{n}$. Indicated is the threshold fidelity of $\frac{1}{2}$ beyond which the state σ_{AB}^0 is entangled (see Proposition C.4). The success probability is shown in a multiplexing setting with $M = 10^5$ (see Remark C.2). Also, we have let $\bar{n} = 10^{-4}$ and $f_S = 1$.

a. Success probability and fidelity. Let us now evaluate the quality of entanglement transmission from a satellite to two ground stations. For illustrative purposes, and for simplicity, we focus primarily on the simple scenario depicted in Fig. 12, in which a satellite passes over the midpoint between two ground stations, although the same analysis can be done even when this is not the case. Since the satellite is an equal distance away from both ground stations, we have $\eta_{\text{sg}}^{(1)} = \eta_{\text{sg}}^{(2)}$. We also let $\bar{n}_1 = \bar{n}_2$. This means that $x_1 = x_2 \equiv x$, $y_1 = y_2 \equiv y$ and $z_1 = z_2 \equiv z$, so that

$$a = x^2 + y^2, \quad b = z^2, \quad c = 2xy \quad (\eta_{\text{sg}}^{(1)} = \eta_{\text{sg}}^{(2)} = \eta_{\text{sg}} \text{ and } \bar{n}_1 = \bar{n}_2 = \bar{n}). \quad (\text{C60})$$

In this scenario, given a distance d between the ground stations and an altitude h for the satellite, by simple geometry the distance L between the satellite and either ground station is given by

$$L = \sqrt{4R_{\oplus}(R_{\oplus} + h) \sin^2\left(\frac{d}{4R_{\oplus}}\right) + h^2}, \quad (\text{C61})$$

where R_{\oplus} is the radius of the earth.

Now, let us consider the transmission-heralding success probability p in (C58). Due to the altitude of the satellites, there typically has to be multiplexing of the signals (see Remark C.2) in order to maintain a high probability of both ground stations

receiving the entangled state. In Fig. 13, we plot the success probability with multiplexing, which is given by $1 - (1 - p)^M$, where M is the number of distinct frequency modes used for multiplexing.

We also plot in Fig. 13 the fidelity of the initial state, which is given by

$$F(1) = \langle \Phi^+ | \sigma_{AB}^0 | \Phi^+ \rangle = \frac{1}{p} \tilde{F}(1), \quad (\text{C62})$$

$$\tilde{F}(1) = \langle \Phi^+ | \tilde{\sigma}_{AB}(1) | \Phi^+ \rangle \quad (\text{C63})$$

$$= \frac{1}{2} f_S (a + b) + \frac{1}{2} \left(\frac{1 - f_S}{3} \right) (a + 2c - b), \quad (\text{C64})$$

with a, b, c given by (C54) in general and by (C60) in the special case depicted in Fig. 12.

The fidelity of σ_{AB}^0 with respect to Φ_{AB}^+ is related in a simple way to the entanglement of σ_{AB}^0 . In particular, by the partial positive transpose (PPT) criterion^{153,154}, σ_{AB}^0 is entangled if and only if its fidelity with respect to Φ_{AB}^+ is strictly greater than $\frac{1}{2}$, and this leads to constraints on the loss and noise parameters of the satellite-to-ground transmission.

Proposition C.4. The quantum state σ_{AB}^0 after successful satellite-to-ground transmission, as defined in (C59), is entangled if and only if the fidelity of the source state in (C48) satisfies $f_S > \frac{1}{2}$, and

$$2(f_S - 1)a + (4f_S - 1)b - (1 + 2f_S)c > 0, \quad (\text{C65})$$

with a, b, c given by (C54) in general and by (C60) in the special case depicted in Fig. 12.

Proof. Observe that the state σ_{AB}^0 is a Bell-diagonal state of the form

$$\sigma_{AB}^0 = (\alpha + \beta) \Phi_{AB}^+ + (\alpha - \beta) \Phi_{AB}^- + \gamma \Psi_{AB}^+ + \gamma \Psi_{AB}^-, \quad (\text{C66})$$

where $\alpha, \beta, \gamma \geq 0$ (when $f_S > \frac{1}{2}$). Indeed, the coefficient of Φ_{AB}^+ in (C53) can be written as

$$\frac{1}{2} f_S a + \frac{1}{2} \left(\frac{1 - f_S}{3} \right) (a + 2c) + \frac{1}{2} f_S b - \frac{1}{2} \left(\frac{1 - f_S}{3} \right) b, \quad (\text{C67})$$

and the coefficient of Φ_{AB}^- in (C53) can be written as

$$\frac{1}{2} f_S a + \frac{1}{2} \left(\frac{1 - f_S}{3} \right) (a + 2c) - \left(\frac{1}{2} f_S b - \frac{1}{2} \left(\frac{1 - f_S}{3} \right) b \right). \quad (\text{C68})$$

We can thus make the following identifications:

$$\alpha \equiv \frac{1}{a + c} \left(\frac{1}{2} f_S a + \frac{1}{2} \left(\frac{1 - f_S}{3} \right) (a + 2c) \right), \quad (\text{C69})$$

$$\beta \equiv \frac{1}{a + c} \left(\frac{1}{2} f_S b - \frac{1}{2} \left(\frac{1 - f_S}{3} \right) b \right), \quad (\text{C70})$$

$$\gamma \equiv \frac{1}{2} f_S c + \frac{1}{2} \left(\frac{1 - f_S}{3} \right) (2a + c). \quad (\text{C71})$$

Now, using the PPT criterion^{153,154}, we have that σ_{AB}^0 is entangled if and only if $\langle \Phi^+ | \sigma_{AB}^0 | \Phi^+ \rangle > \frac{1}{2}$. Then, from (C62), we have that

$$\langle \Phi^+ | \sigma_{AB}^0 | \Phi^+ \rangle = \frac{1}{2} f_S \frac{a + b}{a + c} + \frac{1}{2} \left(\frac{1 - f_S}{3} \right) \frac{a + 2c - b}{a + c}, \quad (\text{C72})$$

so we require

$$\frac{1}{2} f_S \frac{a + b}{a + c} + \frac{1}{2} \left(\frac{1 - f_S}{3} \right) \frac{a + 2c - b}{a + c} > \frac{1}{2}. \quad (\text{C73})$$

Simplifying this leads to

$$2(f_S - 1)a + (4f_S - 1)b - (1 + 2f_S)c > 0, \quad (\text{C74})$$

as required. \square

Now, for the scenario depicted in Fig. 12, we have that $x_1 = x_2 = x$, $y_1 = y_2 = y$, and $z_1 = z_2 = z$, so that from (C60) we have $a = x^2 + y^2$, $b = z^2$, and $c = 2xy$. Substituting this into (C65) leads to $2(f_S - 1)(x^2 + y^2) + (4f_S - 1)z^2 - 2(1 + 2f_S)xy > 0$ as the condition for σ_{AB}^0 to be entangled. We plot this condition in Fig. 14. The inequality gives us the colored regions, and the values within the regions are obtained by evaluating the fidelity according to (C62).

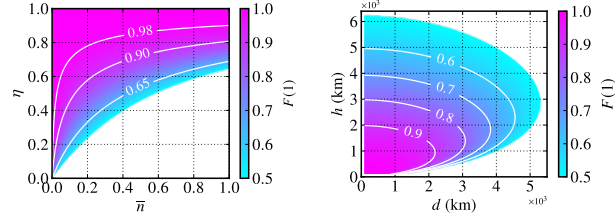


FIG. 14. Plots of the entanglement region for the state σ_{AB}^0 obtained after successful satellite-to-ground transmission for the scenario depicted in Fig. 12. The regions are defined by the condition $F(1) > \frac{1}{2}$, with $F(1)$ the fidelity of the state σ_{AB}^0 with the maximally entangled state; see (C62) and Proposition C.4. For both plots, we assume $f_S = 1$. For the right-hand plot, we take $\bar{n}_1 = \bar{n}_2 = 10^{-4}$.

b. Key rates for QKD. Let us also consider key rates for quantum key distribution (QKD) between Alice and Bob, who are at the ends of the elementary link whose quantum state is σ_{AB}^0 (conditioned on successful transmission and heralding), as given by (C59). We consider the BB84, six-state, and device-independent (DI) QKD protocols, and we calculate the secret key rates using known asymptotic secret key rate formulas, which we review (along with other necessary background on QKD) in Appendix E.

Recalling from the proof of Proposition C.4 that σ_{AB}^0 is a quantum state of the form

$$\sigma_{AB}^0 = (\alpha + \beta)\Phi_{AB}^+ + (\alpha - \beta)\Phi_{AB}^- + \gamma\Psi_{AB}^+ + \gamma\Psi_{AB}^-, \quad (\text{C75})$$

with α, β, γ defined in (C69)–(C71), it is easy to show using (E2)–(E6) that the quantum bit-error rates for the BB84 and six-state protocols are

$$Q_{\text{BB84}}^{(d,h)} = \frac{1}{2}(Q_x + Q_z) = \frac{3}{4} - \frac{1}{2}\beta - \alpha, \quad (\text{C76})$$

$$Q_{\text{6-state}}^{(d,h)} = \frac{1}{3}(Q_x + Q_y + Q_z) = \frac{2}{3}(1 - (\alpha + \beta)). \quad (\text{C77})$$

For the device-independent protocol, we assume that the correlation is such that the quantum bit-error rate is $Q_{\text{DI}}^{(d,h)} = Q_{\text{6-state}}^{(d,h)}$ and $S^{(d,h)} = 2\sqrt{2}(1 - 2Q_{\text{DI}}^{(d,h)})$. Then, assuming that M signals per second are transmitted from the satellite, the secret-key rate (in units of secret key bits per second) is given by $\tilde{K} = pMK$, where $p = a + c$ is the success probability of elementary link generation and K is the asymptotic secret key rate per copy of the state σ_{AB}^0 , which depends on the protocol under consideration. Using the formulas in Appendix E, we obtain

$$\tilde{K}_{\text{BB84}}(d, h) = M(a + c)K_{\text{BB84}}(Q_{\text{BB84}}^{(d,h)}) \quad (\text{C78})$$

$$\tilde{K}_{\text{6-state}}(d, h) = M(a + c)K_{\text{6-state}}(Q_{\text{6-state}}^{(d,h)}) \quad (\text{C79})$$

$$\tilde{K}_{\text{DI}}(d, h) = M(a + c)K_{\text{DI}}(Q_{\text{DI}}^{(d,h)}, S^{(d,h)}) \quad (\text{C80})$$

We plot these secret key rates in Fig. 15.

In Fig. 15, notice that the region of non-zero secret key rate is largest for the six-state protocol, with the region for the BB84 protocol being smaller and the region for the DI protocol being even smaller. This is due to the fact that the error threshold for the DI protocol is the smallest among the three protocols, with the error threshold for the BB84 protocol slightly larger, and the error threshold for the 6-state protocol the largest.

Appendix D: Policies for satellite-to-ground entanglement distribution

In this section, we present an example of an analysis of elementary links based on the satellite-to-ground transmission model presented in Sec. C2 based on Ref. [147].

1. Quantum memory model

Having examined the quantum state immediately after successful transmission and heralding, let us now consider a particular model of decoherence for the quantum memories in which the transmitted qubits are stored. For illustrative purposes, we consider a simple amplitude damping decoherence model for the quantum memories. The amplitude damping channel \mathcal{A}_γ is a qubit channel, with $\gamma \in [0, 1]$, such that¹³³

$$\mathcal{A}_\gamma(|0\rangle\langle 0|) = |0\rangle\langle 0|, \quad (\text{D1})$$

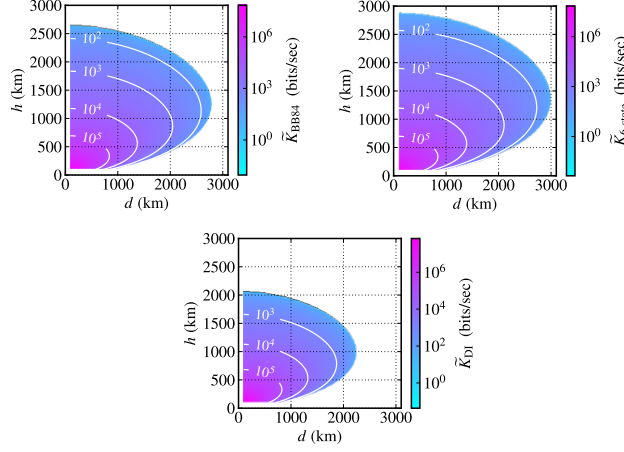


FIG. 15. Asymptotic secret key rates for the BB84, six-state, and device-independent (DI) quantum key distribution protocols for the scenario depicted in Fig. 12. When calculating the error rates in (C76) and (C77), we take $f_S = 1$. To calculate the key rates in (C78), (C79), and (C80), we have taken $M = 10^9$.

$$\mathcal{A}_\gamma(|0\rangle\langle 1|) = \sqrt{1-\gamma}|0\rangle\langle 1|, \quad (\text{D2})$$

$$\mathcal{A}_\gamma(|1\rangle\langle 0|) = \sqrt{1-\gamma}|1\rangle\langle 0|, \quad (\text{D3})$$

$$\mathcal{A}_\gamma(|1\rangle\langle 1|) = \gamma|0\rangle\langle 0| + (1-\gamma)|1\rangle\langle 1|. \quad (\text{D4})$$

Note that for $\gamma = 0$ we recover the noiseless (identity) channel. We can relate γ to the coherence time of the quantum memory, which we denote by t_{coh} , as follows [155, Sec. 3.4.3]:

$$\gamma := 1 - e^{-\frac{1}{t_{\text{coh}}}}. \quad (\text{D5})$$

Note that infinite coherence time corresponds to an ideal quantum memory, meaning that the quantum channel is noiseless. Indeed, by relating the noise parameter γ to the coherence time as in (D5), we have that $t_{\text{coh}} = \infty \Rightarrow \gamma = 0$.

For $m \in \mathbb{N}_0$ applications of the amplitude damping channel, it is straightforward to show that

$$\mathcal{A}_\gamma^{\circ m}(|0\rangle\langle 0|) = |0\rangle\langle 0|, \quad (\text{D6})$$

$$\mathcal{A}_\gamma^{\circ m}(|0\rangle\langle 1|) = \sqrt{\lambda_m}|0\rangle\langle 1|, \quad (\text{D7})$$

$$\mathcal{A}_\gamma^{\circ m}(|1\rangle\langle 0|) = \sqrt{\lambda_m}|1\rangle\langle 0|, \quad (\text{D8})$$

$$\mathcal{A}_\gamma^{\circ m}(|1\rangle\langle 1|) = (1 - \lambda_m)|0\rangle\langle 0| + \lambda_m|1\rangle\langle 1|, \quad (\text{D9})$$

where $\lambda_m := e^{-\frac{m}{t_{\text{coh}}}} = (1 - \gamma)^m$. Then, for all $m \in \mathbb{N}_0$,

$$\sigma_{AB}(m) := (\mathcal{A}_\gamma^{\circ m} \otimes \mathcal{A}_\gamma^{\circ m})(\sigma_{AB}^0) \quad (\text{D10})$$

$$= \left(\alpha \lambda_m^2 + \left(\beta - \frac{1}{2} \right) \lambda_m + \frac{1}{2} \right) \Phi_{AB}^+ + \left(\alpha \lambda_m^2 + \left(-\beta - \frac{1}{2} \right) \lambda_m + \frac{1}{2} \right) \Phi_{AB}^- \quad (\text{D11})$$

$$+ \lambda_m \left(\frac{1}{2} - \alpha \lambda_m \right) \Psi_{AB}^+ + \lambda_m \left(\frac{1}{2} - \alpha \lambda_m \right) \Psi_{AB}^- \quad (\text{D12})$$

$$+ \frac{1}{2} (1 - \lambda_m) (|\Phi^+\rangle\langle\Phi^-|_{AB} + |\Phi^-\rangle\langle\Phi^+|_{AB}), \quad (\text{D13})$$

where α and β are given by (C69) and (C70), respectively. Note that we have assumed that the memories corresponding to systems A and B have the same coherence time. It follows that

$$f(m) = \langle \Phi^+ | (\mathcal{A}_\gamma^{\circ m} \otimes \mathcal{A}_\gamma^{\circ m})(\sigma_{AB}^0) | \Phi^+ \rangle = \alpha \lambda_m^2 + \left(\beta - \frac{1}{2} \right) \lambda_m + \frac{1}{2}, \quad (\text{D14})$$

for all $m \in \mathbb{N}_0$. Note that $f(m) \leq f(0)$ for all $m \in \mathbb{N}_0$.

2. Memory-cutoff policy

Let us now consider the memory-cutoff policy, which we defined in Sec. II C. In what follows, we make use of the following definitions for the deterministic decision functions corresponding to the memory-cutoff policy:

$$d^{t^*}(m) := \begin{cases} 0 & \text{if } m \in \{0, 1, \dots, t^* - 1\}, \\ 1 & \text{if } m = -1, t^*, \end{cases} \quad (\text{D15})$$

$$d^\infty(m) := \begin{cases} 0 & \text{if } m \in \{0, 1, 2, \dots\}, \\ 1 & \text{if } m = -1. \end{cases} \quad (\text{D16})$$

Using (33) and (35), along with the expression for $f(m)$ in (D14), for every cutoff $t^* \in \mathbb{N}_0$ we obtain

$$\lim_{t \rightarrow \infty} \tilde{F}^{t^*}(t) = \frac{p}{1 + t^* p} \sum_{m=0}^{t^*} \left(\alpha \lambda_m^2 + \left(\beta - \frac{1}{2} \right) \lambda_m + \frac{1}{2} \right), \quad (\text{D17})$$

$$\lim_{t \rightarrow \infty} F^{t^*}(t) = \frac{1}{t^* + 1} \sum_{m=0}^{t^*} \left(\alpha \lambda_m^2 + \left(\beta - \frac{1}{2} \right) \lambda_m + \frac{1}{2} \right). \quad (\text{D18})$$

Then, using the fact that $\lambda_m = e^{-\frac{m}{t_{\text{coh}}}}$, it is straightforward to show that

$$\sum_{m=0}^{t^*} \lambda_m = e^{-\frac{t^*}{2t_{\text{coh}}}} \frac{\sinh\left(\frac{1+t^*}{2t_{\text{coh}}}\right)}{\sinh\left(\frac{1}{2t_{\text{coh}}}\right)}, \quad (\text{D19})$$

$$\sum_{m=0}^{t^*} \lambda_m^2 = e^{-\frac{t^*}{t_{\text{coh}}}} \frac{\sinh\left(\frac{1+t^*}{t_{\text{coh}}}\right)}{\sinh\left(\frac{1}{t_{\text{coh}}}\right)}. \quad (\text{D20})$$

Therefore, in the steady-state limit,

$$\lim_{t \rightarrow \infty} \tilde{F}^{t^*}(t) = \frac{\alpha p e^{-\frac{t^*}{t_{\text{coh}}}}}{1 + t^* p} \frac{\sinh\left(\frac{1+t^*}{t_{\text{coh}}}\right)}{\sinh\left(\frac{1}{t_{\text{coh}}}\right)} + \frac{p e^{-\frac{t^*}{2t_{\text{coh}}}}}{1 + t^* p} \left(\beta - \frac{1}{2} \right) \frac{\sinh\left(\frac{1+t^*}{2t_{\text{coh}}}\right)}{\sinh\left(\frac{1}{2t_{\text{coh}}}\right)} + \frac{1}{2} \frac{(t^* + 1)p}{1 + t^* p}, \quad (\text{D21})$$

$$\lim_{t \rightarrow \infty} F^{t^*}(t) = \frac{\alpha e^{-\frac{t^*}{t_{\text{coh}}}}}{t^* + 1} \frac{\sinh\left(\frac{1+t^*}{t_{\text{coh}}}\right)}{\sinh\left(\frac{1}{t_{\text{coh}}}\right)} + \frac{e^{-\frac{t^*}{2t_{\text{coh}}}}}{t^* + 1} \left(\beta - \frac{1}{2} \right) \frac{\sinh\left(\frac{1+t^*}{2t_{\text{coh}}}\right)}{\sinh\left(\frac{1}{2t_{\text{coh}}}\right)} + \frac{1}{2}. \quad (\text{D22})$$

For $t^* = \infty$, from (36), we obtain

$$\tilde{F}^\infty(t) = \sum_{m=0}^{t-1} \left(\alpha \lambda_m^2 + \left(\beta - \frac{1}{2} \right) \lambda_m + \frac{1}{2} \right) p(1-p)^{t-1-m} \quad (\text{D23})$$

for all $t \geq 1$. Evaluating the sums leads to

$$\tilde{F}^\infty(t) = \frac{\alpha p e^{\frac{2}{t_{\text{coh}}}} \left(e^{-\frac{2t}{t_{\text{coh}}}} - (1-p)^t \right)}{1 - e^{\frac{2}{t_{\text{coh}}}} (1-p)} + \left(\beta - \frac{1}{2} \right) \frac{p e^{\frac{1}{t_{\text{coh}}}} \left(e^{-\frac{t}{t_{\text{coh}}}} - (1-p)^t \right)}{1 - e^{\frac{1}{t_{\text{coh}}}} (1-p)} + \frac{1}{2} (1 - (1-p)^t). \quad (\text{D24})$$

Then, for all $p \in (0, 1]$, we obtain $\lim_{t \rightarrow \infty} \tilde{F}^\infty(t) = \frac{1}{2}$.

Let us now focus primarily on the $t^* = \infty$ memory-cutoff policy by considering an example. Consider the situation depicted in Fig. 12, in which we have two ground stations separated by a distance d and a satellite at altitude h that passes over the midpoint between the two ground stations. Now, given that the ground stations are separated by a distance d , it takes time at least $\frac{2d}{c}$ to perform the heralding procedure, as this is the round-trip communication time between the ground stations (c is the speed of light). We thus take the duration of each time step in the decision process for the elementary link to be $\frac{2d}{c}$. If the coherence time of the

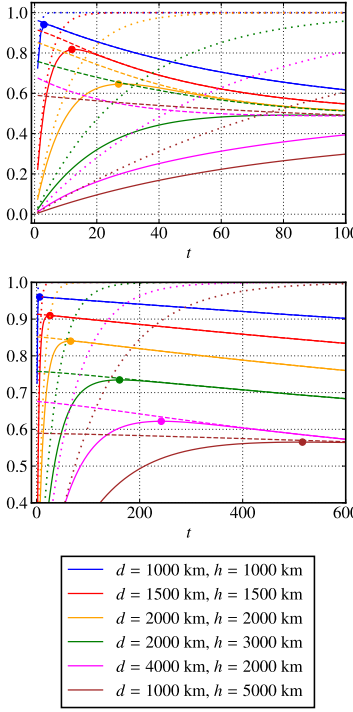


FIG. 16. The $t^* = \infty$ memory-cutoff policy for satellite-to-ground elementary link generation for various ground distances d and satellite altitudes h , according to the situation depicted in Fig. 12. The solid lines are $\tilde{F}^\infty(t)$ (as given by (D24)), the dashed lines are $F^\infty(t)$, and the dotted lines are $X^\infty(t) = 1 - (1 - p)^t$ (see (37)), where $p = 1 - (1 - (a + c))^M$, with a and c given by (C60) and $M = 10^5$. We let $f_S = 1$ be the fidelity of the source, we let $\bar{n}_1 = \bar{n}_2 = 10^{-4}$ be the average number of background photons, and we take the memory coherence times to be 1 s (top) and 60 s (bottom). The dots are placed at the maxima of the curves for $\tilde{F}^\infty(t)$.

quantum memories is x seconds, then $t_{\text{coh}} = \frac{xc}{2d}$ time steps. In Fig. 16, we plot the quantities $\tilde{F}^\infty(t)$ (solid lines), $F^\infty(t)$ (dashed lines), and $X^\infty(t)$ (dotted lines) for the $t^* = \infty$ memory-cutoff policy under this scenario.

In Fig. 16, we can see the trade-off between the quantities \tilde{F} , F , and X . On the one hand, the fidelity $F^\infty(t)$ is always highest at time $t = 1$, as we expect, but at this point the probability $X^\infty(t)$ that the elementary link is active is simply p . Since we want not only a high fidelity for the elementary link but also a high probability that the elementary link is active, by optimizing \tilde{F} it is possible to achieve a higher elementary link activity probability at the expense of a slightly lower fidelity. Specifically, in Fig. 16, we see that for every choice of d and h there exists a time step $t_{\text{crit}} \geq 1$ at which \tilde{F} is maximal. At this point, the elementary link activity probability is $1 - (1 - p)^{t_{\text{crit}}}$, which in many cases is dramatically greater than p , while the fidelity $F^\infty(t_{\text{crit}})$ is only slightly lower than the fidelity at time $t = 1$. Therefore, by waiting until time t_{crit} , it is possible to obtain an elementary link that is almost deterministically active, while incurring only a slight decrease in the fidelity. The time t_{crit} , obtained by optimizing the quantity $\tilde{F}^\infty(t)$ with respect to time t and can be found using the formula in (D24), can be viewed as the optimal time t that should be chosen for the quantum network protocol presented in Fig. 8. We refer to Ref. [116] for an argument similar to the one presented here, except that in Ref. [116] the time t_{crit} is obtained by considering a desired value of the fidelity $F^\infty(t)$ rather than by optimizing $\tilde{F}^\infty(t)$ with respect to t , which is what we do here.

3. Forward recursion policy

The forward recursion policy is defined as the time-homogeneous policy such that the action at time t is equal to the one that maximizes the quantity $\tilde{F}^\pi(t+1)$ at the next time step. The corresponding decision function is⁵⁸

$$d^{\text{FR}}(m) = \begin{cases} 1 & \text{if } m = -1, \\ 0 & \text{if } m \geq 0 \text{ and } f(m+1) > p f(0), \\ 1 & \text{if } m \geq 0 \text{ and } f(m+1) \leq p f(0). \end{cases} \quad (\text{D25})$$

Observe that if $p = 1$, then the second condition in (D25) is always false, because of the fact that $f(m) \leq f(0)$ for all $m \in \mathbb{N}_0$; see (D14). Therefore, when $p = 1$, we have that $d_t^{\text{FR}} = d_t^0$, i.e., the forward recursion policy is equal to the $t^* = 0$ memory-cutoff policy; see (D16). We now show that the forward recursion policy reduces to a memory-cutoff policy even when $p < 1$.

Proposition D.1. Consider satellite-to-ground bipartite elementary link generation with $\bar{n}_1 = \bar{n}_2 = 0$ and $f_S = 1$, and let $p \in (0, 1)$ be the transmission-heralding success probability, as given by (C58). Let t_{coh} be the coherence time of the quantum memories, as defined in Sec. D 1. Then, for all $t \geq 1$,

$$d^{\text{FR}} = \begin{cases} d^\infty & \text{if } p \leq \frac{1}{2}, \\ d^{t^*} & \text{if } p > \frac{1}{2}, \end{cases} \quad (\text{D26})$$

where

$$t^* = \left\lceil -\frac{t_{\text{coh}}}{2} \ln(2p - 1) - 1 \right\rceil. \quad (\text{D27})$$

In other words, if $p \leq \frac{1}{2}$, then the forward recursion policy is equal to the $t^* = \infty$ memory-cutoff policy; if $p > \frac{1}{2}$, then the forward recursion policy is equal to the t^* memory-cutoff policy, with t^* given by (D27).

Remark D.2. The result of Proposition D.1 goes beyond elementary link generation with satellites, because we assumed that $\bar{n}_1 = \bar{n}_2 = 0$ and $f_S = 1$. As a result of these assumptions, the result of Proposition D.1 applies to every elementary link generation scenario (such as ground-based elementary link generation as described in Sec. C 1) in which the transmission channel is a pure-loss channel, the heralding procedure is described by (C24)–(C28), the source state is equal to the target state, and the quantum memories are modeled as in Sec. D 1.

Proof. For the state σ_{AB}^0 as given by (2), using (D14) the second condition in (D25) translates to

$$\alpha \lambda_{m+1}^2 + \left(\beta - \frac{1}{2} \right) \lambda_{m+1} + \frac{1}{2} > p(\alpha + \beta) \quad (\text{D28})$$

$$\Rightarrow p < \frac{\alpha \lambda_{m+1}^2}{\alpha + \beta} + \frac{\left(\beta - \frac{1}{2} \right) \lambda_{m+1}}{\alpha + \beta} + \frac{1}{2(\alpha + \beta)}. \quad (\text{D29})$$

In the case $\bar{n}_1 = \bar{n}_2 = 0$ and $f_S = 1$, we have that $\alpha = \beta = \frac{1}{2}$, so that the inequality in (D29) becomes

$$p < \frac{1}{2} \left(e^{-\frac{2(m+1)}{t_{\text{coh}}}} + 1 \right), \quad (\text{D30})$$

Now, this inequality is satisfied for all $m \in \mathbb{N}_0$ if and only if $p \leq \frac{1}{2}$. In other words, if $p \leq \frac{1}{2}$, then for all possible memory times the action is to wait if the elementary link is currently active, meaning that the decision function in (D25) becomes

$$d^{\text{FR}}(m) = \begin{cases} 1 & \text{if } m = -1, \\ 0 & \text{if } m \geq 0, \end{cases} \quad (\text{D31})$$

which is precisely the decision function d^∞ for the $t^* = \infty$ memory-cutoff policy; see (D16).

For $p \in \left(\frac{1}{2}, 1 \right)$, whether or not the inequality in (D30) is satisfied depends on the memory time m . Consider the largest value of m for which the inequality is satisfied, and denote that value by m_{max} . Since the action is to wait, at the next time step the memory value will be $m_{\text{max}} + 1$, which by definition will not satisfy the inequality in (D28). This means that, for all memory times strictly less than $m_{\text{max}} + 1$, the forward recursion policy dictates that the “wait” action should be performed if the elementary link is currently active. As soon as the memory time is equal to $m_{\text{max}} + 1$, then the forward recursion policy dictates that the “request” action should be performed. This means that $m_{\text{max}} + 1$ is a cutoff value. In particular, by rearranging the inequality in (D30), we obtain

$$m < -\frac{t_{\text{coh}}}{2} \ln(2p - 1) - 1, \quad (\text{D32})$$

which means that

$$m_{\text{max}} = \left\lceil -\frac{t_{\text{coh}}}{2} \ln(2p - 1) - 1 \right\rceil, \quad (\text{D33})$$

and

$$t^* = 1 + m_{\text{max}} = \left\lceil -\frac{t_{\text{coh}}}{2} \ln(2p - 1) - 1 \right\rceil, \quad (\text{D34})$$

as required. \square

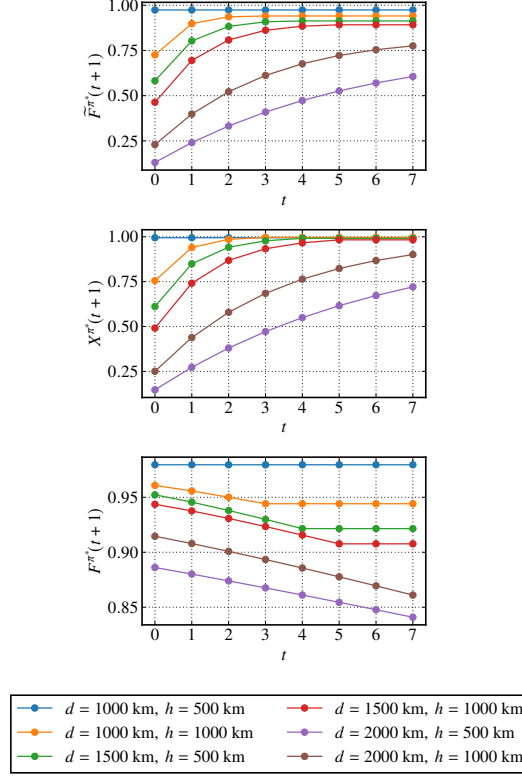


FIG. 17. Optimal values of $\tilde{F}^\pi(t+1)$, along with the associated values of $X^\pi(t+1)$ and fidelities $F^\pi(t+1)$, for a single elementary link distributed by a satellite to two ground stations, according to the symmetric situation depicted in Fig. 12. We assume that $f_S = 1$ and that $\bar{n}_1 = \bar{n}_2 = 10^{-4}$, and we assume that the quantum memories have a coherence time of 1 s. We also assume multiplexing with $M = 10^5$ distinct frequency modes per transmission.

Observe that the cutoff in (D27) is equal to zero for all $p \geq \frac{1}{2} \left(1 + e^{-\frac{2}{t_{\text{coh}}}}\right)$. This means that $p = 1$ is not the only transmission-heralding success probability for which the forward recursion policy is equal to the $t^* = 0$ memory-cutoff policy. Intuitively, for $\frac{1}{2} \left(1 + e^{-\frac{2}{t_{\text{coh}}}}\right) \leq p \leq 1$, the transmission-heralding success probability is high enough that it is not necessary to store the quantum state in memory—for the purposes of maximizing the value of \tilde{F} , it suffices to request a new quantum state at every time step. At the other extreme, for $0 \leq p \leq \frac{1}{2}$, the probability is too low to keep requesting—for the purposes of maximizing the value of \tilde{F} , it is better to keep the quantum state in memory indefinitely.

4. Backward recursion policy

Finally, to end this section, let us consider the backward recursion policy, which we know to be optimal from Theorem II.1. We perform the policy optimization for small times, just as a proof of concept.

In Fig. 17, we plot optimal values of $\tilde{F}^\pi(t+1)$ for a single elementary link, except now we plot them as a function of the ground station distance d and the satellite altitude h as per the situation depicted in Fig. 12. We also plot the elementary link activity probability $X^\pi(t+1)$ and the expected fidelities $F^\pi(t+1)$ associated with the optimal policies. As before, we assume that $f_S = 1$, but unlike before we assume that $\bar{n}_1 = \bar{n}_2 = 10^{-4}$, and we consider multiplexing with $M = 10^5$ distinct frequency modes per transmission. We assume a coherence time of 1 s throughout. For small distance-altitude pairs, we find that the optimal value is reached within five time steps. For these cases, it is worth pointing out that the optimal value of $\tilde{F}^\pi(t+1)$ corresponds to an elementary link activity probability $X^\pi(t+1)$ of nearly one, while the fidelity (although it drops, as expected) does not drop significantly, meaning that the elementary link can still be useful for performing entanglement distillation of parallel elementary links or for creating virtual links. It is also interesting to point out that for a ground distance separation of $d = 2000$ km, the optimal values for satellite altitude $h = 1000$ km is higher than for $h = 500$ km. This result can be traced back to the top-left panel of Fig. 13, in which we see that the transmission-heralding success probability curves for $h = 500$ km and $h = 1000$ km cross over

at around 1700 km, so that $h = 1000$ km has a higher probability than $h = 500$ km when $d = 2000$ km.

Appendix E: Overview of quantum key distribution

In this section, we provide a brief overview of quantum key distribution (QKD). We refer to Refs. [8–11, 156–158] for pedagogical introductions and reviews of state-of-the-art QKD research.

Let us consider the following scenario of so-called entanglement-based QKD. Suppose that Alice and Bob have access to a source that distributes entangled states ρ_{AB} to them, and that their task is to use many copies of this quantum state to distill a secret key. The general strategy of Alice and Bob is to measure their quantum systems. Based on their measurement statistics, they decide whether or not to use their classical measurement data to distill a secret key. The measurement statistics are of the form

$$p_{AB}(x, y|a, b) := \text{Tr}\left[\left(\Pi_A^{a,x} \otimes \Lambda_B^{b,y}\right)\rho_{AB}\right], \quad x \in \mathcal{X}, y \in \mathcal{Y}, a \in \mathcal{A}, b \in \mathcal{B}, \quad (\text{E1})$$

where \mathcal{A} and \mathcal{B} are finite sets of POVMs, such that $\{\Pi_A^{a,x}\}_{x \in \mathcal{X}}$ is a POVM for Alice's measurement for all $a \in \mathcal{A}$ and $\{\Lambda_B^{b,y}\}_{y \in \mathcal{Y}}$ is a POVM for Bob's measurement for all $b \in \mathcal{B}$.

BB84 and six-state protocols. Two well-known device-dependent protocols that we discuss here are the BB84⁶ and six-state^{159,160} protocols. The original formulation of these protocols is as so-called prepare-and-measure protocols, which do not require Alice and Bob to share entanglement. However, these protocols can be viewed from an entanglement-based point of view, in which Alice and Bob possess an entangled state; see Ref. [157] for a discussion on the equivalence of entanglement-based and prepare-and-measure-based protocols, and Ref. [161] for a more general discussion of the security of prepare-and-measure-based and entanglement-based QKD protocols. In this device-dependent scenario, we explicitly assume that the state ρ_{AB} is a two-qubit state, and the correlation in (E1) is given by measurement of the qubit Pauli observables X , Z , and $Y = iXZ$. In other words, the sets \mathcal{A} and \mathcal{B} indicate which observable to be measured, and the sets \mathcal{X} and \mathcal{Y} contain the outcomes of the measurements. It can be shown via certain symmetrization procedures that, without loss of generality, ρ_{AB} is a Bell-diagonal state; see Refs. [157] and [162] for details. It then suffices to estimate the following three quantities, called *quantum bit-error rates* (QBERs), in order to characterize the eavesdropper's knowledge:

$$Q_x := \text{Tr}[(|+\rangle\langle+|_A \otimes |-\rangle\langle-|_B)\rho_{AB}] + \text{Tr}[(|-\rangle\langle-|_A \otimes |+\rangle\langle+|_B)\rho_{AB}] \quad (\text{E2})$$

$$= \frac{1}{2}(1 - \text{Tr}[(X \otimes X)\rho_{AB}]), \quad (\text{E3})$$

$$Q_y := \text{Tr}[(|+i\rangle\langle+i|_A \otimes |-i\rangle\langle-i|_B)\rho_{AB}] + \text{Tr}[(|-i\rangle\langle-i|_A \otimes |+i\rangle\langle+i|_B)\rho_{AB}] \quad (\text{E4})$$

$$= \frac{1}{2}(1 + \text{Tr}[(Y \otimes Y)\rho_{AB}]), \quad (\text{E5})$$

$$Q_z := \text{Tr}[(|0\rangle\langle 0|_A \otimes |1\rangle\langle 1|_B)\rho_{AB}] + \text{Tr}[(|1\rangle\langle 1|_A \otimes |0\rangle\langle 0|_B)\rho_{AB}] \quad (\text{E6})$$

$$= \frac{1}{2}(1 - \text{Tr}[(Z \otimes Z)\rho_{AB}]), \quad (\text{E7})$$

where $|\pm\rangle = \frac{1}{\sqrt{2}}(|0\rangle \pm |1\rangle)$ and $|i\rangle = \frac{1}{\sqrt{2}}(|0\rangle \pm i|1\rangle)$. For example, Q_x is simply the probability that Alice and Bob's measurement outcomes disagree when they both measure the observable X , and similarly for Q_y and Q_z .

A standard figure of merit for QKD protocols is the number of secret key bits obtained per copy of the source state; see, e.g., Ref. [162] for precise definitions. For the BB84 protocol, the asymptotic secret key rate is^{163–168}

$$K_{\text{BB84}}(Q) = 1 - 2h_2(Q), \quad (\text{E8})$$

where $Q = \frac{1}{3}(Q_x + Q_y + Q_z)$ and

$$h_2(Q) := -Q \log_2(Q) - (1 - Q) \log_2(1 - Q) \quad (\text{E9})$$

is the binary entropy. For the six-state protocol, the asymptotic secret key rate is^{159,169}.

$$K_{\text{6-state}}(Q) = 1 + \left(1 - \frac{3Q}{2}\right) \log_2 \left(1 - \frac{3Q}{2}\right) + \frac{3Q}{2} \log_2 \left(\frac{Q}{2}\right), \quad (\text{E10})$$

where $Q = \frac{1}{3}(Q_x + Q_y + Q_z)$.

Remark E.1. The QBERs Q_x, Q_y, Q_z in (E2), (E4), and (E6) have a useful interpretation in terms of the fidelity of an arbitrary two-qubit state ρ_{AB} to the maximally entangled state Φ_{AB} . In particular,

$$\langle \Phi | \rho_{AB} | \Phi \rangle = 1 - \frac{1}{2}(Q_x + Q_y + Q_z) \quad (\text{E11})$$

for every two-qubit state ρ_{AB} . It is easy to see this by noting that

$$\Phi_{AB} = \frac{1}{4} (\mathbb{1}_A \otimes \mathbb{1}_B + X_A \otimes X_B - Y_A \otimes Y_B + Z_A \otimes Z_B). \quad (\text{E12})$$

Then, using the definitions in (E2), (E4), and (E6), we obtain (E11).

Device-independent protocols. The device-independent protocol that we present here is the one introduced in Refs. [170 and 171], and the basic idea behind the protocol comes from the protocol in Ref. [7]. The security of the protocol is based on violation of a Bell inequality, specifically the CHSH inequality¹⁷² (see Ref. [173] for a pedagogical introduction). In this protocol, unlike the device-dependent protocols shown above, it is not required to assume that ρ_{AB} is a two-qubit state. However, like the device-dependent protocols considered above, there are symmetrization procedures and other reductions from which it can be argued that ρ_{AB} is a two-qubit Bell-diagonal state without loss of generality; see Refs. [170 and 171] for details. The correlation in (E1) is given by measurement of observables P_A^0, P_A^1, P_A^2 for system A and observables Q_B^1, Q_B^2 for system B , and we assume that they all have spectral decompositions of the form

$$P_A^j = \Pi_A^{j,0} - \Pi_A^{j,1}, \quad j \in \{0, 1, 2\}, \quad (\text{E13})$$

$$T_B^k = \Lambda_B^{k,0} - \Lambda_B^{k,1}, \quad k \in \{1, 2\}. \quad (\text{E14})$$

In other words, $A = \{0, 1, 2\}$, $B = \{1, 2\}$, and $X = Y = \{0, 1\}$.

Two quantities in this case characterize the secret key rate:

$$S := \text{Tr} \left[\left(P_A^1 \otimes T_B^1 + P_A^1 \otimes T_B^2 + P_A^2 \otimes T_B^1 - P_A^2 \otimes T_B^2 \right) \rho_{AB} \right], \quad (\text{E15})$$

and the quantum bit-error rate (QBER) Q , which is defined as

$$Q := \text{Tr}[(\Pi_A^{0,0} \otimes \Lambda_B^{1,1})\rho_{AB}] + \text{Tr}[(\Pi_A^{0,1} \otimes \Lambda_B^{1,0})\rho_{AB}]. \quad (\text{E16})$$

As with the QBERs defined previously, the QBER here is the probability that the outcomes of Alice and Bob disagree when a measurement of P_A^0 is performed by Alice and a measurement of T_B^1 is performed by Bob. The asymptotic secret key rate is then^{171,174}

$$K_{\text{DI}}(Q, S) = 1 - h_2(Q) - h_2 \left(\frac{1 + \sqrt{(S/2)^2 - 1}}{2} \right). \quad (\text{E17})$$

Appendix F: Proof of Theorem II.2

To prove this, we use (A44). First of all, it is straightforward to show that the transition matrix P^d given by the definition in (A23) is equal to

$$\begin{aligned} P^d = & (1 - p\bar{\alpha}(-1)) | -1 \rangle \langle -1 | + p\bar{\alpha}(-1) | 0 \rangle \langle -1 | \\ & + (1 - p\bar{\alpha}(m^*)) | -1 \rangle \langle m^* | + p\bar{\alpha}(m^*) | 0 \rangle \langle m^* | \\ & + \sum_{m=0}^{m^*-1} (\alpha(m) | m+1 \rangle \langle m | + p\bar{\alpha}(m) | 0 \rangle \langle m | + (1-p)\bar{\alpha}(m) | -1 \rangle \langle m |). \end{aligned} \quad (\text{F1})$$

With this, we can verify that the vector $|M(\infty)\rangle_d := \sum_{m=-1}^{m^*} s_d(m) |m\rangle$ is a unit-eigenvalue probability vector of P^d , i.e., that $P^d |M(\infty)\rangle_d = |M(\infty)\rangle_d$. This is the unique such vector, because the Markov chain defined by the transition matrix P^d is ergodic, which can be straightforwardly verified. Therefore, by ergodicity, the stationary vector $|M(\infty)\rangle$ is unique and $\lim_{t \rightarrow \infty} (P^d)^{t-1} = |M(\infty)\rangle \langle \gamma|$; see, e.g., Ref. [128, Theorem A.2]. Therefore, using (A44), we obtain the desired result.

Appendix G: Proof of Theorem II.4

The inequality

$$\sup_d \lim_{t \rightarrow \infty} \widetilde{F}^{(d,d,\dots)}(t) \geq \lim_{t \rightarrow \infty} \widetilde{F}^{t*}(t) \quad (\text{G1})$$

is certainly true for all $t^* \in \{0, 1, \dots, m^*\}$, which implies that

$$\sup_d \lim_{t \rightarrow \infty} \tilde{F}^{(d, d, \dots)}(t) \geq \max_{t^* \in \{0, 1, \dots, m^*\}} \lim_{t \rightarrow \infty} \tilde{F}^{t^*}(t). \quad (\text{G2})$$

Now, to prove the opposite inequality, we show that for every decision function d there exists a $t^* \in \{0, 1, \dots, m^*\}$ such that $\lim_{t \rightarrow \infty} \tilde{F}^{(d, d, \dots)}(t) \leq \lim_{t \rightarrow \infty} \tilde{F}^{t^*}(t)$. To this end, let d be an arbitrary decision function. We first observe that, from Theorem II.2, the steady-state probability distribution s_d of the memory storage time is such that $s_d(m) \leq s_d(0)$ for all $m \in \{1, 2, \dots, m^*\}$. On the other hand, for all $t^* \in \mathbb{N}_0$, we have $s_d(m) = \frac{p}{1+t^*p}$ for all $m \in \{0, 1, \dots, t^*\}$. We thus need a cutoff value $t^* \in \{0, 1, \dots, m^*\}$ satisfying $\frac{p}{1+t^*p} \geq s_d(0)$. Rearranging this inequality leads to the condition

$$t^* \leq \frac{1}{s_d(0)} - \frac{1}{p} = \frac{N_d}{p(1 - \alpha(-1))} - \frac{1}{p}. \quad (\text{G3})$$

Now, from (29), we have that

$$N_d \leq 1 + p(1 - \alpha(-1))(1 + m^*), \quad (\text{G4})$$

which implies that

$$t^* \leq \frac{1}{p(1 - \alpha(-1))} + 1 + m^* - \frac{1}{p} \leq \frac{1}{p} \left(\frac{1}{1 - \alpha(-1)} - 1 \right) + 1 + m^*. \quad (\text{G5})$$

Now, because $\alpha(-1)$ is a probability, if $\alpha(-1) \in [0, 1)$, then $\frac{1}{1 - \alpha(-1)} - 1 \geq 0$, which implies that the right-most quantity in the above inequality is positive and strictly greater than m^* . (Note that if $\alpha(-1) = 1$, then $\lim_{t \rightarrow \infty} \tilde{F}^{(d, d, \dots)}(t) = 0$.) Therefore, we can set $t^* = m^*$, resulting in

$$\lim_{t \rightarrow \infty} \tilde{F}^{(d, d, \dots)}(t) = \sum_{m=0}^{m^*} f(m) s_d(m) \leq \frac{p}{1 + m^* p} \sum_{m=0}^{m^*} f(m) = \lim_{t \rightarrow \infty} \tilde{F}^{m^*}(t) \leq \max_{t^* \in \{0, 1, \dots, m^*\}} \lim_{t \rightarrow \infty} \tilde{F}^{t^*}(t), \quad (\text{G6})$$

as required. This completes the proof.

Appendix H: Proofs from Sec. III B

1. Proof of Proposition III.1

Let $\rho_{A\vec{R}_1 \dots \vec{R}_n B}$ be an arbitrary state. Then,

$$\begin{aligned} \langle \Phi |_{AB} \mathcal{L}_{A\vec{R}_1 \dots \vec{R}_n B \rightarrow AB}^{\text{ES}_n} \left(\rho_{A\vec{R}_1 \dots \vec{R}_n B} \right) | \Phi \rangle_{AB} \\ = \sum_{\vec{x}, \vec{z} \in [d]^{\times n}} \left(\langle \Phi^{a, b} |_{AB} \otimes \langle \Phi^{z_1, x_1} |_{R_1^1 R_1^2} \otimes \dots \otimes \langle \Phi^{z_n, x_n} |_{R_n^1 R_n^2} \right) \left(\rho_{A\vec{R}_1 \dots \vec{R}_n B} \right) \\ \left(| \Phi^{a, b} \rangle_{AB} \otimes | \Phi^{z_1, x_1} \rangle_{R_1^1 R_1^2} \otimes \dots \otimes | \Phi^{z_n, x_n} \rangle_{R_n^1 R_n^2} \right), \end{aligned} \quad (\text{H1})$$

where

$$a := z_1 + \dots + z_n, \quad b := x_1 + \dots + x_n. \quad (\text{H2})$$

Using

$$| \Phi^{z, x} \rangle = (Z^z X^x \otimes \mathbb{1}) | \Phi \rangle \quad (\text{H3})$$

$$= \frac{1}{\sqrt{d}} \sum_{k=0}^{d-1} e^{\frac{2\pi i (k+x)z}{d}} | k+x, k \rangle \quad (\text{H4})$$

and

$$| j, k \rangle = \frac{1}{\sqrt{d}} \sum_{z, x=0}^{d-1} e^{\frac{-2\pi i j z}{d}} \delta_{j, k+x} | \Phi^{z, x} \rangle, \quad (\text{H5})$$

we obtain

$$\begin{aligned}
& |\Phi^{a,b}\rangle_{AB} \otimes |\Phi^{z_1,x_1}\rangle_{\vec{R}_1} \otimes |\Phi^{z_2,x_2}\rangle_{\vec{R}_2} \otimes \cdots \otimes |\Phi^{z_n,x_n}\rangle_{\vec{R}_n} \\
&= \frac{1}{\sqrt{d^{n+1}}} \sum_{k_0,k_1,\dots,k_n=0}^{d-1} e^{\frac{2\pi i (k_0+b)a}{d}} \left(\prod_{\ell=1}^n e^{\frac{2\pi i (k_\ell+x_\ell)z_\ell}{d}} \right) |k_0+b, k_0\rangle_{AB} |k_1+x_1, k_1\rangle_{R_1^1 R_1^2} \\
&\quad |k_2+x_2, k_2\rangle_{R_2^1 R_2^2} \cdots |k_n+x_n, k_n\rangle_{R_n^1 R_n^2} \tag{H6}
\end{aligned}$$

$$\begin{aligned}
&= \frac{1}{\sqrt{d^{n+1}}} \sum_{k_0,k_1,\dots,k_n=0}^{d-1} e^{\frac{2\pi i (k_0+b)a}{d}} \left(\prod_{\ell=1}^n e^{\frac{2\pi i (k_\ell+x_\ell)z_\ell}{d}} \right) |k_0+b, k_1+x_1\rangle_{AR_1^1} \\
&\quad |k_1, k_2+x_2\rangle_{R_1^2 R_2^1} \cdots |k_n, k_0\rangle_{R_n^2 B}. \tag{H7}
\end{aligned}$$

Now,

$$|k_0+b, k_1+x_1\rangle_{AR_1^1} = \frac{1}{\sqrt{d}} \sum_{z'_0, x'_0=0}^{d-1} e^{\frac{-2\pi i (k_0+b)z'_0}{d}} \delta_{k_0+b, k_1+x_1+x'_0} |\Phi^{z'_0, x'_0}\rangle_{AR_1^1} \tag{H8}$$

$$\ell \in \{1, \dots, n-1\} : |k_\ell, k_{\ell+1}+x_{\ell+1}\rangle_{R_\ell^2 R_{\ell+1}^1} = \frac{1}{\sqrt{d}} \sum_{z'_\ell, x'_\ell=0}^{d-1} e^{\frac{-2\pi i k_\ell z'_\ell}{d}} \delta_{k_\ell, k_{\ell+1}+x_{\ell+1}+x'_\ell} |\Phi^{z'_\ell, x'_\ell}\rangle_{R_\ell^2 R_{\ell+1}^1}, \tag{H9}$$

$$|k_n, k_0\rangle_{R_n^2 B} = \frac{1}{\sqrt{d}} \sum_{z'_n, x'_n=0}^{d-1} e^{\frac{-2\pi i k_n z'_n}{d}} \delta_{k_n, k_0+x'_n} |\Phi^{z'_n, x'_n}\rangle_{R_n^2 B} \tag{H10}$$

Therefore,

$$\begin{aligned}
& |\Phi^{a,b}\rangle_{AB} \otimes |\Phi^{z_1,x_1}\rangle_{\vec{R}_1} \otimes |\Phi^{z_2,x_2}\rangle_{\vec{R}_2} \otimes \cdots \otimes |\Phi^{z_n,x_n}\rangle_{\vec{R}_n} \\
&= \frac{1}{d^{n+1}} \sum_{\substack{k_0, \dots, k_n=0 \\ z'_0, \dots, z'_n=0 \\ x'_0, \dots, x'_n=0}}^{d-1} e^{\frac{2\pi i (k_0+b)a}{d}} \left(\prod_{\ell=1}^n e^{\frac{2\pi i (k_\ell+x_\ell)z_\ell}{d}} \right) e^{\frac{-2\pi i (k_0+b)z'_0}{d}} \delta_{k_0+b, k_1+x_1+x'_0} \left(\prod_{\ell=1}^{n-1} e^{\frac{-2\pi i k_\ell z'_\ell}{d}} \delta_{k_\ell, k_{\ell+1}+x_{\ell+1}+x'_\ell} \right) e^{\frac{-2\pi i k_n z'_n}{d}} \delta_{k_n, k_0+x'_n} \\
&\quad |\Phi^{z'_0, x'_0}\rangle_{AR_1^1} \bigotimes_{\ell=1}^{n-1} |\Phi^{z'_\ell, x'_\ell}\rangle_{R_\ell^2 R_{\ell+1}^1} |\Phi^{z'_n, x'_n}\rangle_{R_n^2 B}. \tag{H11}
\end{aligned}$$

Evaluating the sums with respect to k_0, \dots, k_n , starting with k_n and proceeding backwards to k_0 , we obtain

$$\begin{aligned}
& |\Phi^{a,b}\rangle_{AB} \otimes |\Phi^{z_1,x_1}\rangle_{\vec{R}_1} \otimes |\Phi^{z_2,x_2}\rangle_{\vec{R}_2} \otimes \cdots \otimes |\Phi^{z_n,x_n}\rangle_{\vec{R}_n} \\
&= \frac{1}{d^n} \sum_{\substack{z'_0, \dots, z'_n=0 \\ x'_0, \dots, x'_n=0}}^{d-1} e^{-\frac{2\pi i}{d} ab} \left(\prod_{\ell=1}^n e^{\frac{2\pi i}{d} (x_\ell+x'_\ell+\dots+x_n+x'_n)z_\ell} \right) \left(\prod_{\ell=1}^n e^{-\frac{2\pi i}{d} (x'_\ell+x_{\ell+1}+x'_{\ell+1}+\dots+x_n+x'_n)z'_\ell} \right) e^{\frac{2\pi i}{d} (z'_1+\dots+z'_n)b} \\
&\quad |\Phi^{2a-z'_1-\dots-z'_n, -x'_1-\dots-x'_n}\rangle_{AR_1^1} \bigotimes_{\ell=1}^{n-1} |\Phi^{z'_\ell, x'_\ell}\rangle_{R_\ell^2 R_{\ell+1}^1} |\Phi^{z'_n, x'_n}\rangle_{R_n^2 B}, \tag{H12}
\end{aligned}$$

where for the sum with respect to k_0 we used the identity

$$\sum_{k=0}^{d-1} e^{\frac{2\pi i k \alpha}{d}} = d \delta_{\alpha,0}, \tag{H13}$$

which holds for all $\alpha \in \{0, 1, \dots, d-1\}$. Now, observe that

$$|\Phi^{2a-z'_1-\dots-z'_n, -x'_1-\dots-x'_n}\rangle_{AR_1^1} = Z_A^{2a} |\Phi^{-z'_1-\dots-z'_n, -x'_1-\dots-x'_n}\rangle_{AR_1^1}. \tag{H14}$$

Using this, along with the fact that $(Z_A^z)^\dagger Z_A^z = \mathbb{1}$ for all $z \in \{0, 1, \dots, d-1\}$, and after much simplification and repeated use of (H13), we obtain

$$\begin{aligned}
& \sum_{\vec{x}, \vec{z} \in [d]^{\times n}} \left(\langle \Phi^{a,b} |_{AB} \otimes \langle \Phi^{z_1, x_1} |_{R_1^1 R_1^2} \otimes \cdots \otimes \langle \Phi^{z_n, x_n} |_{R_n^1 R_n^2} \right) \left(\rho_{A\vec{R}_1 \cdots \vec{R}_n B} \right) \\
& \quad \left(| \Phi^{a,b} \rangle_{AB} \otimes | \Phi^{z_1, x_1} \rangle_{R_1^1 R_1^2} \otimes \cdots \otimes | \Phi^{z_n, x_n} \rangle_{R_n^1 R_n^2} \right) \\
& = \sum_{\vec{z}', \vec{x}' \in [d]^{\times n}} \left(\langle \Phi^{-z'_1 - \cdots - z'_n, -x'_1 - \cdots - x'_n} |_{AR_1^1} \bigotimes_{\ell=1}^{n-1} \langle \Phi^{z'_\ell, x'_\ell} |_{R_\ell^2 R_{\ell+1}^1} \langle \Phi^{z'_n, x'_n} |_{R_n^2 B} \right) \left(\rho_{A\vec{R}_1 \cdots \vec{R}_n B} \right) \\
& \quad \left(| \Phi^{-z'_1 - \cdots - z'_n, -x'_1 - \cdots - x'_n} \rangle_{AR_1^1} \bigotimes_{\ell=1}^{n-1} | \Phi^{z'_\ell, x'_\ell} \rangle_{R_\ell^2 R_{\ell+1}^1} | \Phi^{z'_n, x'_n} \rangle_{R_n^2 B} \right), \quad (\text{H15})
\end{aligned}$$

which leads to the desired result.

2. Proof of Proposition III.2

Let $\rho_{A\vec{R}_1 \cdots \vec{R}_n B}$ be an arbitrary state. We then have

$$\begin{aligned}
& \langle \text{GHZ}_{n+2} | \mathcal{L}_{A\vec{R}_1 \cdots \vec{R}_n B \rightarrow AR_1^1 \cdots R_n^1 B}^{\text{GHZ};n} \left(\rho_{A\vec{R}_1 \cdots \vec{R}_n B} \right) | \text{GHZ}_{n+2} \rangle \\
& = \frac{1}{2} \sum_{x, x'=0}^1 \sum_{\vec{x} \in \{0,1\}^n} \langle x, x, \dots, x | L_n^{x_n} \cdots L_2^{x_2} L_1^{x_1} \left(\rho_{A\vec{R}_1 \cdots \vec{R}_n B} \right) L_1^{x_1^\dagger} L_2^{x_2^\dagger} \cdots L_n^{x_n^\dagger} | x', x', \dots, x' \rangle, \quad (\text{H16})
\end{aligned}$$

where

$$L_j^{x_j} := \langle x_j |_{R_j^2} \text{CNOT}_{\vec{R}_j} X_{R_{j+1}^1}^{x_j} \quad (\text{H17})$$

$$= \langle x_j |_{R_j^2} \left(\sum_{x'=0}^1 |x' \rangle \langle x' |_{R_j^1} \otimes X_{R_j^2}^{x'} \right) (\mathbb{1}_{\vec{R}_j} \otimes X_{R_{j+1}^1}^{x_j}) \quad (\text{H18})$$

$$= \sum_{x'=0}^1 |x' \rangle \langle x' |_{R_j^1} \otimes \langle x_j + x' |_{R_j^2} \otimes X_{R_{j+1}^1}^{x_j}. \quad (\text{H19})$$

Then,

$$\begin{aligned}
L_n^{x_n} \cdots L_2^{x_2} L_1^{x_1} &= \sum_{x'_1, \dots, x'_n=0}^1 |x'_1, \dots, x'_n \rangle \langle x'_1, x'_2 + x_1, x'_3 + x_2, \dots, x'_n + x_{n-1} |_{R_1^1 R_2^1 \cdots R_n^1} \\
&\quad \otimes \langle x_1 + x'_1, x_2 + x'_2, \dots, x_n + x'_n |_{R_1^2 R_2^2 \cdots R_n^2} \otimes X_B^{x_n}, \quad (\text{H20})
\end{aligned}$$

so that, using (H5) with $d = 2$,

$$\begin{aligned}
& \langle x, x, \dots, x |_{AR_1^1 R_2^1 \cdots R_n^1 B} L_n^{x_n} \cdots L_2^{x_2} L_1^{x_1} \\
& = \langle x |_A \langle x, x + x_1, x + x_2, \dots, x + x_{n-1} |_{R_1^1 R_2^1 \cdots R_n^1} \langle x_1 + x, x_2 + x, \dots, x_n + x |_{R_1^2 R_2^2 \cdots R_n^2} \langle x + x_n |_B \quad (\text{H21})
\end{aligned}$$

$$= \langle x, x |_{AR_1^1} \langle x + x_1, x + x_1 |_{R_1^2 R_2^1} \langle x + x_2, x + x_2 |_{R_2^2 R_3^1} \cdots \langle x + x_n, x + x_n |_{R_n^2 B} \quad (\text{H22})$$

$$= \frac{1}{\sqrt{2^{n+1}}} \sum_{\vec{z} \in \{0,1\}^n}^1 (-1)^{z_1 x} (-1)^{z_2 (x+x_1)} \cdots (-1)^{z_{n+1} (x+x_n)} \langle \Phi^{z_1, 0} |_{AR_1^1} \langle \Phi^{z_2, 0} |_{R_1^2 R_2^1} \cdots \langle \Phi^{z_{n+1}, 0} |_{R_n^2 B}. \quad (\text{H23})$$

We substitute this into (H16), simplify, and then make use of the following identity:

$$\sum_{\vec{y} \in \{0,1\}^n} (-1)^{\vec{y}^\top \vec{x}} = 2^n \delta_{\vec{x}, \vec{0}}. \quad (\text{H24})$$

This leads to

$$\langle \text{GHZ}_{n+2} | \mathcal{L}_{A\vec{R}_1 \cdots \vec{R}_n B \rightarrow AR_1^1 \cdots R_n^1 B}^{\text{GHZ};n} \left(\rho_{A\vec{R}_1 \cdots \vec{R}_n B} \right) | \text{GHZ}_{n+2} \rangle$$

$$= \sum_{z_2, \dots, z_{n+1}=0}^1 \langle \Phi^{z_2+\dots+z_{n+1},0} | \langle \Phi^{z_2,0} | \dots \langle \Phi^{z_{n+1},0} | \left(\rho_{A\vec{R}_1 \dots \vec{R}_n B} \right) | \Phi^{z_2+\dots+z_{n+1},0} \rangle | \Phi^{z_2,0} \rangle \dots | \Phi^{z_{n+1},0} \rangle. \quad (\text{H25})$$

This holds for every state $\rho_{A\vec{R}_1 \dots \vec{R}_n B}$, so it holds for the tensor product state in the statement of the proposition, thus completing the proof.

3. Proof of Proposition III.3

Let $\rho_{A_1^n B_1^n}$ be an arbitrary $2n$ -qubit state. Then, by definition of the channel $\mathcal{L}^{(G)}$, we have that

$$\langle G | \mathcal{L}^{(G)} \left(\rho_{A_1^n R_1^n} \right) | G \rangle = \sum_{\vec{\gamma} \in \{0,1\}^n} \left(\langle G^{\vec{\gamma}} |_{A_1^n} \otimes \langle G^{\vec{\gamma}} |_{R_1^n} \right) \left(\rho_{A_1^n R_1^n} \right) \left(|G^{\vec{\gamma}}\rangle_{A_1^n} \otimes |G^{\vec{\gamma}}\rangle_{R_1^n} \right), \quad (\text{H26})$$

where we recall the definition of $|G^{\vec{\gamma}}\rangle$ in (84). Now,

$$|G^{\vec{\gamma}}\rangle_{A_1^n} \otimes |G^{\vec{\gamma}}\rangle_{R_1^n} = \frac{1}{2^n} \sum_{\vec{\alpha}, \vec{\beta} \in \{0,1\}^n} (-1)^{\gamma_1(\alpha_1+\beta_1) + \dots + \gamma_n(\alpha_n+\beta_n)} (-1)^{\frac{1}{2} \vec{\alpha}^\top A(G) \vec{\alpha} + \frac{1}{2} \vec{\beta}^\top A(G) \vec{\beta}} |\vec{\alpha}\rangle_{A_1^n} \otimes |\vec{\beta}\rangle_{R_1^n}, \quad (\text{H27})$$

and, for all $\vec{\alpha}, \vec{\beta} \in \{0,1\}^n$,

$$|\vec{\alpha}\rangle_{A_1^n} \otimes |\vec{\beta}\rangle_{R_1^n} = \frac{1}{\sqrt{2^n}} \sum_{\vec{x}, \vec{z} \in \{0,1\}^n} (-1)^{\alpha_1 z_1 + \dots + \alpha_n z_n} \delta_{\beta_1, \alpha_1 + x_1} \dots \delta_{\beta_n, \alpha_n + x_n} |\Phi^{z_1, x_1}\rangle_{A_1 R_1} \otimes \dots \otimes |\Phi^{z_n, x_n}\rangle_{A_n R_n}, \quad (\text{H28})$$

where we have used (H5). Then,

$$\begin{aligned} |G^{\vec{\gamma}}\rangle_{A_1^n} \otimes |G^{\vec{\gamma}}\rangle_{R_1^n} &= \frac{1}{(2^n)^{\frac{3}{2}}} \sum_{\vec{\alpha}, \vec{x}, \vec{z} \in \{0,1\}^n} (-1)^{\vec{\gamma}^\top \vec{x} + \vec{\alpha}^\top \vec{z}} (-1)^{\frac{1}{2} \vec{\alpha}^\top A(G) \vec{\alpha} + \frac{1}{2} (\vec{\alpha} + \vec{x})^\top A(G) (\vec{\alpha} + \vec{x})} |\Phi^{x_1, z_1}\rangle_{A_1 R_1} \otimes \dots \otimes |\Phi^{z_n, x_n}\rangle_{A_n R_n}. \end{aligned} \quad (\text{H29})$$

Now, because $A(G)$ is a symmetric matrix, we have that $\vec{\alpha}^\top A(G) \vec{x} = \vec{x}^\top A(G) \vec{\alpha}$. We thus obtain

$$(-1)^{\frac{1}{2} \vec{\alpha}^\top A(G) \vec{\alpha} + \frac{1}{2} (\vec{\alpha} + \vec{x})^\top A(G) (\vec{\alpha} + \vec{x})} = (-1)^{\vec{\alpha}^\top A(G) \vec{x} + \frac{1}{2} \vec{x}^\top A(G) \vec{x}}, \quad (\text{H30})$$

so that

$$|G^{\vec{\gamma}}\rangle_{A_1^n} \otimes |G^{\vec{\gamma}}\rangle_{R_1^n} = \frac{1}{(2^n)^{\frac{3}{2}}} \sum_{\vec{\alpha}, \vec{x}, \vec{z} \in \{0,1\}^n} (-1)^{\vec{\gamma}^\top \vec{x} + \vec{\alpha}^\top \vec{z}} (-1)^{\frac{1}{2} \vec{x}^\top A(G) \vec{x} + \vec{\alpha}^\top A(G) \vec{x}} |\Phi^{z_1, x_1}\rangle_{A_1 R_1} \otimes \dots \otimes |\Phi^{z_n, x_n}\rangle_{A_n R_n}. \quad (\text{H31})$$

Therefore, using (H24), we find that

$$\begin{aligned} \sum_{\vec{\gamma} \in \{0,1\}^n} &\left(\langle G^{\vec{\gamma}} |_{A_1^n} \otimes \langle G^{\vec{\gamma}} |_{R_1^n} \right) \left(\rho_{A_1^n R_1^n} \right) \left(|G^{\vec{\gamma}}\rangle_{A_1^n} \otimes |G^{\vec{\gamma}}\rangle_{R_1^n} \right) \\ &= \frac{1}{(2^n)^2} \sum_{\vec{\alpha}, \vec{\alpha}', \vec{z}, \vec{z}', \vec{x} \in \{0,1\}^n} (-1)^{\vec{\alpha}^\top (A(G) \vec{x} + \vec{z}) + \vec{\alpha}'^\top (A(G) \vec{x} + \vec{z}')} (\langle \Phi^{z_1, x_1} |_{A_1 R_1} \otimes \dots \otimes \langle \Phi^{z_n, x_n} |_{A_n R_n}) \left(\rho_{A_1^n R_1^n} \right) \\ &\quad \left(|\Phi^{z'_1, x'_1}\rangle_{A_1 R_1} \otimes \dots \otimes |\Phi^{z'_n, x_n}\rangle_{A_n R_n} \right). \end{aligned} \quad (\text{H32})$$

Using (H24) two more times in the summation with respect to $\vec{\alpha}$ and $\vec{\alpha}'$ finally leads to

$$\begin{aligned} \sum_{\vec{\gamma} \in \{0,1\}^n} &\left(\langle G^{\vec{\gamma}} |_{A_1^n} \otimes \langle G^{\vec{\gamma}} |_{R_1^n} \right) \left(\rho_{A_1^n R_1^n} \right) \left(|G^{\vec{\gamma}}\rangle_{A_1^n} \otimes |G^{\vec{\gamma}}\rangle_{R_1^n} \right) \\ &= \sum_{\vec{x} \in \{0,1\}^n} (\langle \Phi^{z_1, x_1} |_{A_1 R_1} \otimes \dots \otimes \langle \Phi^{z_n, x_n} |_{A_n R_n}) \left(\rho_{A_1^n R_1^n} \right) (\langle \Phi^{z_1, x_1} |_{A_1 R_1} \otimes \dots \otimes \langle \Phi^{z_n, x_n} |_{A_n R_n}), \end{aligned} \quad (\text{H33})$$

where $\vec{z} = A(G)\vec{x}$. Since this holds for every state $\rho_{A_1^n R_1^n}$, it holds for the tensor product state in the statement of the proposition, which completes the proof.

Appendix I: Proof of Eq. (96)

By definition,

$$\Pr[W_{E'}(t_{\text{req}}) = t]_{\infty} = \Pr[X_{E'}(t_{\text{req}} + 1) = 0, \dots, X_{E'}(t_{\text{req}} + t) = 1]_{\infty}. \quad (\text{I1})$$

Note that

$$\Pr[W_{E'}(t_{\text{req}}) = 1]_{\infty} = \Pr[X_{E'}(t_{\text{req}} + 1) = 1]_{\infty} = (1 - (1 - p)^{t_{\text{req}}+1})^M = p_{t_{\text{req}}+1}^M, \quad (\text{I2})$$

which holds because all of the elementary links are generated independently and because they all have the same success probability.

Now, for $t \geq 2$, our first goal is to prove that

$$\Pr[W_{E'}(t_{\text{req}}) = t]_{\infty} = (1 - (1 - p_{t_{\text{req}}+1})(1 - p)^{t-1})^M - (1 - (1 - p_{t_{\text{req}}+1})(1 - p)^{t-2})^M. \quad (\text{I3})$$

In order to prove this, let us for the moment take $t_{\text{req}} = 0$. Then, $X_{E'}(1) = 0$ means that at least one of the M elementary links is not active in the first time step, and the same for all subsequent time steps except for the t^{th} time step, in which all of the M elementary links are active. Then, because $t^* = \infty$, the links that are active in the first time step always remain active. This means that we can evaluate $\Pr[W_{E'}(0) = t]_{\infty}$ by counting the number of elementary links that are inactive at each time step. For example, for $t = 2$, we obtain

$$\Pr[X_{E'}(1) = 0, X_{E'}(2) = 1]_{\infty} = \sum_{k_1=1}^M \binom{M}{k_1} \underbrace{(1-p)^{k_1}}_{\substack{k_1 \text{ inactive links} \\ \text{in the first} \\ \text{time step}}} \underbrace{p^{M-k_1}}_{\substack{M-k_1 \text{ active} \\ \text{links in the} \\ \text{first time step}}} \underbrace{p^{k_1}}_{\substack{\text{remaining} \\ \text{inactive links} \\ \text{suceed in the} \\ \text{second time step}}} \quad (\text{I4})$$

$$= p^M \sum_{k_1=1}^M \binom{M}{k_1} (1-p)^{k_1}. \quad (\text{I5})$$

Similarly, for $t = 3$, we find that

$$\begin{aligned} \Pr[X_{E'}(1) = 0, X_{E'}(2) = 0, X_{E'}(3) = 1]_{\infty} &= \sum_{k_1=1}^M \binom{M}{k_1} (1-p)^{k_1} p^{M-k_1} \sum_{k_2=1}^{k_1} \binom{k_1}{k_2} (1-p)^{k_2} p^{k_1-k_2} p^{k_2} \\ &= p^M \sum_{k_1=1}^M \sum_{k_2=1}^{k_1} \binom{M}{k_1} \binom{k_1}{k_2} (1-p)^{k_1} (1-p)^{k_2}. \end{aligned} \quad (\text{I6})$$

$$= p^M \sum_{k_1=1}^M \sum_{k_2=1}^{k_1} \binom{M}{k_1} \binom{k_1}{k_2} (1-p)^{k_1} (1-p)^{k_2}. \quad (\text{I7})$$

In general, then, for all $t \geq 2$,

$$\begin{aligned} \Pr[W_{E'}(0) = t]_{\infty} &= \Pr[X_{E'}(1) = 0, \dots, X_{E'}(t) = 1]_{\infty} \\ &= p^M \sum_{k_1=1}^M \sum_{k_2=1}^{k_1} \sum_{k_3=1}^{k_2} \dots \sum_{k_{t-1}=1}^{k_{t-2}} \binom{M}{k_1} \binom{k_1}{k_2} \binom{k_2}{k_3} \dots \binom{k_{t-2}}{k_{t-1}} (1-p)^{k_1} (1-p)^{k_2} \dots (1-p)^{k_{t-1}} \end{aligned} \quad (\text{I8})$$

$$= \sum_{k_1=1}^M \binom{M}{k_1} (1-p)^{k_1} p^{M-k_1} \underbrace{p^{k_1} \sum_{k_2=1}^{k_1} \sum_{k_3=1}^{k_2} \dots \sum_{k_{t-1}=1}^{k_{t-2}} \binom{k_1}{k_2} \binom{k_2}{k_3} \dots \binom{k_{t-2}}{k_{t-1}} (1-p)^{k_2} \dots (1-p)^{k_{t-1}}}_{\Pr[W_{k_1}^{(\infty)}(0) = t-1]} \quad (\text{I9})$$

$$= \sum_{k_1=1}^M \binom{M}{k_1} (1-p)^{k_1} p^{M-k_1} \Pr[W_{k_1}(0) = t-1]_{\infty} \quad (\text{I10})$$

Using this, we can immediately prove the following result by induction on t :

$$\Pr[W_{E'}(0) = t]_{\infty} = (1 - (1 - p)^t)^M - (1 - (1 - p)^{t-1})^M. \quad (\text{I11})$$

Indeed, from (I2), we immediately have that this result holds for $t = 1$. Similarly, using the fact that

$$\sum_{k_1=1}^M \binom{M}{k_1} (1-p)^{k_1} = -1 + (2-p)^M = \frac{1}{p^M} \left((1-(1-p)^2)^M - (1-(1-p))^M \right), \quad (\text{I12})$$

we see that (I11) holds for $t = 2$ as well. Now, assuming that (I11) holds for all $t \geq 2$, using (I10) we find that

$$\Pr[W_{E'}(0) = t+1]_\infty = \sum_{k_1=1}^M \binom{M}{k_1} (1-p)^{k_1} p^{M-k_1} \Pr[W_{k_1}(0) = t]_\infty \quad (\text{I13})$$

$$= \sum_{k_1=1}^M \binom{M}{k_1} (1-p)^{k_1} p^{M-k_1} \left((1-(1-p)^t)^{k_1} - (1-(1-p)^{t-1})^{k_1} \right) \quad (\text{I14})$$

$$= (1-(1-p)^{t+1})^M - (1-(1-p)^t)^M, \quad (\text{I15})$$

as required. Therefore, (I11) holds for all $t \geq 1$.

We are now in a position to prove (I3). Recall that for the $t^\star = \infty$ policy, $\Pr[X(t) = 1]_\infty = 1 - (1-p)^t = p_t$. Therefore, at time step $t_{\text{req}} + 1$, the probability that $k_1 \geq 1$ elementary links are inactive is $(1-p_{t_{\text{req}}+1})^{k_1}$ and the probability that $M - k_1$ elementary links are active is $p_{t_{\text{req}}+1}^{M-k_1}$. In the subsequent time steps, each inactive elementary link from the previous time step is active with probability p and inactive with probability $1-p$. Therefore,

$$\Pr[W_{E'}(t_{\text{req}}) = t]_\infty = \sum_{k_1=1}^M \binom{M}{k_1} (1-p_{t_{\text{req}}+1})^{k_1} p_{t_{\text{req}}+1}^{M-k_1} \sum_{k_2=1}^{k_1} \binom{k_1}{k_2} (1-p)^{k_2} p^{k_2-k_1} \dots \sum_{k_{t-1}=1}^{k_{t-2}} \binom{k_{t-2}}{k_{t-1}} (1-p)^{k_{t-1}} p^{k_{t-2}-k_{t-1}} p^{k_{t-1}} \quad (\text{I16})$$

$$= \sum_{k_1=1}^M \binom{M}{k_1} (1-p_{t_{\text{req}}+1})^{k_1} p_{t_{\text{req}}+1}^{M-k_1} p^{k_1} \sum_{k_2=1}^{k_1} \dots \sum_{k_{t-1}=1}^{k_{t-2}} \binom{k_1}{k_2} \dots \binom{k_{t-2}}{k_{t-1}} (1-p)^{k_2} \dots (1-p)^{k_{t-1}} \quad (\text{I17})$$

$$= \sum_{k_1=1}^M \binom{M}{k_1} (1-p_{t_{\text{req}}+1})^{k_1} p_{t_{\text{req}}+1}^{M-k_1} \Pr[W_{k_1}(0) = t-1]_\infty \quad (\text{I18})$$

$$= (1-(1-p_{t_{\text{req}}+1})(1-p)^{t-1})^M - (1-(1-p_{t_{\text{req}}+1})(1-p)^{t-2})^M, \quad (\text{I19})$$

which is precisely (I3).

Now, for brevity, let $\tilde{q} \equiv 1 - p_{t_{\text{req}}+1}$, $q \equiv 1 - p$. Then,

$$\Pr[W_{E'}(t_{\text{req}}) = t]_\infty = (1-\tilde{q}q^{t-1})^M - (1-\tilde{q}q^{t-2})^M \quad (\text{I20})$$

$$= \sum_{k=0}^M \binom{M}{k} (-1)^k (\tilde{q}q^{t-1})^k - \sum_{k=0}^M \binom{M}{k} (-1)^k (\tilde{q}q^{t-2})^k \quad (\text{I21})$$

$$= \sum_{k=1}^M \binom{M}{k} (-1)^k \tilde{q}^k (q^{t-1})^k (1-q^{-k}). \quad (\text{I22})$$

Then, using the fact that

$$\sum_{t=2}^{\infty} t(q^k)^{t-1} = \frac{q^k(2-q^k)}{(1-q^k)^2}, \quad (\text{I23})$$

we obtain

$$\mathbb{E}[W_{E'}(t_{\text{req}})]_\infty = \sum_{t=1}^{\infty} t \Pr[W_{E'}(t_{\text{req}}) = t]_\infty \quad (\text{I24})$$

$$= (1 - \tilde{q})^M + \sum_{k=1}^M \binom{M}{k} (-1)^k \tilde{q}^k \left(\frac{q^k (2 - q^k)}{(1 - q^k)^2} \right) (1 - q^{-k}) \quad (I25)$$

$$= (1 - \tilde{q})^M + \sum_{k=1}^M \binom{M}{k} (-1)^{k+1} \tilde{q}^k \left(1 + \frac{1}{1 - q^k} \right) \quad (I26)$$

$$= (1 - \tilde{q})^M + \sum_{k=1}^M \binom{M}{k} (-1)^{k+1} \tilde{q}^k \left(1 + \frac{1}{p_k} \right) \quad (I27)$$

$$= (1 - \tilde{q})^M + \sum_{k=1}^M \binom{M}{k} (-1)^{k+1} \tilde{q}^k + \sum_{k=1}^M \binom{M}{k} (-1)^{k+1} \frac{(1 - p_k)^{t_{\text{req}}+1}}{p_k} \quad (I28)$$

$$= 1 + \sum_{k=1}^M \binom{M}{k} (-1)^{k+1} \frac{(1 - p_k)^{t_{\text{req}}+1}}{p_k}, \quad (I29)$$

where in the second-last line we used the fact that $\tilde{q}^k = (1 - p_k)^{t_{\text{req}}+1}$. Finally, using the fact that $1 = \sum_{k=1}^M \binom{M}{k} (-1)^{k+1}$, we obtain

$$\mathbb{E}[W_{E'}(t_{\text{req}})]_{\infty} = \sum_{k=1}^M \binom{M}{k} (-1)^{k+1} \left(1 + \frac{(1 - p_k)^{t_{\text{req}}+1}}{p_k} \right), \quad (I30)$$

as required.

¹H. J. Kimble, “The quantum internet,” *Nature* **453** (2008).

²C. Simon, “Towards a global quantum network,” *Nature Photonics* **11**, 678–680 (2017).

³D. Castelvecchi, “The quantum internet has arrived (and it hasn’t),” *Nature* **554**, 289–292 (2018).

⁴S. Wehner, D. Elkouss, and R. Hanson, “Quantum internet: A vision for the road ahead,” *Science* **362** (2018).

⁵J. Dowling, *Schrödinger’s Web: Race to Build the Quantum Internet* (Taylor & Francis, 2020).

⁶C. H. Bennett and G. Brassard, “Quantum cryptography: Public key distribution and coin tossing,” in *International Conference on Computer System and Signal Processing, IEEE* (1984) pp. 175–179.

⁷A. K. Ekert, “Quantum cryptography based on Bell’s theorem,” *Physical Review Letters* **67**, 661–663 (1991).

⁸N. Gisin, G. Ribordy, W. Tittel, and H. Zbinden, “Quantum cryptography,” *Reviews of Modern Physics* **74**, 145–195 (2002).

⁹V. Scarani, H. Bechmann-Pasquinucci, N. J. Cerf, M. Dušek, N. Lütkenhaus, and M. Peev, “The security of practical quantum key distribution,” *Reviews of Modern Physics* **81**, 1301–1350 (2009).

¹⁰F. Xu, X. Ma, Q. Zhang, H.-K. Lo, and J.-W. Pan, “Secure quantum key distribution with realistic devices,” *Reviews of Modern Physics* **92**, 025002 (2020).

¹¹S. Pirandola, U. L. Andersen, L. Banchi, M. Berta, D. Bunandar, R. Colbeck, D. Englund, T. Gehring, C. Lupo, C. Ottaviani, J. Pereira, M. Razavi, J. S. Shaari, M. Tomamichel, V. C. Usenko, G. Vallone, P. Villoresi, and P. Wallden, “Advances in Quantum Cryptography,” [arXiv:1906.01645](https://arxiv.org/abs/1906.01645) (2019).

¹²C. H. Bennett, G. Brassard, C. Crépeau, R. Jozsa, A. Peres, and W. K. Wootters, “Teleporting an unknown quantum state via dual classical and Einstein-Podolsky-Rosen channels,” *Physical Review Letters* **70**, 1895–1899 (1993).

¹³L. Vaidman, “Teleportation of quantum states,” *Physical Review A* **49**, 1473–1476 (1994).

¹⁴S. L. Braunstein, C. A. Fuchs, and H. J. Kimble, “Criteria for continuous-variable quantum teleportation,” *Journal of Modern Optics* **47**, 267–278 (2000).

¹⁵R. Jozsa, D. S. Abrams, J. P. Dowling, and C. P. Williams, “Quantum clock synchronization based on shared prior entanglement,” *Physical Review Letters* **85**, 2010–2013 (2000).

¹⁶J. Preskill, “Quantum clock synchronization and quantum error correction,” [arXiv:quant-ph/0010098](https://arxiv.org/abs/quant-ph/0010098) (2000).

¹⁷U. Yurtsever and J. P. Dowling, “Lorentz-invariant look at quantum clock synchronization protocols based on distributed entanglement,” *Physical Review A* **65**, 052317 (2002).

¹⁸E. O. Ilo-Okeke, L. Tessler, J. P. Dowling, and T. Byrnes, “Remote quantum clock synchronization without synchronized clocks,” *npj Quantum Information* **4**, 40 (2018).

¹⁹J. I. Cirac, A. K. Ekert, S. F. Huelga, and C. Macchiavello, “Distributed quantum computation over noisy channels,” *Physical Review A* **59**, 4249–4254 (1999).

²⁰C. L. Degen, F. Reinhard, and P. Cappellaro, “Quantum sensing,” *Reviews of Modern Physics* **89**, 035002 (2017).

²¹Q. Zhuang, Z. Zhang, and J. H. Shapiro, “Distributed quantum sensing using continuous-variable multipartite entanglement,” *Physical Review A* **97**, 032329 (2018).

²²Y. Xia, Q. Zhuang, W. Clark, and Z. Zhang, “Repeater-enhanced distributed quantum sensing based on continuous-variable multipartite entanglement,” *Physical Review A* **99**, 012328 (2019).

²³D. E. Bruschi, C. Sabín, A. White, V. Baccetti, D. K. L. Oi, and I. Fuentes, “Testing the effects of gravity and motion on quantum entanglement in space-based experiments,” *New Journal of Physics* **16**, 053041 (2014).

²⁴P. Kómár, E. M. Kessler, M. Bishop, L. Jiang, A. S. Sørensen, J. Ye, and M. D. Lukin, “A quantum network of clocks,” *Nature Physics* **10**, 582 (2014).

²⁵M. Peev, C. Pacher, R. Alléaume, C. Barreiro, *et al.*, “The SECOQC quantum key distribution network in Vienna,” *New Journal of Physics* **11**, 075001 (2009).

²⁶T.-Y. Chen, J. Wang, H. Liang, W.-Y. Liu, *et al.*, “Metropolitan all-pass and inter-city quantum communication network,” *Optics Express* **18**, 27217–27225 (2010).

²⁷A. Mirza and F. Petruccione, “Realizing long-term quantum cryptography,” *Journal of the Optical Society of America B* **27**, A185–A188 (2010).

²⁸D. Stucki, M. Legré, F. Buntzschu, B. Clausen, *et al.*, “Long-term performance of the SwissQuantum quantum key distribution network in a field environment,” *New Journal of Physics* **13**, 123001 (2011).

²⁹M. Sasaki, M. Fujiwara, H. Ishizuka, W. Klaus, *et al.*, “Field test of quantum key distribution in the Tokyo QKD Network,” *Optics Express* **19**, 10387–10409 (2011).

³⁰S. Wang, W. Chen, Z.-Q. Yin, H.-W. Li, *et al.*, “Field and long-term demonstration of a wide area quantum key distribution network,” *Optics Express* **22**, 21739–21756 (2014).

³¹D. Bunandar, A. Lentine, C. Lee, H. Cai, *et al.*, “Metropolitan quantum key

distribution with silicon photonics," *Physical Review X* **8**, 021009 (2018).

³²Q. Zhang, F. Xu, Y.-A. Chen, C.-Z. Peng, and J.-W. Pan, "Large scale quantum key distribution: challenges and solutions," *Optics Express* **26**, 24260–24273 (2018).

³³O. Svelto, *Principles of Lasers*, 5th ed. (Springer US, 2010).

³⁴H. Kaushal, V. K. Jain, and S. Kar, *Free Space Optical Communication* (Springer Nature, 2017).

³⁵S. Karp, R. M. Gagliardi, S. E. Moran, and L. B. Stotts, *Optical Channels: Fibers, Clouds, Water, and the Atmosphere*, 1st ed., Applications of Communications Theory (Springer US, 1988).

³⁶C. H. Bennett, G. Brassard, S. Popescu, B. Schumacher, J. A. Smolin, and W. K. Wootters, "Purification of noisy entanglement and faithful teleportation via noisy channels," *Physical Review Letters* **76**, 722–725 (1996).

³⁷D. Deutsch, A. Ekert, R. Jozsa, C. Macchiavello, S. Popescu, and A. Sanpera, "Quantum privacy amplification and the security of quantum cryptography over noisy channels," *Physical Review Letters* **77**, 2818–2821 (1996).

³⁸C. H. Bennett, D. P. DiVincenzo, J. A. Smolin, and W. K. Wootters, "Mixed-state entanglement and quantum error correction," *Physical Review A* **54**, 3824–3851 (1996).

³⁹M. Żukowski, A. Zeilinger, M. A. Horne, and A. K. Ekert, "Event-ready-detectors' Bell experiment via entanglement swapping," *Physical Review Letters* **71**, 4287–4290 (1993).

⁴⁰S. Pirandola, "Capacities of repeater-assisted quantum communications," *arXiv:1601.00966* (2016).

⁴¹K. Azuma, A. Mizutani, and H.-K. Lo, "Fundamental rate-loss trade-off for the quantum internet," *Nature Communications* **7**, 13523 (2016).

⁴²K. Azuma and G. Kato, "Aggregating quantum repeaters for the quantum internet," *Physical Review A* **96**, 032332 (2017).

⁴³S. Bäuml and K. Azuma, "Fundamental limitation on quantum broadcast networks," *Quantum Science and Technology* **2**, 024004 (2017).

⁴⁴L. Rigovacca, G. Kato, S. Bäuml, M. S. Kim, W. J. Munro, and K. Azuma, "Versatile relative entropy bounds for quantum networks," *New Journal of Physics* **20**, 013033 (2018).

⁴⁵S. Pirandola, "End-to-end capacities of a quantum communication network," *Communications Physics* **2**, 51 (2019).

⁴⁶S. Pirandola, "Bounds for multi-end communication over quantum networks," *Quantum Science and Technology* **4**, 045006 (2019).

⁴⁷S. Das, S. Bäuml, M. Winczewski, and K. Horodecki, "Universal Limitations on Quantum Key Distribution over a Network," *Physical Review X* **11**, 041016 (2021).

⁴⁸S. Bäuml, M. Christandl, K. Horodecki, and A. Winter, "Limitations on quantum key repeaters," *Nature Communications* **6**, 6908 (2015).

⁴⁹K. P. Seshadreesan, M. Takeoka, and M. M. Wilde, "Bounds on Entanglement Distillation and Secret Key Agreement for Quantum Broadcast Channels," *IEEE Transactions on Information Theory* **62**, 2849–2866 (2016).

⁵⁰M. Takeoka, K. P. Seshadreesan, and M. M. Wilde, "Unconstrained capacities of quantum key distribution and entanglement distillation for pure-loss bosonic broadcast channels," *Physical Review Letters* **119**, 150501 (2017).

⁵¹R. Laurenza and S. Pirandola, "General bounds for sender-receiver capacities in multipoint quantum communications," *Physical Review A* **96**, 032318 (2017).

⁵²M. Christandl and A. Müller-Hermes, "Relative entropy bounds on quantum, private and repeater capacities," *Communications in Mathematical Physics* **353**, 821–852 (2017).

⁵³S. Bäuml, K. Azuma, G. Kato, and D. Elkouss, "Linear programs for entanglement and key distribution in the quantum internet," *Communications Physics* **3**, 55 (2020).

⁵⁴C. Harney and S. Pirandola, "Analytical methods for high-rate global quantum networks," *PRX Quantum* **3**, 010349 (2022).

⁵⁵W. Dai, T. Peng, and M. Z. Win, "Optimal Remote Entanglement Distribution," *IEEE Journal on Selected Areas in Communications* **38**, 540–556 (2020).

⁵⁶K. Chakraborty, D. Elkouss, B. Rijssman, and S. Wehner, "Entanglement Distribution in a Quantum Network, a Multi-Commodity Flow-Based Approach," *arXiv:2005.14304* (2020).

⁵⁷K. Goodenough, D. Elkouss, and S. Wehner, "Optimizing repeater schemes for the quantum internet," *Physical Review A* **103**, 032610 (2021).

⁵⁸S. Khatri, "Policies for elementary links in a quantum network," *Quantum* **5**, 537 (2021).

⁵⁹O. A. Collins, S. D. Jenkins, A. Kuzmich, and T. A. B. Kennedy, "Multiplexed memory-insensitive quantum repeaters," *Physical Review Letters* **98**, 060502 (2007).

⁶⁰H.-J. Briegel, W. Dür, J. I. Cirac, and P. Zoller, "Quantum repeaters: The role of imperfect local operations in quantum communication," *Physical Review Letters* **81**, 5932–5935 (1998).

⁶¹W. Dür, H.-J. Briegel, J. I. Cirac, and P. Zoller, "Quantum repeaters based on entanglement purification," *Physical Review A* **59**, 169–181 (1999).

⁶²L.-M. Duan, M. D. Lukin, J. I. Cirac, and P. Zoller, "Long-distance quantum communication with atomic ensembles and linear optics," *Nature* **414** (2001).

⁶³C. Simon, H. de Riedmatten, M. Afzelius, N. Sangouard, H. Zbinden, and N. Gisin, "Quantum repeaters with photon pair sources and multimode memories," *Physical Review Letters* **98**, 190503 (2007).

⁶⁴N. Sangouard, C. Simon, J. Minář, H. Zbinden, H. de Riedmatten, and N. Gisin, "Long-distance entanglement distribution with single-photon sources," *Physical Review A* **76**, 050301 (2007).

⁶⁵N. K. Bernardez, L. Praxmeyer, and P. van Loock, "Rate analysis for a hybrid quantum repeater," *Physical Review A* **83**, 012323 (2011).

⁶⁶M. Zwerger, W. Dür, and H. J. Briegel, "Measurement-based quantum repeaters," *Physical Review A* **85**, 062326 (2012).

⁶⁷K. Azuma, K. Tamaki, and H.-K. Lo, "All-photonic quantum repeaters," *Nature Communications* **6** (2015).

⁶⁸M. Zwerger, H. J. Briegel, and W. Dür, "Measurement-based quantum communication," *Applied Physics B* **122**, 50 (2016).

⁶⁹M. Epping, H. Kampermann, and D. Bruß, "Large-scale quantum networks based on graphs," *New Journal of Physics* **18**, 053036 (2016).

⁷⁰J. Wallnöfer, M. Zwerger, C. Muschik, N. Sangouard, and W. Dür, "Two-dimensional quantum repeaters," *Physical Review A* **94**, 052307 (2016).

⁷¹X. Liu, Z.-Q. Zhou, Y.-L. Hua, C.-F. Li, and G.-C. Guo, "Semi-hierarchical quantum repeaters based on moderate lifetime quantum memories," *Physical Review A* **95**, 012319 (2017).

⁷²S. E. Vinay and P. Kok, "Practical repeaters for ultralong-distance quantum communication," *Physical Review A* **95**, 052336 (2017).

⁷³C. Meignan, D. Markham, and F. Grosshans, "Distributing graph states over arbitrary quantum networks," *Physical Review A* **100**, 052333 (2019).

⁷⁴M. Zwerger, A. Pirker, V. Dunjko, H. J. Briegel, and W. Dür, "Long-range big quantum-data transmission," *Physical Review Letters* **120**, 030503 (2018).

⁷⁵A. Pirker, J. Wallnöfer, and W. Dür, "Modular architectures for quantum networks," *New Journal of Physics* **20**, 053054 (2018).

⁷⁶S. Das, S. Khatri, and J. P. Dowling, "Robust quantum network architectures and topologies for entanglement distribution," *Physical Review A* **97**, 012335 (2018).

⁷⁷J. Wallnöfer, A. Pirker, M. Zwerger, and W. Dür, "Multipartite state generation in quantum networks with optimal scaling," *Scientific Reports* **9**, 314 (2019).

⁷⁸A. Pirker and W. Dür, "A quantum network stack and protocols for reliable entanglement-based networks," *New Journal of Physics* **21**, 033003 (2019).

⁷⁹P. Hilaire, E. Barnes, and S. E. Economou, "Resource requirements for efficient quantum communication using all-photonic graph states generated from a few matter qubits," *Quantum* **5**, 397 (2021).

⁸⁰R. M. Gingrich, P. Kok, H. Lee, F. Vatan, and J. P. Dowling, "All Linear Optical Quantum Memory Based on Quantum Error Correction," *Physical Review Letters* **91**, 217901 (2003).

⁸¹T. C. Ralph, A. J. F. Hayes, and A. Gilchrist, "Loss-tolerant optical qubits," *Physical Review Letters* **95**, 100501 (2005).

⁸²L. Jiang, J. M. Taylor, K. Nemoto, W. J. Munro, R. Van Meter, and M. D. Lukin, "Quantum repeater with encoding," *Physical Review A* **79**, 032325 (2009).

⁸³A. G. Fowler, D. S. Wang, C. D. Hill, T. D. Ladd, R. Van Meter, and L. C. L. Hollenberg, "Surface code quantum communication," *Physical Review Letters* **104**, 180503 (2010).

⁸⁴W. J. Munro, A. M. Stephens, S. J. Devitt, K. A. Harrison, and K. Nemoto, "Quantum communication without the necessity of quantum memories," *Nature Photonics* **6**, 777 (2012).

⁸⁵S. Muralidharan, J. Kim, N. Lütkenhaus, M. D. Lukin, and L. Jiang, "Ultrafast and fault-tolerant quantum communication across long distances," *Physical Review Letters* **112**, 250501 (2014).

⁸⁶R. Namiki, L. Jiang, J. Kim, and N. Lütkenhaus, "Role of syndrome information on a one-way quantum repeater using teleportation-based error correction," *Physical Review A* **94**, 052304 (2016).

⁸⁷S. Muralidharan, L. Li, J. Kim, N. Lütkenhaus, M. D. Lukin, and L. Jiang, "Optimal architectures for long distance quantum communication," *Scientific Reports* **6**, 20463 (2016).

⁸⁸F. M. Miatto, M. Epping, and N. Lütkenhaus, "Hamiltonians for one-way quantum repeaters," *Quantum* **2**, 75 (2018).

⁸⁹F. da Silva, A. Torres-Knoop, T. Coopmans, D. Maier, and S. Wehner, "Optimizing Entanglement Generation and Distribution Using Genetic Algorithms," *arXiv:2010.16373* (2020).

⁹⁰W. Dai and D. Towsley, "Entanglement Swapping for Repeater Chains with Finite Memory Sizes," *arXiv:2111.10994* (2021).

⁹¹F. Rozpędek, K. Noh, Q. Xu, S. Guha, and L. Jiang, "Quantum repeaters based on concatenated bosonic and discrete-variable quantum codes," *npj Quantum Information* **7** (2021).

⁹²N. Sangouard, C. Simon, H. de Riedmatten, and N. Gisin, "Quantum repeaters based on atomic ensembles and linear optics," *Reviews of Modern Physics* **83**, 33–80 (2011).

⁹³W. J. Munro, K. Azuma, K. Tamaki, and K. Nemoto, "Inside Quantum Repeaters," *IEEE Journal of Selected Topics in Quantum Electronics* **21**, 78–90 (2015).

⁹⁴R. Van Meter, *Quantum Networking* (John Wiley & Sons, Ltd, 2014).

⁹⁵K. Azuma, S. Bäuml, T. Coopmans, D. Elkouss, and B. Li, "Tools for quantum network design," *AVS Quantum Science* **3**, 014101 (2021).

⁹⁶W. J. Munro, N. L. Piparo, J. Dias, M. Hanks, and K. Nemoto, "Designing tomorrow's quantum internet," *AVS Quantum Science* **4**, 020503 (2022).

⁹⁷M. Aspelmeyer, T. Jennewein, M. Pfennigbauer, W. R. Leeb, and A. Zeilinger, "Long-distance quantum communication with entangled photons using satellites," *IEEE Journal of Selected Topics in Quantum Electronics* **9**, 1541–1551 (2003).

⁹⁸C. Jones, D. Kim, M. T. Rakher, P. G. Kwiat, and T. D. Ladd, "Design and analysis of communication protocols for quantum repeater networks," *New Journal of Physics* **18**, 083015 (2016).

⁹⁹S. Khatri, C. T. Matyas, A. U. Siddiqui, and J. P. Dowling, "Practical figures of merit and thresholds for entanglement distribution in quantum networks," *Physical Review Research* **1**, 023032 (2019).

¹⁰⁰F. Rozpędek, K. Goodenough, J. Ribeiro, N. Kalb, V. C. Vivoli, A. Reiserer, R. Hanson, S. Wehner, and D. Elkouss, "Parameter regimes for a single sequential quantum repeater," *Quantum Science and Technology* **3**, 034002 (2018).

¹⁰¹F. Rozpędek, R. Yehia, K. Goodenough, M. Ruf, P. C. Humphreys, R. Hanson, S. Wehner, and D. Elkouss, "Near-term quantum-repeater experiments with nitrogen-vacancy centers: Overcoming the limitations of direct transmission," *Physical Review A* **99**, 052330 (2019).

¹⁰²A. Dahlberg, M. Skrzypczyk, T. Coopmans, L. Wubben, F. Rozpędek, M. Pompili, A. Stolk, P. Pawełczak, R. Knegjens, J. de Oliveira Filho, R. Hanson, and S. Wehner, "A Link Layer Protocol for Quantum Networks," in *Proceedings of the ACM Special Interest Group on Data Communication, SIGCOMM '19* (Association for Computing Machinery, New York, NY, USA, 2019) p. 159–173.

¹⁰³W. Kozłowski, A. Dahlberg, and S. Wehner, "Designing a Quantum Network Protocol," in *Proceedings of the 16th International Conference on Emerging Networking EXperiments and Technologies*, CoNEXT '20 (Association for Computing Machinery, New York, NY, USA, 2020) pp. 1–16.

¹⁰⁴T. Coopmans, R. Knegjens, A. Dahlberg, D. Maier, L. Nijsten, J. Oliveira, M. Papendrecht, J. Rabbie, F. Rozpędek, M. Skrzypczyk, L. Wubben, W. de Jong, D. Podareanu, A. T. Knoop, D. Elkouss, and S. Wehner, "NetSquid, a NETwork Simulator for QUantum Information using Discrete events," *Communications Physics* **4**, 164 (2021).

¹⁰⁵M. Pompili, S. L. N. Hermans, S. Baier, H. K. C. Beukers, P. C. Humphreys, R. N. Schouten, R. F. L. Vermeulen, M. J. Tiggelman, L. dos Santos Martins, B. Dirks, S. Wehner, and R. Hanson, "Realization of a multi-node quantum network of remote solid-state qubits," *Science* **372**, 259–264 (2021).

¹⁰⁶S. B. van Dam, P. C. Humphreys, F. Rozpędek, S. Wehner, and R. Hanson, "Multiplexed entanglement generation over quantum networks using multi-qubit nodes," *Quantum Science and Technology* **2**, 034002 (2017).

¹⁰⁷E. Shchukin, F. Schmidt, and P. van Loock, "Waiting time in quantum repeaters with probabilistic entanglement swapping," *Physical Review A* **100**, 032322 (2019).

¹⁰⁸S. Santra, L. Jiang, and V. S. Malinovsky, "Quantum repeater architecture with hierarchically optimized memory buffer times," *Quantum Science and Technology* **4**, 025010 (2019).

¹⁰⁹B. Li, T. Coopmans, and D. Elkouss, "Efficient Optimization of Cutoffs in Quantum Repeater Chains," *IEEE Transactions on Quantum Engineering* **2**, 1–15 (2021).

¹¹⁰J. Watrous, *The Theory of Quantum Information* (Cambridge University Press, 2018).

¹¹¹D. M. Greenberger, M. A. Horne, and A. Zeilinger, "Going Beyond Bell's Theorem," in *Bell's Theorem, Quantum Theory and Conceptions of the Universe*, edited by M. Kafatos (Springer Netherlands, Dordrecht, 1989) pp. 69–72.

¹¹²H. J. Briegel and R. Raussendorf, "Persistent entanglement in arrays of interacting particles," *Physical Review Letters* **86**, 910–913 (2001).

¹¹³R. Raussendorf and H. J. Briegel, "A one-way quantum computer," *Physical Review Letters* **86**, 5188–5191 (2001).

¹¹⁴H. J. Briegel, "Cluster States," in *Compendium of Quantum Physics*, edited by D. Greenberger, K. Hentschel, and F. Weinert (Springer Berlin Heidelberg, Berlin, Heidelberg, 2009) pp. 96–105.

¹¹⁵E. Schouten, L. Mancinska, T. Islam, I. Kerenidis, and S. Wehner, "Shortcuts to quantum network routing," *arXiv:1610.05238* (2016).

¹¹⁶K. Chakraborty, F. Rozpędek, A. Dahlberg, and S. Wehner, "Distributed routing in a quantum internet," *arXiv:1907.11630* (2019).

¹¹⁷M. Pant, H. Krovi, D. Towsley, L. Tassiulas, L. Jiang, P. Basu, D. Englund, and S. Guha, "Routing entanglement in the quantum internet," *npj Quantum Information* **5**, 25 (2019).

¹¹⁸S. E. Vinay and P. Kok, "Statistical analysis of quantum-entangled-network generation," *Physical Review A* **99**, 042313 (2019).

¹¹⁹S. Brand, T. Coopmans, and D. Elkouss, "Efficient Computation of the Waiting Time and Fidelity in Quantum Repeater Chains," *IEEE Journal on Selected Areas in Communications* **38**, 619–639 (2020).

¹²⁰T. Coopmans, S. Brand, and D. Elkouss, "Improved analytical bounds on delivery times of long-distance entanglement," *Physical Review A* **105**, 012608 (2022).

¹²¹L. Praxmeyer, "Reposition time in probabilistic imperfect memories," *arXiv:1309.3407* (2013).

¹²²S. Guha, H. Krovi, C. A. Fuchs, Z. Dutton, J. A. Slater, C. Simon, and W. Tittel, "Rate-loss analysis of an efficient quantum repeater architecture," *Physical Review A* **92**, 022357 (2015).

¹²³E. Shchukin and P. van Loock, "Optimal entanglement swapping in quantum repeaters," *arXiv:2109.00793* (2021).

¹²⁴W. J. Stewart, *Probability, Markov Chains, Queues, and Simulation: The Mathematical Basis of Performance Modeling* (Princeton University Press, 2009).

¹²⁵P. Nain, G. Vardoyan, S. Guha, and D. Towsley, "On the Analysis of a Multipartite Entanglement Distribution Switch," *Proc. ACM Meas. Anal. Comput. Syst.* **4** (2020).

¹²⁶S. Khatri, *Towards a General Framework for Practical Quantum Network Protocols*, Ph.D. thesis, Louisiana State University (2021), https://digitalcommons.lsu.edu/gradschool_dissertations/5456/.

¹²⁷T. A. Caswell, M. Droettboom, A. Lee, E. S. de Andrade, J. Hunter, T. Hoffmann, E. Firing, J. Klymak, D. Stansby, N. Varoquaux, J. H. Nielsen, B. Root, R. May, P. Elson, J. K. Seppänen, D. Dale, J.-J. Lee, D. McDougall, A. Straw, P. Hobson, C. Gohlke, T. S. Yu, E. Ma, hannah, A. F. Vincent, S. Silvester, C. Moad, N. Kniazev, E. Ernest, and P. Ivanov, "matplotlib," (2021).

¹²⁸M. L. Puterman, *Markov Decision Processes: Discrete Stochastic Dynamic Programming*, Wiley Series in Probability and Statistics (Wiley, 2014).

¹²⁹C. Derman, "On Sequential Decisions and Markov Chains," *Management Science* **9**, 16–24 (1962).

¹³⁰Y. Kislev and A. Amiad, "Linear and Dynamic Programming in Markov Chains," *American Journal of Agricultural Economics* **50**, 111–129 (1968).

¹³¹S. Osaki and H. Mine, "Linear programming algorithms for semi-Markovian decision processes," *Journal of Mathematical Analysis and Applications* **22**, 356–381 (1968).

¹³²E. A. Feinberg and A. Shwartz, eds., *Handbook of Markov Decision Processes*, International Series in Operations Research & Management Science (Springer, 2002).

¹³³M. A. Nielsen and I. L. Chuang, *Quantum Computation and Quantum Information* (Cambridge University Press, 2000).

¹³⁴A. S. Holevo, *Quantum Systems, Channels, Information: A Mathematical Introduction* (Walter de Gruyter GmbH, 2012).

¹³⁵M. M. Wilde, *Quantum Information Theory*, 2nd ed. (Cambridge University Press, 2017).

¹³⁶S. Khatri and M. M. Wilde, “Principles of Quantum Communication Theory: A Modern Approach,” [arXiv:2011.04672](https://arxiv.org/abs/2011.04672) (2020).

¹³⁷A. Uhlmann, “The ‘transition probability’ in the state space of a * -algebra,” *Reports on Mathematical Physics* **9**, 273–279 (1976).

¹³⁸E. Chitambar, D. Leung, L. Mančinska, M. Ozols, and A. Winter, “Everything You Always Wanted to Know About LOCC (But Were Afraid to Ask),” *Communications in Mathematical Physics* **328**, 303–326 (2014).

¹³⁹A. Serafini, *Quantum Continuous Variables: A Primer of Theoretical Methods* (Taylor & Francis, 2017).

¹⁴⁰P. Kok and S. L. Braunstein, “Postselected versus nonpostselected quantum teleportation using parametric down-conversion,” *Physical Review A* **61**, 042304 (2000).

¹⁴¹H. Krovi, S. Guha, Z. Dutton, J. A. Slater, C. Simon, and W. Tittel, “Practical quantum repeaters with parametric down-conversion sources,” *Applied Physics B* **122**, 52 (2016).

¹⁴²A. Bognat and P. Hayden, “Privacy from Accelerating Eavesdroppers: The Impact of Losses,” in *Horizons of the Mind. A Tribute to Prakash Panangaden: Essays Dedicated to Prakash Panangaden on the Occasion of His 60th Birthday*, edited by F. van Breugel, E. Kashefi, C. Palamidessi, and J. Rutten (Springer International Publishing, Cham, 2014) pp. 180–190.

¹⁴³C. H. Bennett, D. P. DiVincenzo, and J. A. Smolin, “Capacities of quantum erasure channels,” *Physical Review Letters* **78**, 3217–3220 (1997).

¹⁴⁴M. Grassl, T. Beth, and T. Pellizzari, “Codes for the quantum erasure channel,” *Physical Review A* **56**, 33–38 (1997).

¹⁴⁵H.-y. Fan and L.-y. Hu, “New approach for analyzing time evolution of density operator in a dissipative channel by the entangled state representation,” *Optics Communications* **281**, 5571–5573 (2008).

¹⁴⁶J. S. Ivan, K. K. Sabapathy, and R. Simon, “Operator-sum representation for bosonic Gaussian channels,” *Physical Review A* **84**, 042311 (2011).

¹⁴⁷S. Khatri, A. J. Brady, R. A. Desportes, M. P. Bart, and J. P. Dowling, “Spooky action at a global distance: analysis of space-based entanglement distribution for the quantum internet,” *npj Quantum Information* **7**, 4 (2021).

¹⁴⁸J. S. Sidhu, S. K. Joshi, M. Gündoğan, T. Brougham, D. Lowndes, L. Mazzarella, M. Krutzik, S. Mohapatra, D. Dequal, G. Vallone, P. Villoresi, A. Ling, T. Jennewein, M. Mohageg, J. G. Rarity, I. Fuentes, S. Pirandola, and D. K. L. Oi, “Advances in space quantum communications,” *IET Quantum Communication* **2**, 182–217 (2021).

¹⁴⁹J.-P. Bourgoin, E. Meyer-Scott, B. L. Higgins, B. Helou, *et al.*, “A comprehensive design and performance analysis of low earth orbit satellite quantum communication,” *New Journal of Physics* **15**, 023006 (2013).

¹⁵⁰D. Vasylyev, A. A. Semenov, W. Vogel, K. Günthner, A. Thurn, O. Bayraktar, and C. Marquardt, “Free-space quantum links under diverse weather conditions,” *Physical Review A* **96**, 043856 (2017).

¹⁵¹C. Liorni, H. Kampermann, and D. Bruß, “Satellite-based links for quantum key distribution: beam effects and weather dependence,” *New Journal of Physics* **21**, 093055 (2019).

¹⁵²D. Vasylyev, W. Vogel, and F. Moll, “Satellite-mediated quantum atmospheric links,” *Physical Review A* **99**, 053830 (2019).

¹⁵³A. Peres, “Separability criterion for density matrices,” *Physical Review Letters* **77**, 1413–1415 (1996).

¹⁵⁴M. Horodecki, P. Horodecki, and R. Horodecki, “Separability of mixed states: necessary and sufficient conditions,” *Physics Letters A* **223**, 1–8 (1996).

¹⁵⁵J. Preskill, “Quantum Computation,” *Lecture Notes* (2020).

¹⁵⁶N. Lütkenhaus, “Quantum Key Distribution,” in *Quantum Information and Coherence*, edited by E. Andersson and P. Ohberg (Springer International Publishing, 2014) pp. 107–146.

¹⁵⁷G. O. Myhr, *Symmetric Extension of Bipartite Quantum States and its Use in Quantum Key Distribution with Two-Way Postprocessing*, Ph.D. thesis, Friedrich-Alexander-Universität Erlangen-Nürnberg (2010).

¹⁵⁸E. Kaur, *Limitations on Protecting Information Against Quantum Adversaries*, Ph.D. thesis, Louisiana State University (2020).

¹⁵⁹D. Bruß, “Optimal eavesdropping in quantum cryptography with six states,” *Physical Review Letters* **81**, 3018–3021 (1998).

¹⁶⁰H. Bechmann-Pasquinucci and N. Gisin, “Incoherent and coherent eavesdropping in the six-state protocol of quantum cryptography,” *Physical Review A* **59**, 4238–4248 (1999).

¹⁶¹M. Tomamichel and A. Leverrier, “A largely self-contained and complete security proof for quantum key distribution,” *Quantum* **1**, 14 (2017).

¹⁶²S. Khatri, E. Kaur, S. Guha, and M. M. Wilde, “Second-order coding rates for key distillation in quantum key distribution,” [arXiv:1910.03883](https://arxiv.org/abs/1910.03883) (2019).

¹⁶³D. Mayers and A. Yao, “Quantum cryptography with imperfect apparatus,” in *Proceedings of the 39th Annual Symposium on Foundations of Computer Science*, FOCS ’98 (IEEE Computer Society, Washington, DC, USA, 1998) pp. 503–509.

¹⁶⁴H.-K. Lo and H. F. Chau, “Unconditional Security of Quantum Key Distribution over Arbitrarily Long Distances,” *Science* **283**, 2050–2056 (1999).

¹⁶⁵E. Biham, M. Boyer, P. O. Boykin, T. Mor, and V. Roychowdhury, “A Proof of the Security of Quantum Key Distribution (Extended Abstract),” in *Proceedings of the Thirty-Second Annual ACM Symposium on Theory of Computing*, STOC ’00 (Association for Computing Machinery, New York, NY, USA, 2000) pp. 715–724.

¹⁶⁶P. W. Shor and J. Preskill, “Simple Proof of Security of the BB84 Quantum Key Distribution Protocol,” *Physical Review Letters* **85**, 441–444 (2000).

¹⁶⁷D. Mayers, “Unconditional security in quantum cryptography,” *Journal of the ACM* **48**, 351–406 (2001).

¹⁶⁸E. Biham, M. Boyer, P. O. Boykin, T. Mor, and V. Roychowdhury, “A Proof of the Security of Quantum Key Distribution,” *Journal of Cryptology* **19**, 381–439 (2006).

¹⁶⁹H.-K. Lo, “Proof of Unconditional Security of Six-State Quantum Key Distribution Scheme,” *Quantum Information & Computation* **1**, 81–94 (2001).

¹⁷⁰A. Acín, S. Massar, and S. Pironio, “Efficient quantum key distribution secure against no-signalling eavesdroppers,” *New Journal of Physics* **8**, 126–126 (2006).

¹⁷¹A. Acín, N. Brunner, N. Gisin, S. Massar, S. Pironio, and V. Scarani, “Device-independent security of quantum cryptography against collective attacks,” *Physical Review Letters* **98**, 230501 (2007).

¹⁷²J. F. Clauser, M. A. Horne, A. Shimony, and R. A. Holt, “Proposed Experiment to Test Local Hidden-Variable Theories,” *Physical Review Letters* **23**, 880–884 (1969).

¹⁷³V. Scarani, “The device-independent outlook on quantum physics,” *Acta Physical Slovaca* **62**, 347–409 (2013).

¹⁷⁴S. Pironio, A. Acín, N. Brunner, N. Gisin, S. Massar, and V. Scarani, “Device-independent quantum key distribution secure against collective attacks,” *New Journal of Physics* **11**, 045021 (2009).